IGFAE

AEFIS
aefis.usc.es
Agrupación Estratéxica de Física

USC
UNIVERSIDADE DE SANTIAGO DE COMPOSTELA

Hot QCD Matters
May 18th 2017, Laboratori Nazionali di Frascati

Coherence phenomena in high-energy nuclear collisions: from initial to final state

Néstor Armesto

Departamento de Física de Partículas, AEFIS and IGFAE
Universidade de Santiago de Compostela
nestor.armesto@usc.es

Comisión Europea

Unión Europea
Fondo Europeo de Desarrollo Regional
"Una manera de hacer Europa"

erc
European Research Council
Established by the European Commission

EXCELENCIA MARÍA DE MAEZTU

XUNTA DE GALICIA
CONSELLERÍA DE EDUCACIÓN E ORDENACIÓN UNIVERSITARIA

XUNTA DE GALICIA
CONSELLERÍA DE ECONOMÍA, EMPREGO E INDUSTRIA

GOBIERNO DE ESPAÑA
MINISTERIO DE ECONOMÍA Y COMPETITIVIDAD

Contents:

See the talks by Jean-Paul Blaizot, Leticia Cunqueiro, Enrico Scomparin and Urs Wiedemann.

Disclaimer: this a personal selection of topics, not a comprehensive overview.

This talk:

- **<u>Aim</u>**: analysing how a coherent behaviour underlies explanations of phenomena observed in high-energy hadronic collisions.
- I will discuss some examples in small systems (pp, pA) and not only in heavy-ion collisions: they may be closely related.

This talk:

- **Aim**: analysing how a coherent behaviour underlies explanations of phenomena observed in high-energy hadronic collisions.
- I will discuss some examples in small systems (pp, pA) and not only in heavy-ion collisions: they may be closely related.

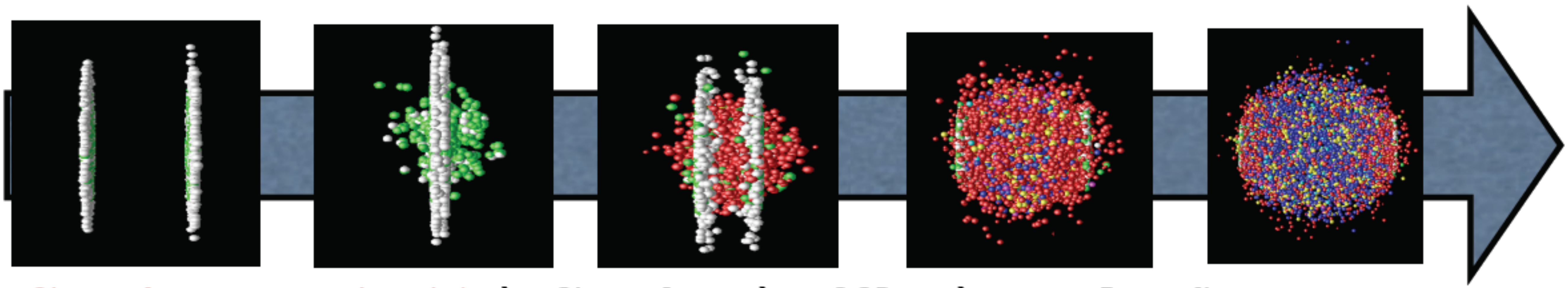

This talk:

- **Aim**: analysing how a coherent behaviour underlies explanations of phenomena observed in high-energy hadronic collisions.
- I will discuss some examples in small systems (pp, pA) and not only in heavy-ion collisions: they may be closely related.

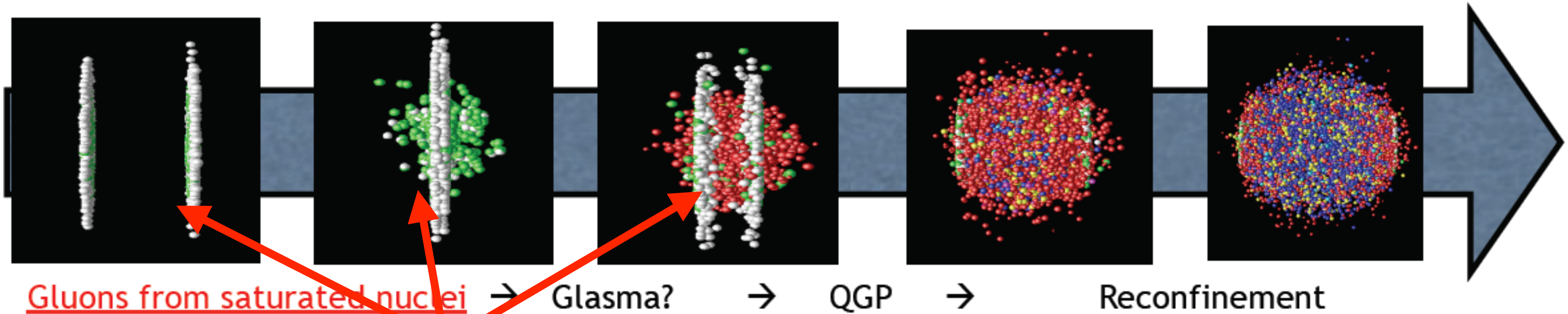

- Nuclear wave function.
- Particle production in the very early stages.

→ Thermalisation problem? / why relativistic hydrodynamics works so well, even in small systems?

This talk:

- **Aim**: analysing how a coherent behaviour underlies explanations of phenomena observed in high-energy hadronic collisions.
- I will discuss some examples in small systems (pp, pA) and not only in heavy-ion collisions: they may be closely related.

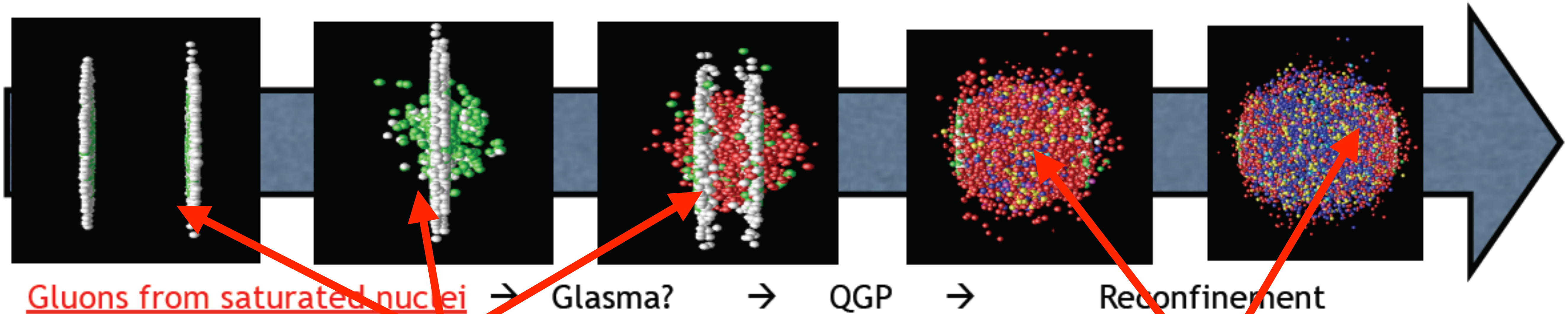

- Nuclear wave function.
- Particle production in the very early stages.

➜ Thermalisation problem? / why relativistic hydrodynamics works so well, even in small systems?

- Energy loss of high-energy partons in a coloured medium.

➜ Analysis of such medium through hard probes.

Why small systems:

- Many physical mechanisms need not be qualitatively different on p or A as they are density effects e.g.:

➜ MPIs (MC models including nuclear collisions).

➜ Non-linear dynamics, perturbative or non-perturbative.

$$\frac{xG_A(x,Q_s^2)}{\pi R_A^2 Q_s^2} \sim 1 \Longrightarrow Q_s^2 \propto A^{1/3} x^{\sim -0.3}$$

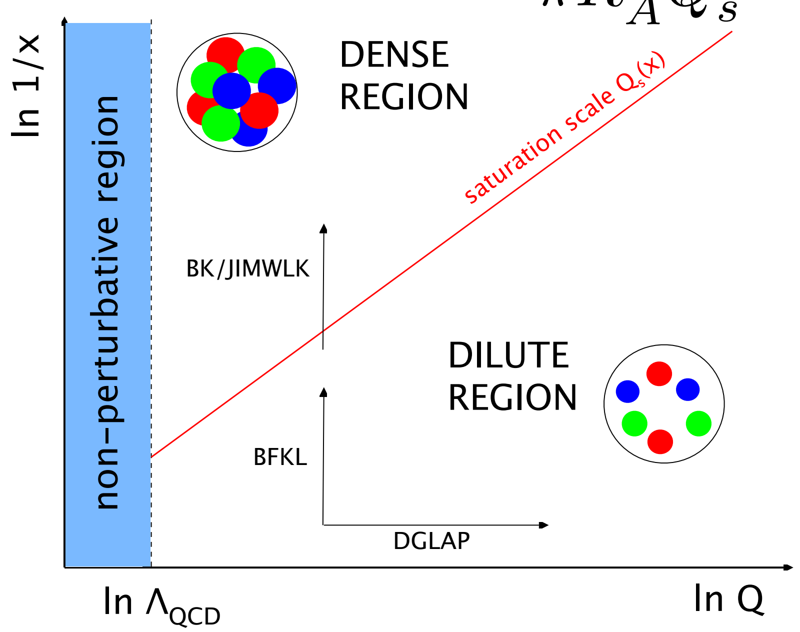

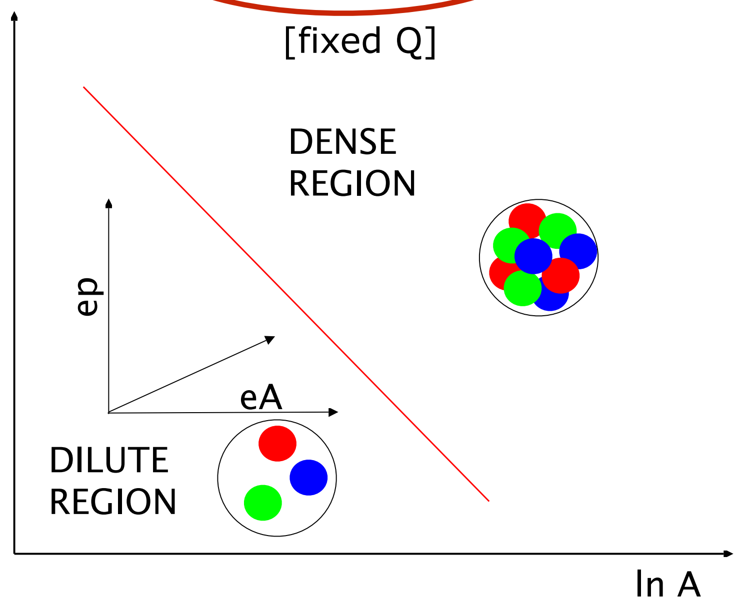

Why small systems:

- Many physical mechanisms need not be qualitatively different on p or A as they are density effects e.g.:

➜ MPIs (MC models including nuclear collisions).

➜ Non-linear dynamics, perturbative or non-perturbative.

$$\frac{xG_A(x,Q_s^2)}{\pi R_A^2 Q_s^2} \sim 1 \Longrightarrow Q_s^2 \propto A^{1/3} x^{\sim -0.3}$$

[fixed Q]

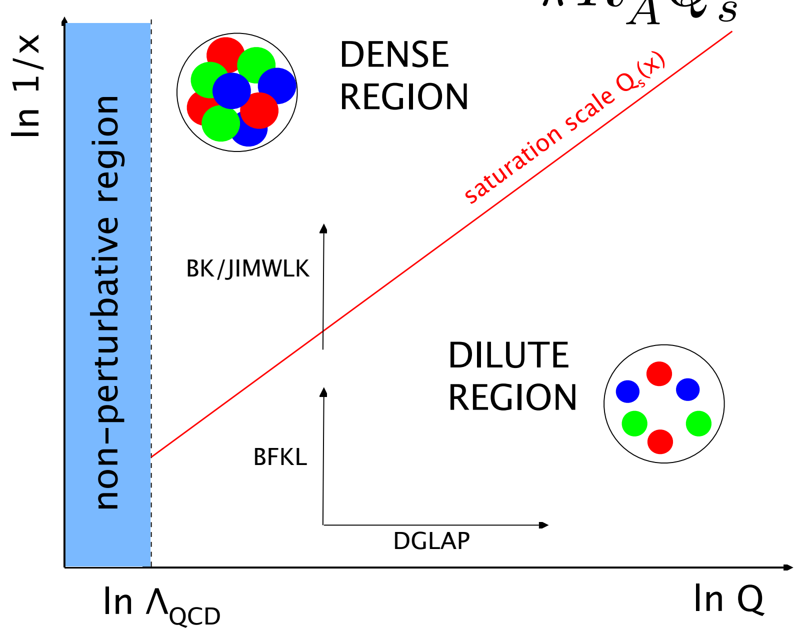

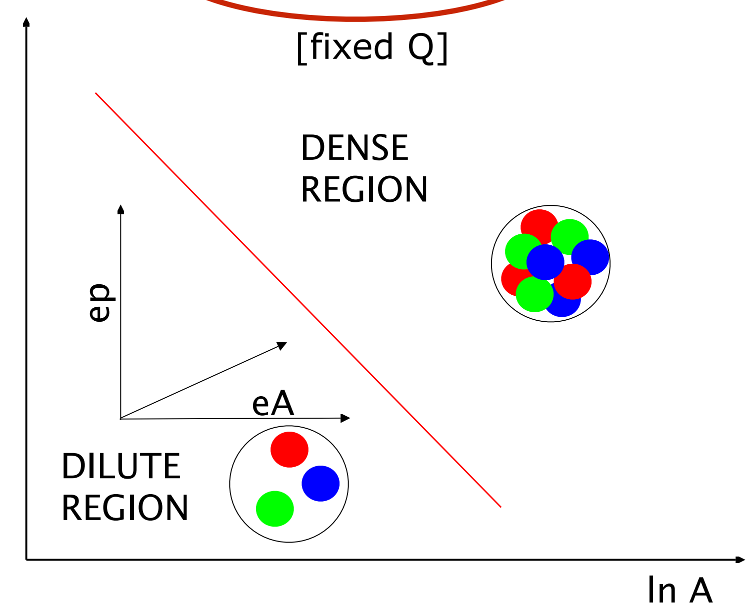

- **LHC data show several similarities, and a smooth transition, between physics in pp, pPb and PbPb**.
- In systems smaller than AA, initial state effects may have a better chance not to be obscured by final state interactions.

Contents:

1. Introduction.

2. Coherence in the initial stages:
   - ➜ Nuclear shadowing.
   - ➜ Correlations and the ridge.
   - ➜ Single inclusive particle production.

3. Coherence in the final stages:
   - ➜ Radiation off a single colour charge.
   - ➜ The antenna setup.

4. Summary and outlook.

See the talks by Jean-Paul Blaizot, Leticia Cunqueiro, Enrico Scomparin and Urs Wiedemann.

Disclaimer: this a personal selection of topics, not a comprehensive overview.

DIS on nuclei:

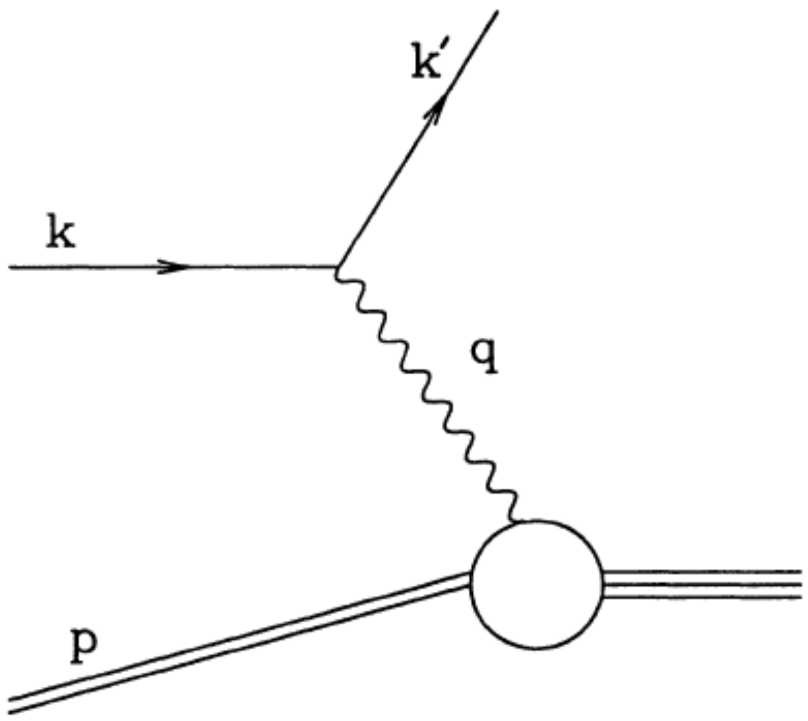

$$M^2 = p^2$$
$$\nu = p\cdot q = M(E'-E)$$
$$x = \frac{Q^2}{2\nu} = \frac{Q^2}{2M(E-E')}$$
$$y = \frac{q\cdot p}{k\cdot p} = 1 - E'/E\ ,$$

$$\frac{d^2\sigma^{em}}{dx dy} = \frac{8\pi\alpha^2 ME}{Q^4}\left[\left(\frac{1+(1-y)^2}{2}\right)2xF_1^{em} + (1-y)(F_2^{em} - 2xF_1^{em}) - (M/2E)xyF_2^{em}\right]$$

DIS on nuclei:

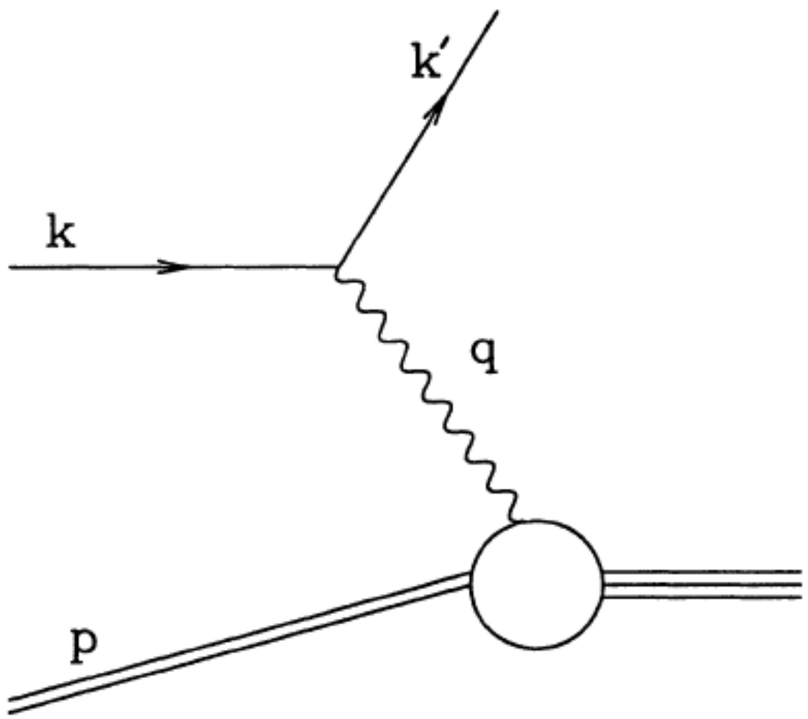

$$M^2 = p^2$$
$$\nu = p \cdot q = M(E' - E)$$
$$x = \frac{Q^2}{2\nu} = \frac{Q^2}{2M(E - E')}$$
$$y = \frac{q \cdot p}{k \cdot p} = 1 - E'/E\ ,$$

$$\frac{d^2\sigma^{em}}{dxdy} = \frac{8\pi\alpha^2 ME}{Q^4}\left[\left(\frac{1+(1-y)^2}{2}\right)2xF_1^{em} + (1-y)(F_2^{em} - 2xF_1^{em}) - (M/2E)xyF_2^{em}\right]$$

$$R_{F_2}^A(x, Q^2) = \frac{F_2^A(x, Q^2)}{AF_2^{\text{nucleon}}(x, Q^2)}$$

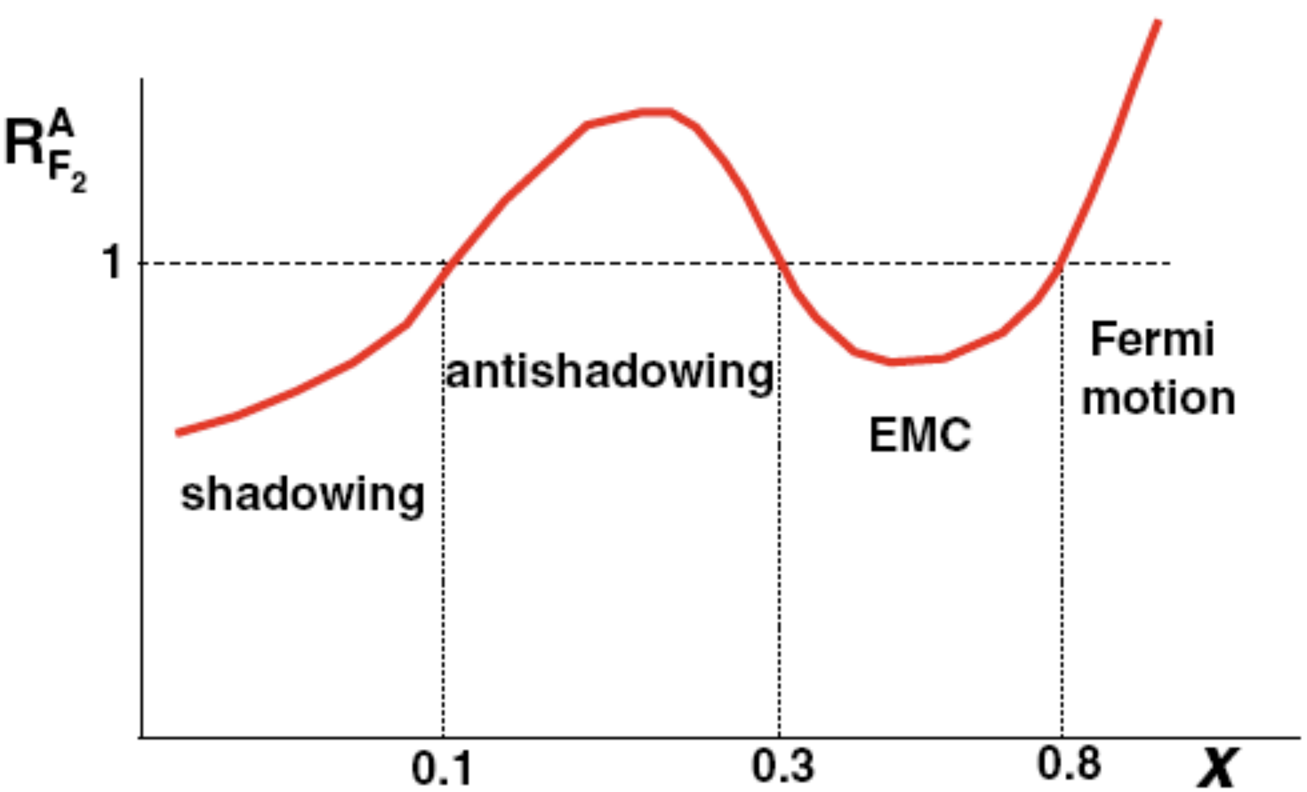

DIS on nuclei:

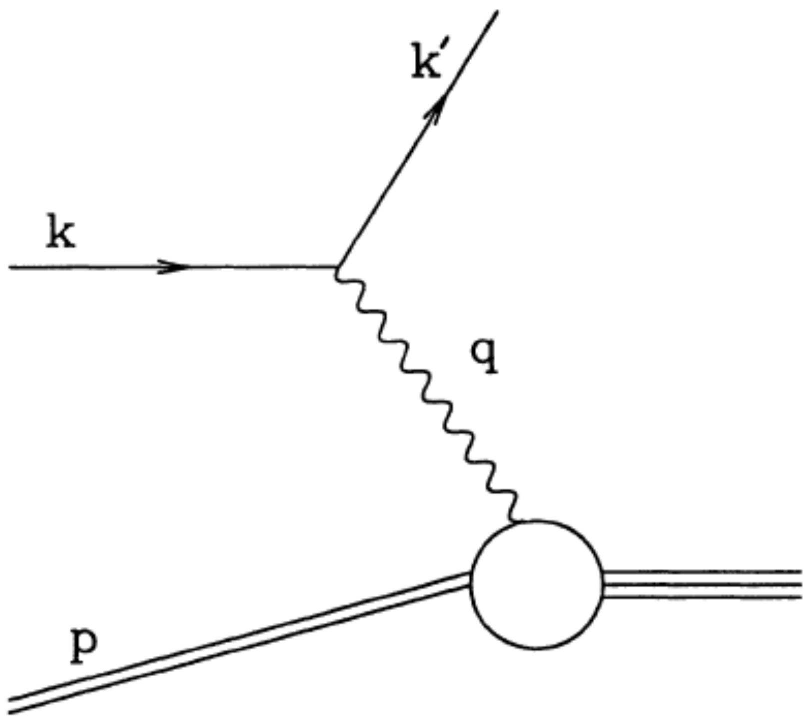

$$M^2 = p^2$$
$$\nu = p \cdot q = M(E' - E)$$
$$x = \frac{Q^2}{2\nu} = \frac{Q^2}{2M(E - E')}$$
$$y = \frac{q \cdot p}{k \cdot p} = 1 - E'/E \, ,$$

$$\frac{d^2\sigma^{em}}{dxdy} = \frac{8\pi\alpha^2 ME}{Q^4}\left[\left(\frac{1+(1-y)^2}{2}\right)2xF_1^{em} + (1-y)(F_2^{em} - 2xF_1^{em}) - (M/2E)xyF_2^{em}\right]$$

$$R_{F_2}^A(x, Q^2) = \frac{F_2^A(x, Q^2)}{AF_2^{\text{nucleon}}(x, Q^2)}$$

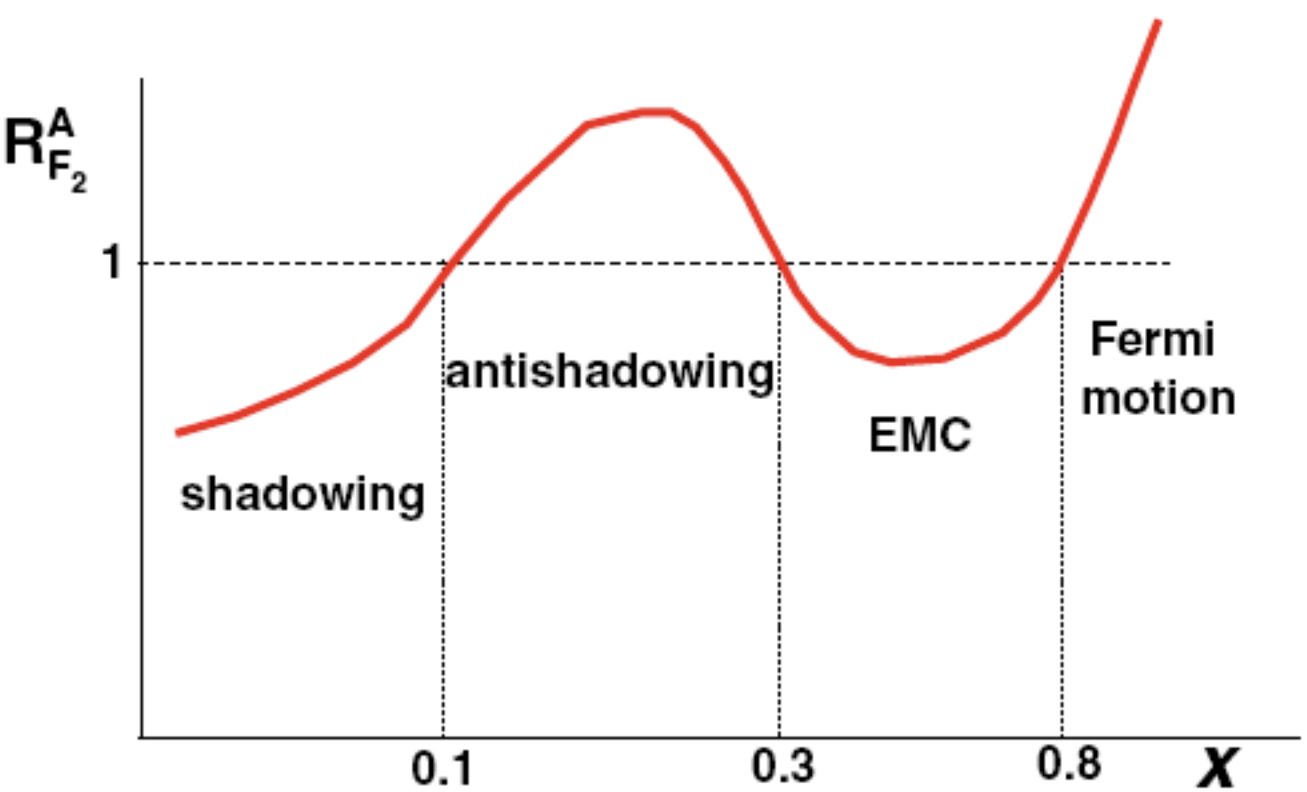

- R=1 indicates the absence of nuclear effects.
- R≠1 discovered in the early 70's.
- I will be mostly interested in small x (<0.1) relevant for high energies: isospin effects neglected.

DIS on nuclei:

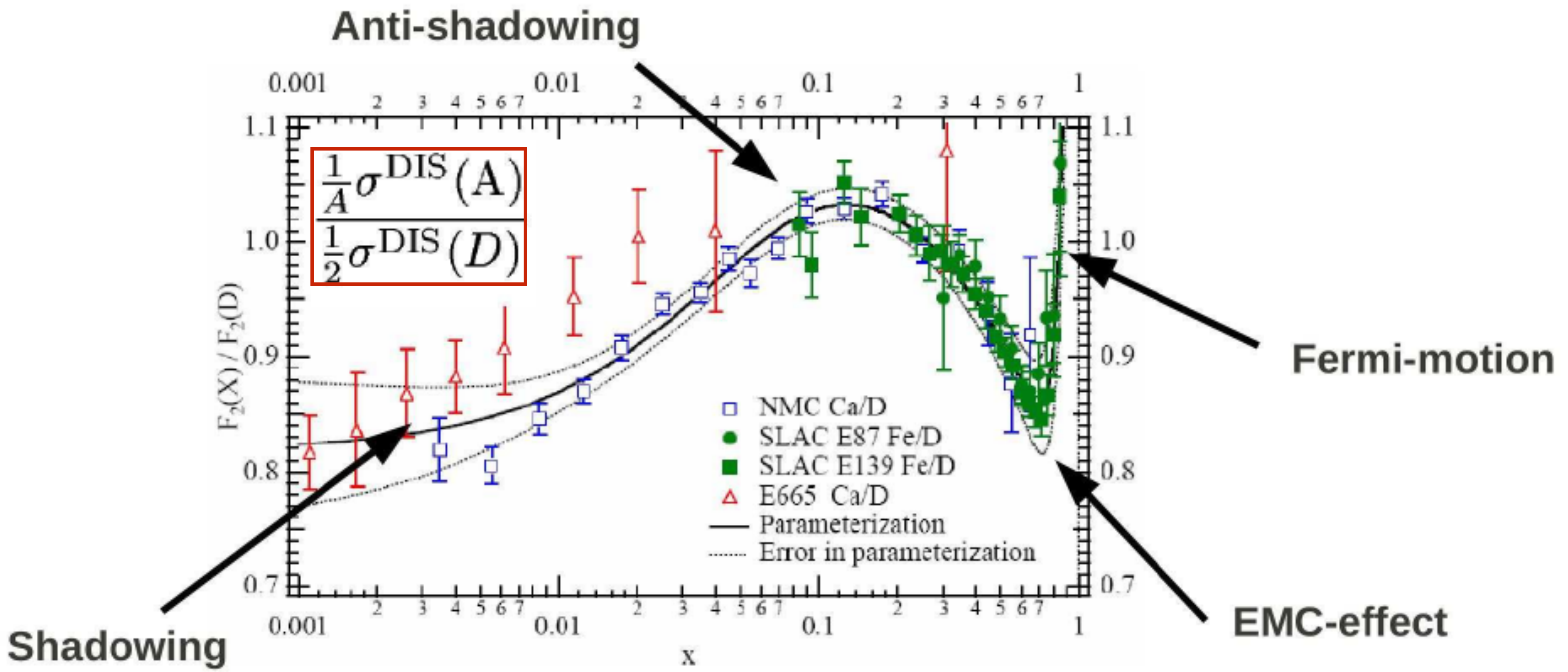

- Different explanations for the different regions (many of them not based on a partonic picture).

DIS on nuclei:

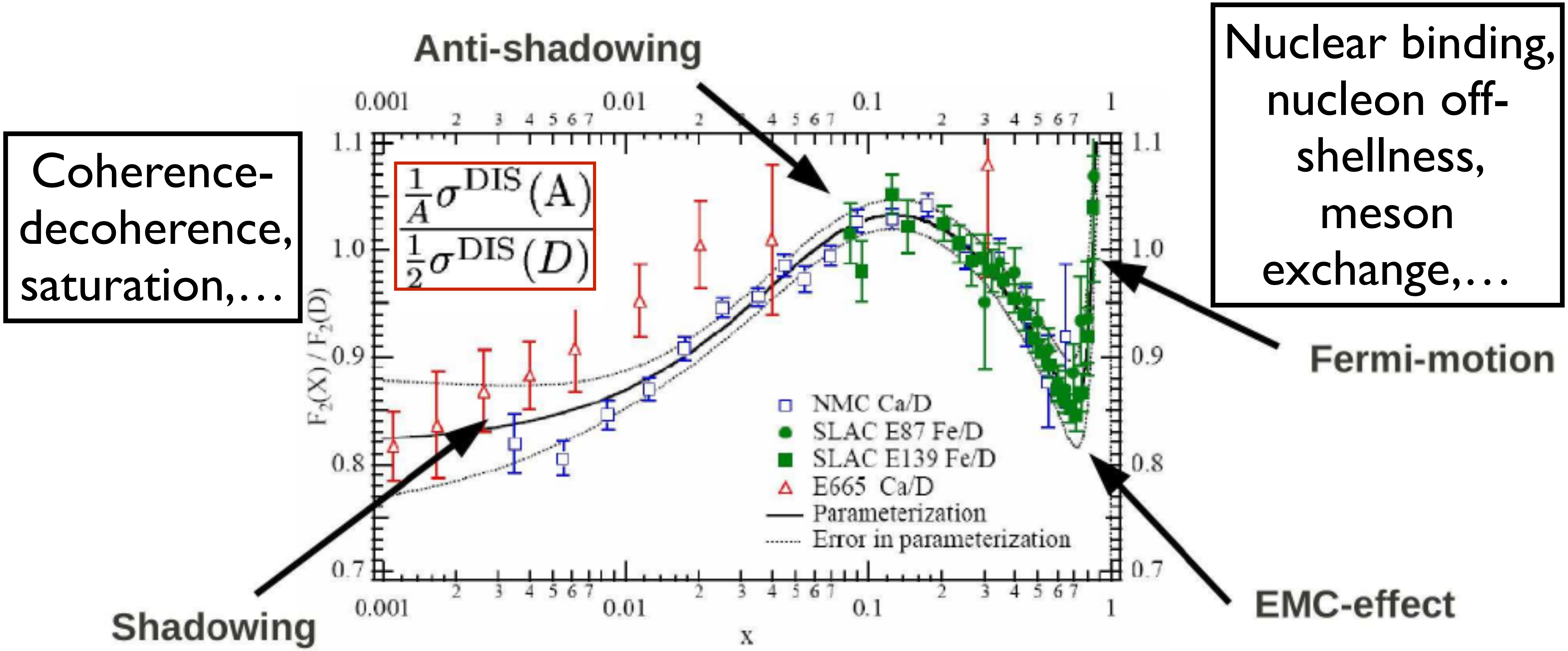

- Different explanations for the different regions (many of them not based on a partonic picture).

DIS on nuclei:

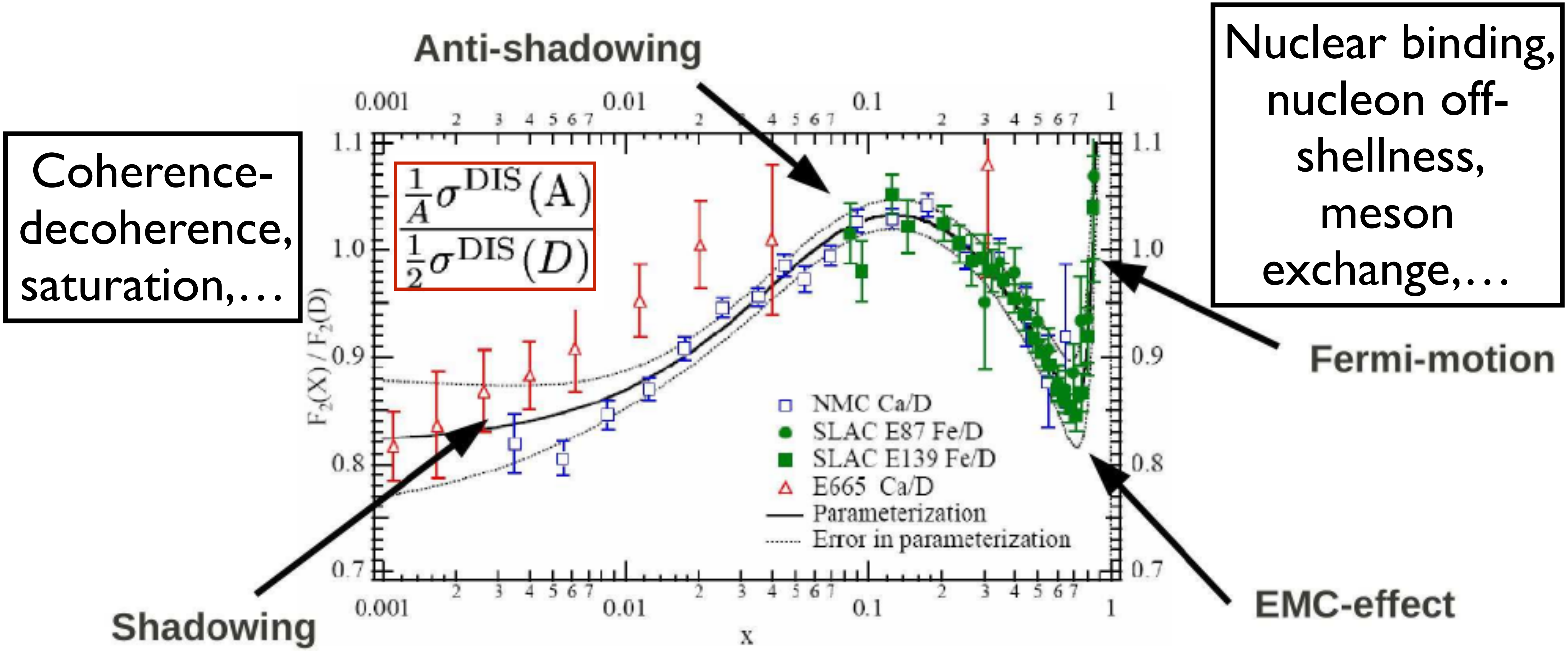

• Bound nucleon≠free nucleon: search for process independent nPDFs that realise this condition in collinear factorisation.

$$\sigma_{\rm DIS}^{\ell+A\to\ell+X} = \sum_{i=q,\bar{q},g} f_i^A(\mu^2)\otimes\hat{\sigma}_{\rm DIS}^{\ell+i\to\ell+X}(\mu^2)$$

Nuclear PDFs, obeying the standard DGLAP

Usual perturbative coefficient functions

nPDFs in HI data:

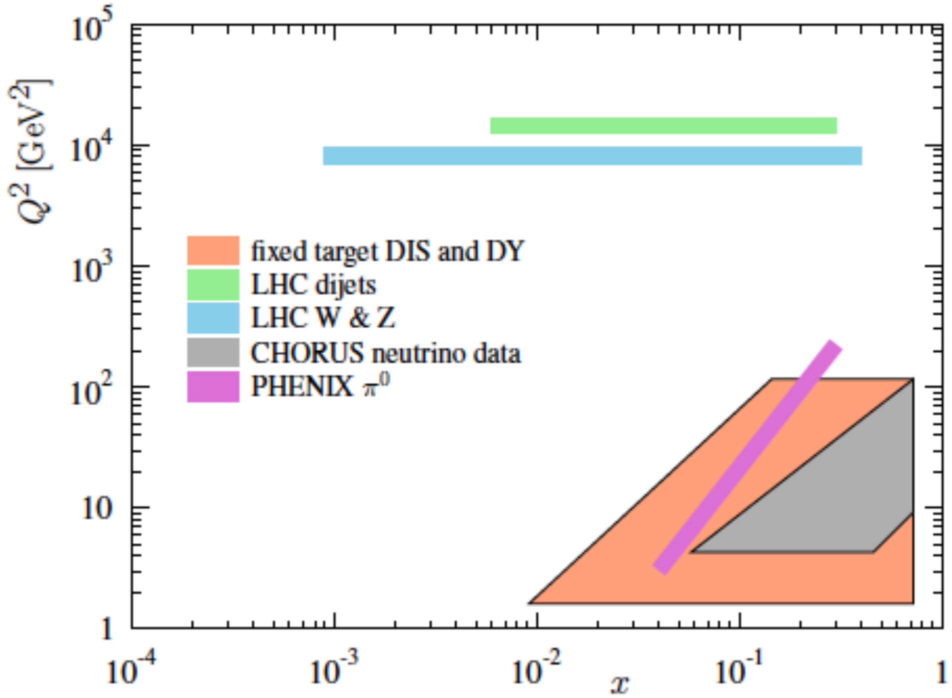

- Lack of data ⇒ large uncertainties for the nuclear PDFs at small scales and x: problem for benchmarking in HIC in order to extract 'medium' parameters.

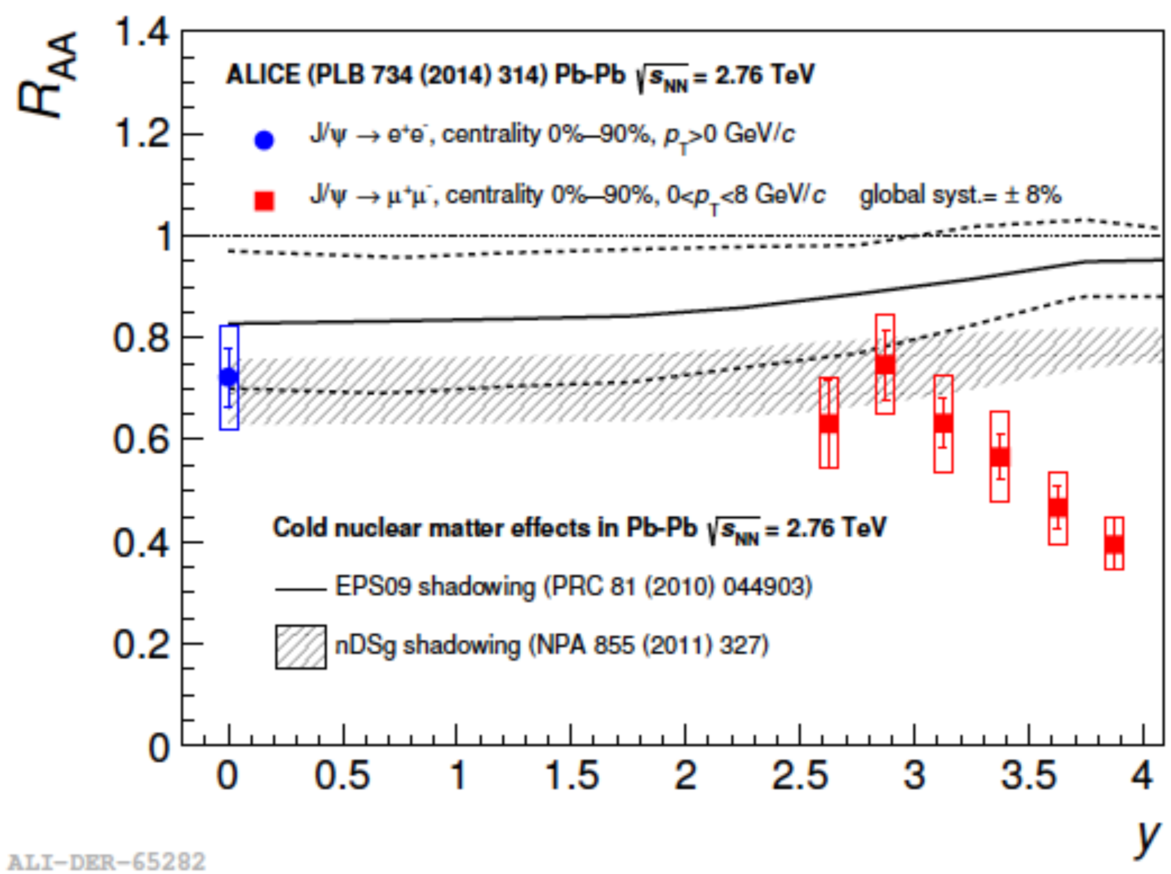

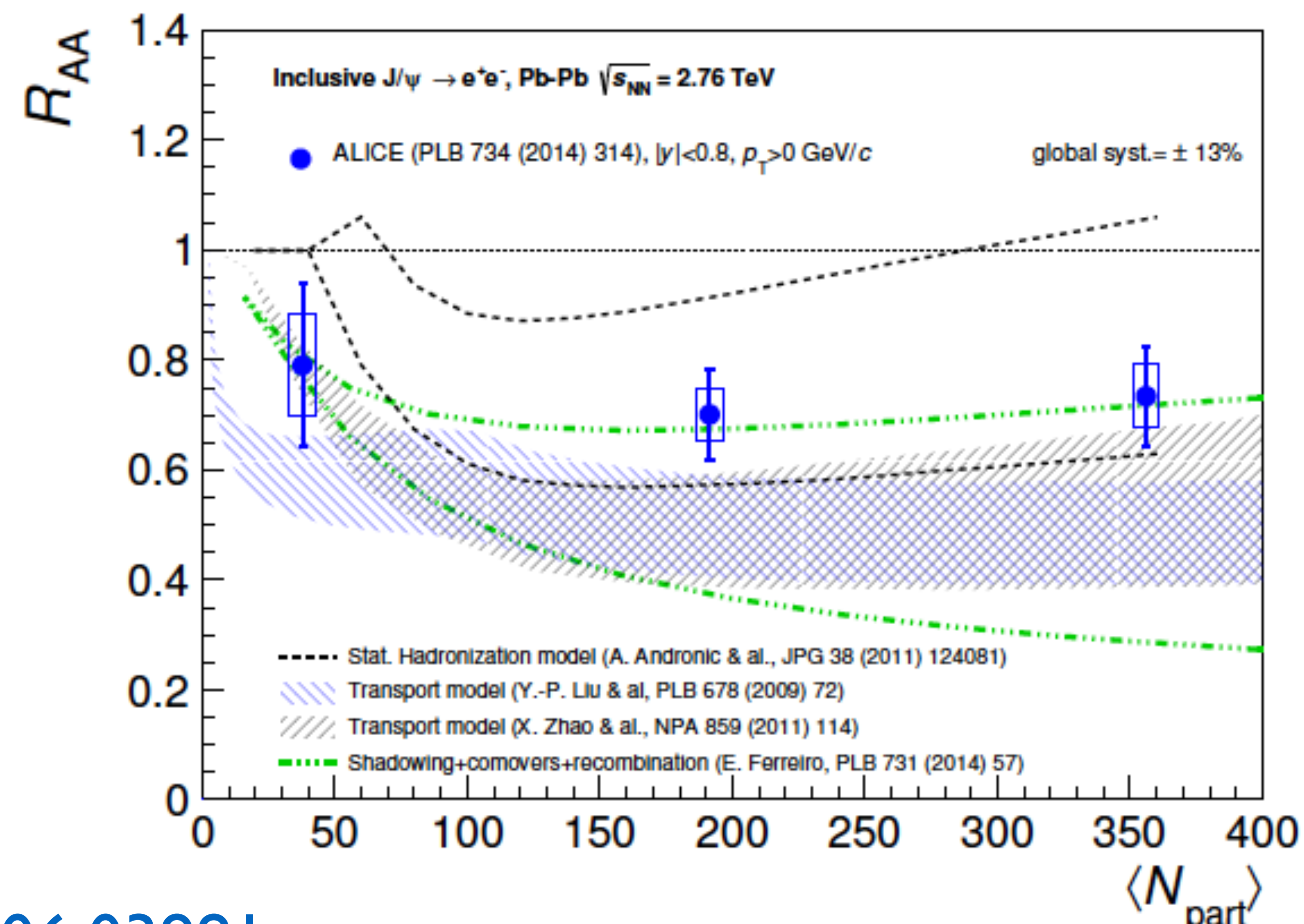

1506.03981

Procedure of extraction:

PDFs, or nuclear effects on them, parametrised at initial scale $Q_0 \gg \Lambda_{QCD}$ employing sum rules (parametrisation biases)

Procedure of extraction:

PDFs, or nuclear effects on them, parametrised at initial scale $Q_0 \gg \Lambda_{QCD}$ employing sum rules (parametrisation biases)

DGLAP evolution, available up to NNLO

PDFs at all required scales

Procedure of extraction:

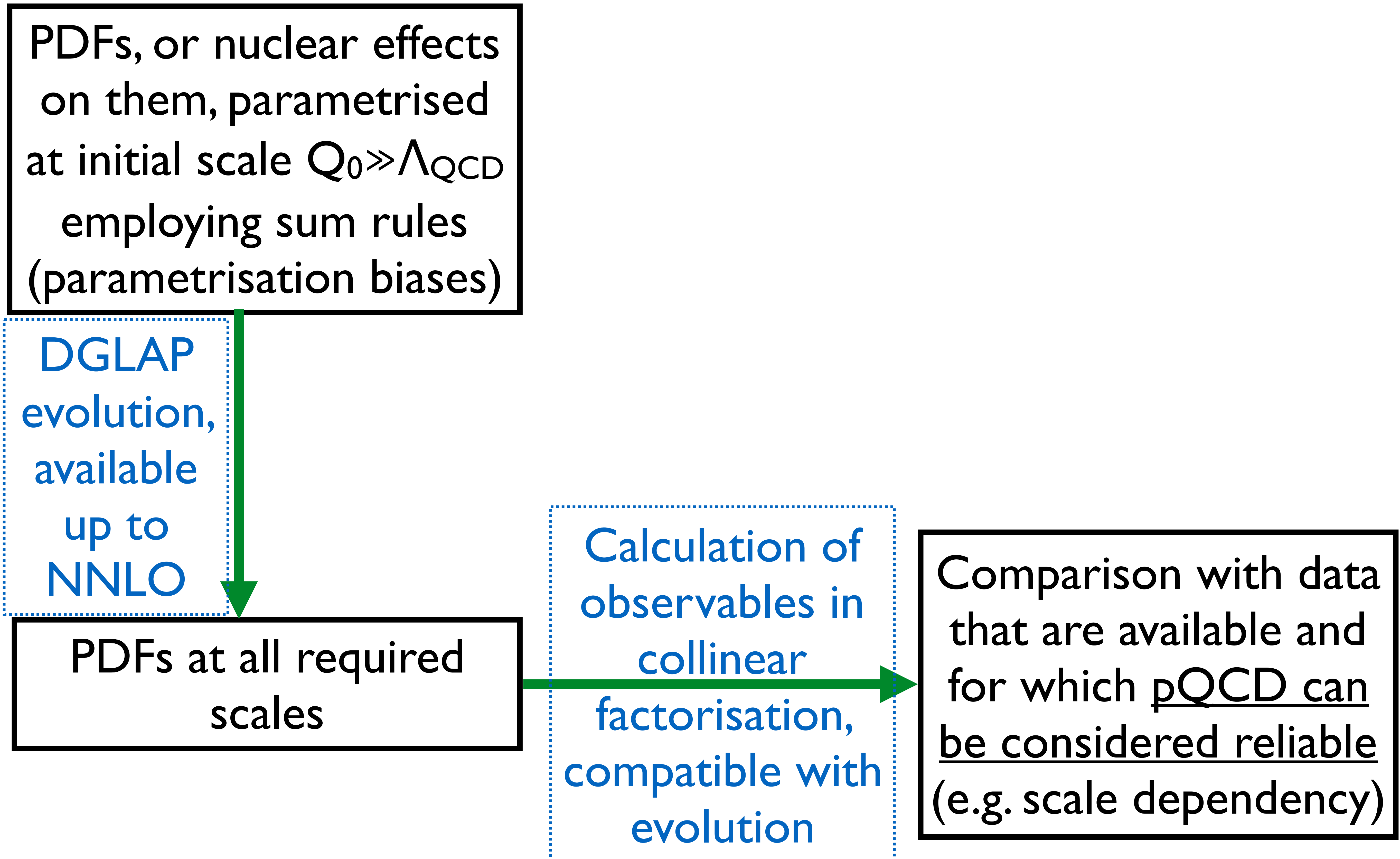

Procedure of extraction:

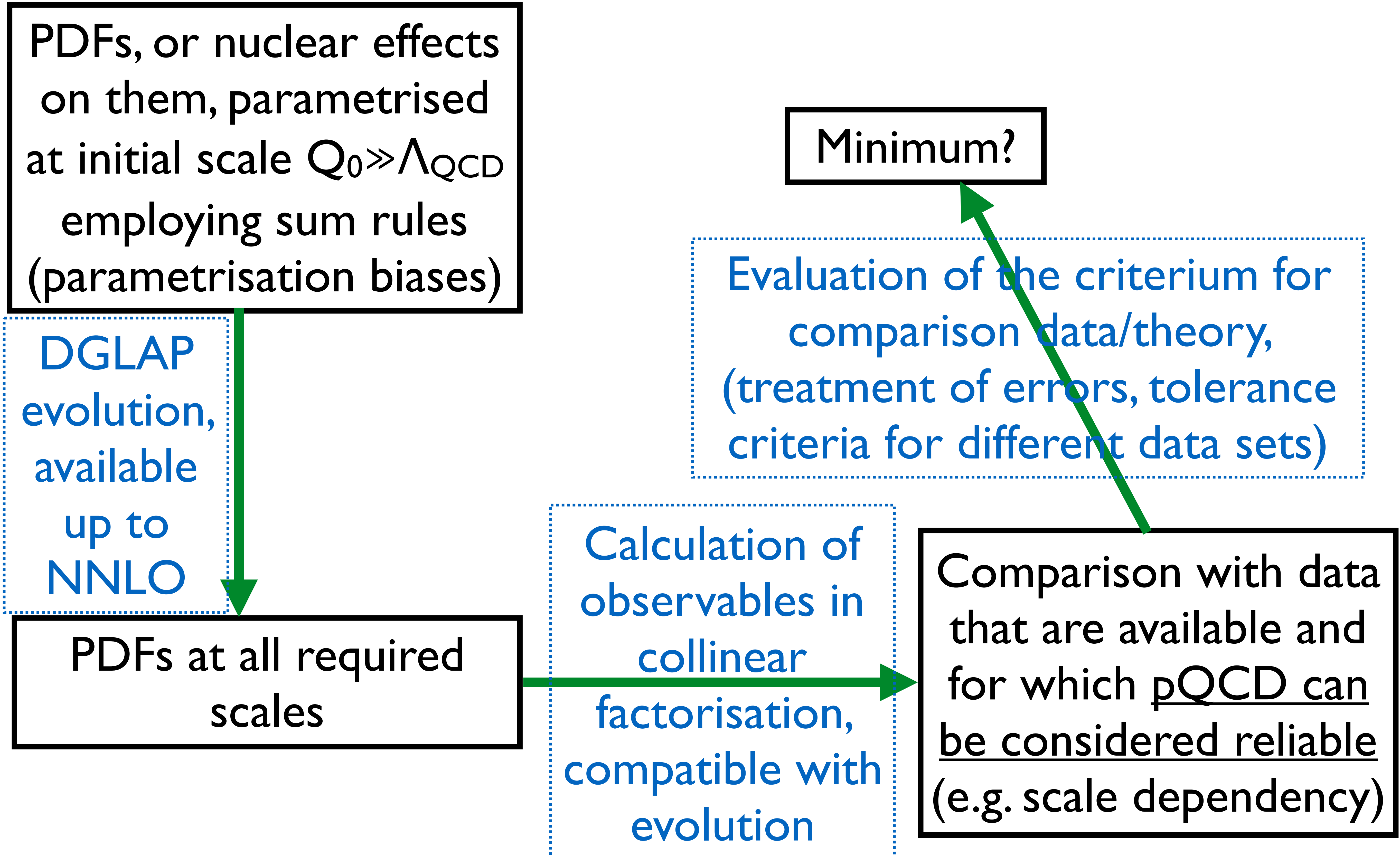

Procedure of extraction:

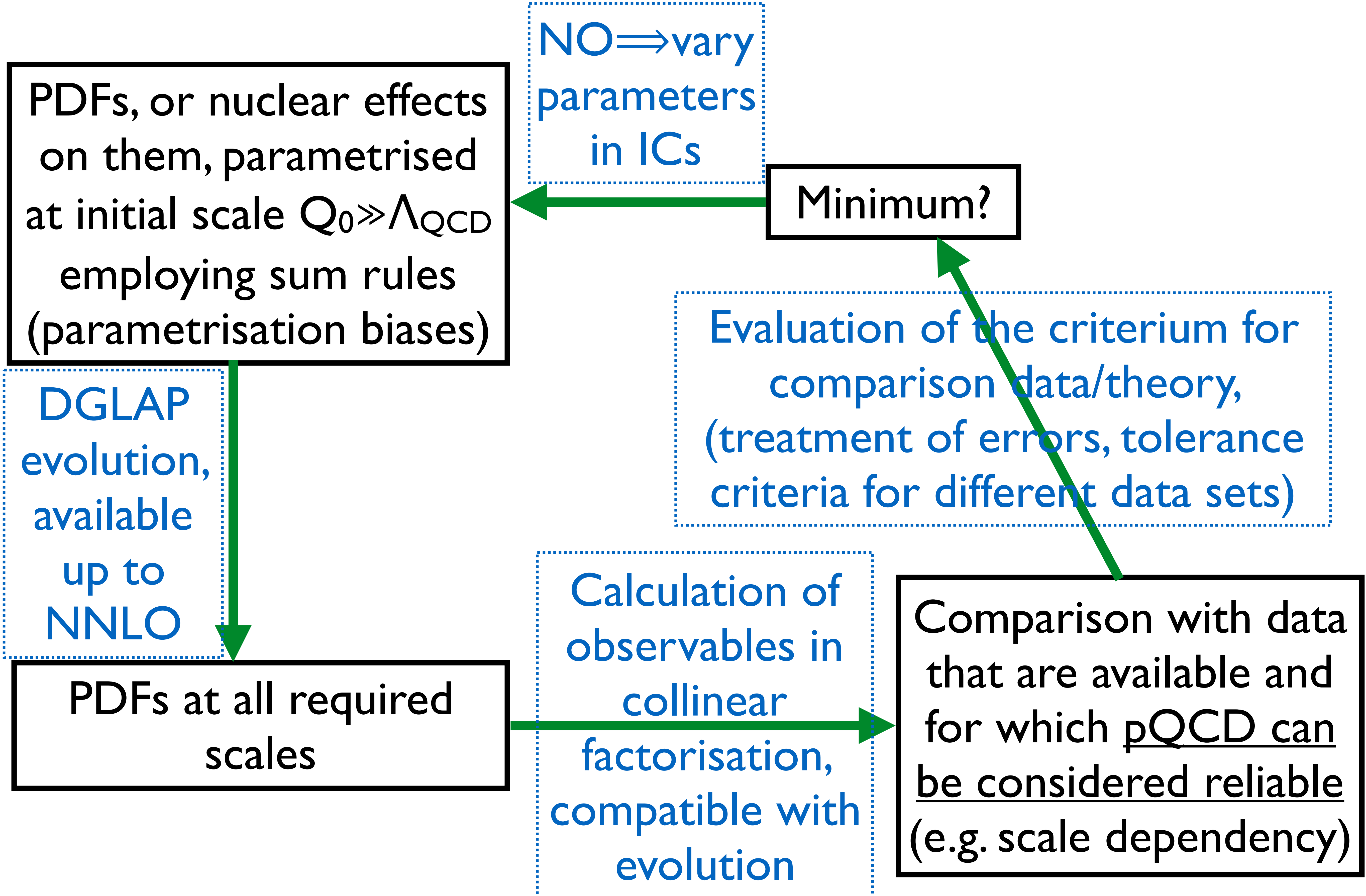

Procedure of extraction:

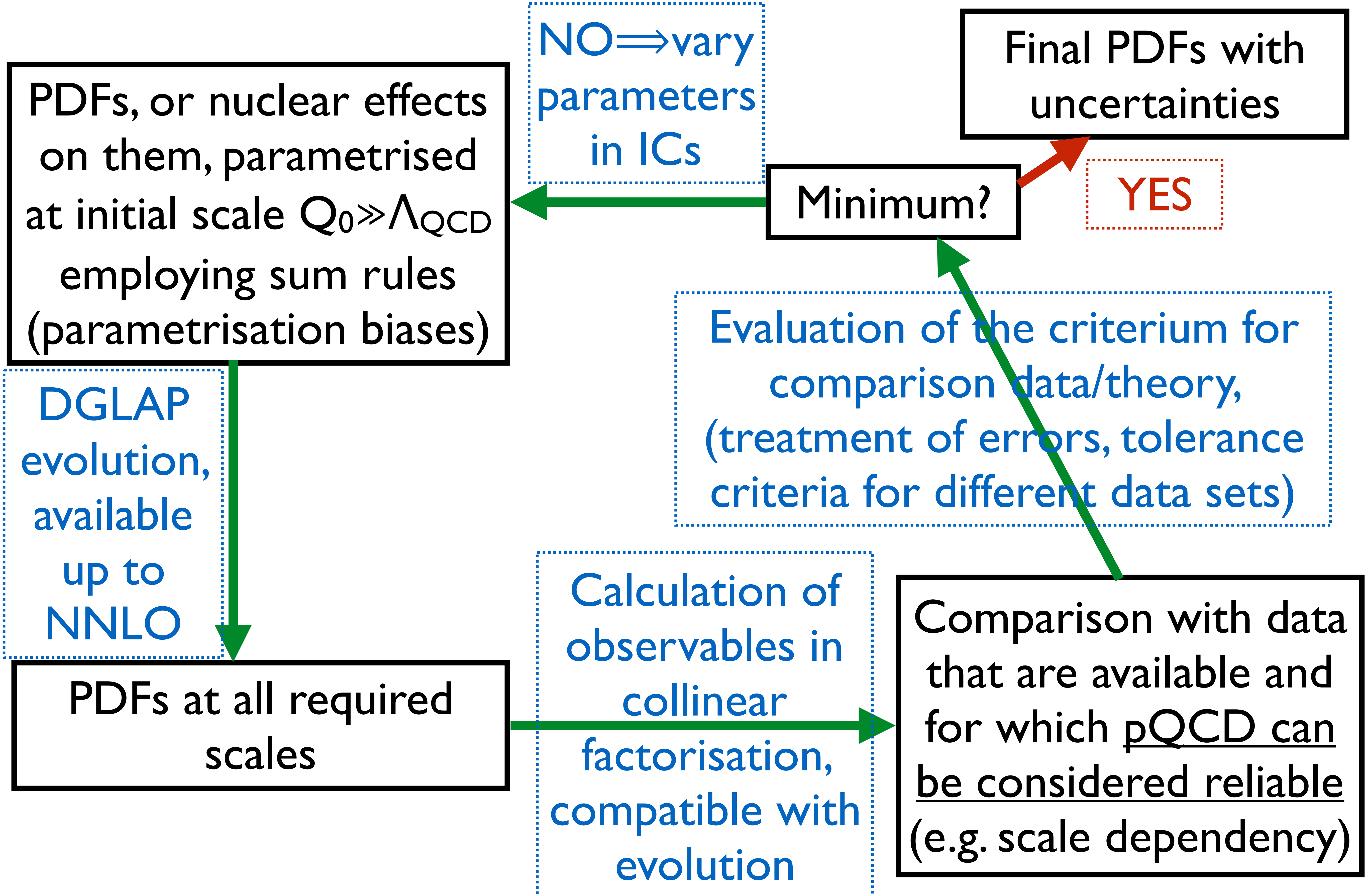

Procedure of extraction:

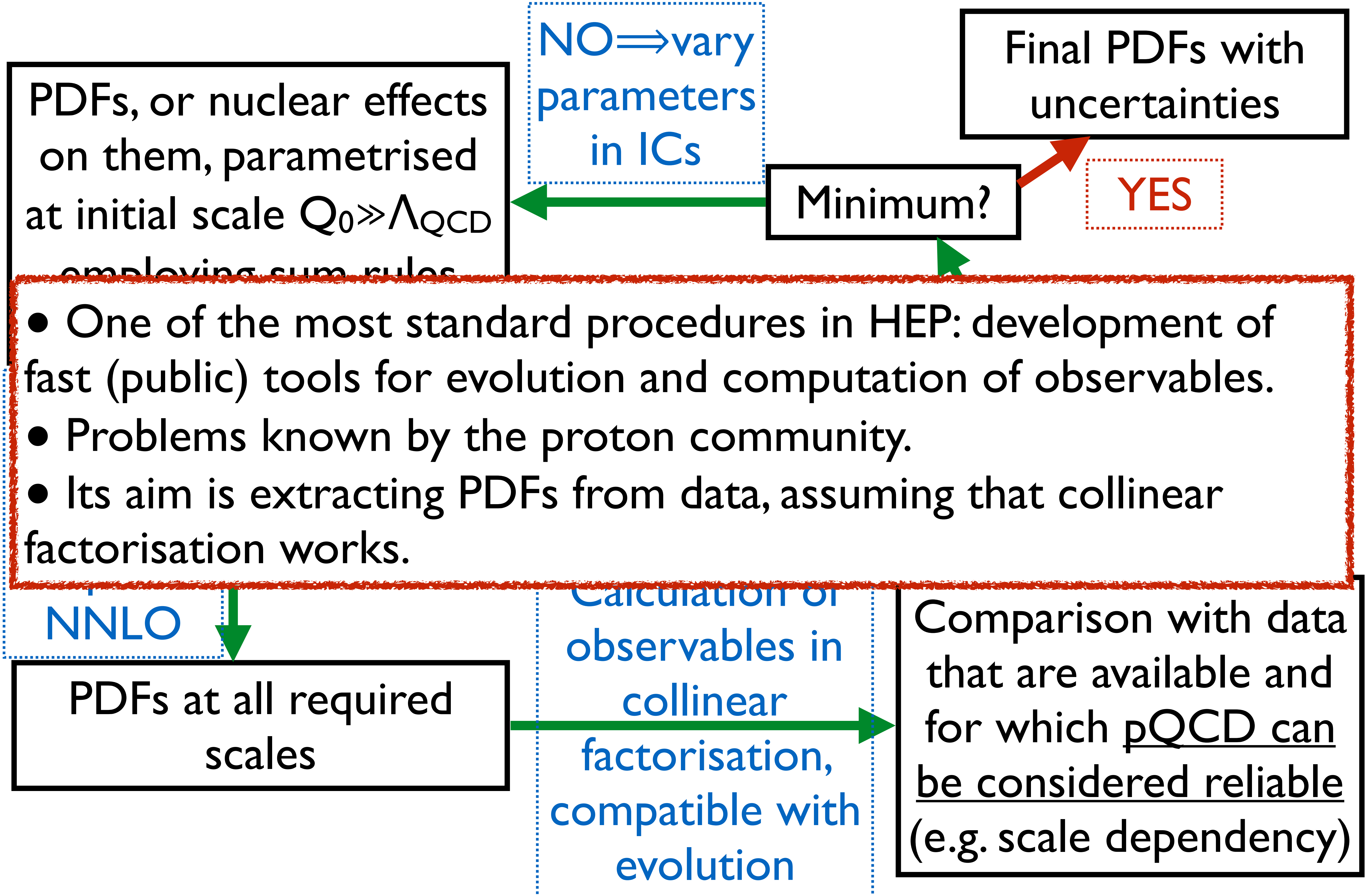

- One of the most standard procedures in HEP: development of fast (public) tools for evolution and computation of observables.
- Problems known by the proton community.
- Its aim is extracting PDFs from data, assuming that collinear factorisation works.

nPDFs at present:

SET		**HKN07** PRC76 (2007) 065207	**EPS09** JHEP 0904 (2009) 065	**DSSZ** PRD85 (2012) 074028	**nCTEQ15** PRD93 (2016) 085037	**KA15** PRD93 (2016) 014036	**EPPS16** EPJC C77 (2017)163
data	eDIS	✔	✔	✔	✔	✔	✔
	DY	✔	✔	✔	✔	✔	✔
	π^0	✘	✔	✔	✔	✘	✔
	νDIS	✘	✘	✔	✘	✘	✔
	pPb	✘	✘	✘	✘	✘	✔
# data		1241	929	1579	740	1479	1811
order		NLO	NLO	NLO	NLO	NNLO	NLO
proton PDF		MRST98	CTEQ6.1	MSTW2008	~CTEQ6.1	JR09	CT14NLO
mass scheme		ZM-VFNS	ZM-VFNS	GM-VFNS	GM-VFNS	ZM-VFNS	GM-VFNS
comments		$\Delta\chi^2$=13.7, ratios, no EMC for gluons	$\Delta\chi^2$=50, ratios, huge shadowing-antishadowing	$\Delta\chi^2$=30, ratios, medium-modified FFs for π^0	$\Delta\chi^2$=35, PDFs, flavour sep., not enough sensitivity	PDFs, deuteron data included	$\Delta\chi^2$=52, ratios, LHC pPb data

nPDFs at present:

SET		HKN07 PRC76 (2007) 065207	EPS09 JHEP 0904 (2009) 065	DSSZ PRD85 (2012) 074028	nCTEQ15 PRD93 (2016) 085037	KA15 PRD93 (2016) 014036	EPPS16 EPJC C77 (2017)163
data	eDIS	✔	✔	✔	✔	✔	✔
				✔	✔	✔	✔
				✔	✔	✘	✔
				✔	✘	✘	✔
				✘	✘	✘	✔
#				1579	740	1479	1811
o				NLO	NLO	NNLO	NLO
pr P				MSTW2008	~CTEQ6.1	JR09	CT14NLO
mass scheme		ZM-VFNS	ZM-VFNS	GM-VFNS	GM-VFNS	ZM-VFNS	GM-VFNS
comments		$\Delta\chi^2$=13.7, ratios, no EMC for gluons	$\Delta\chi^2$=50, ratios, huge shadowing-antishadowing	$\Delta\chi^2$=30, ratios, medium-modified FFs for π^0	$\Delta\chi^2$=35, PDFs, flavour sep., not enough sensitivity	PDFs, deuteron data included	$\Delta\chi^2$=52, ratios, LHC pPb data

- Centrality dependence (EPS09s) not from data but from the A-dependence of the parameters.
- Several models provide it: Vogt et al., FGS, Ferreiro et al.,…

nPDFs at present:

- nCTEQ15 vs. EPPS16: beware of the parametrisation bias.

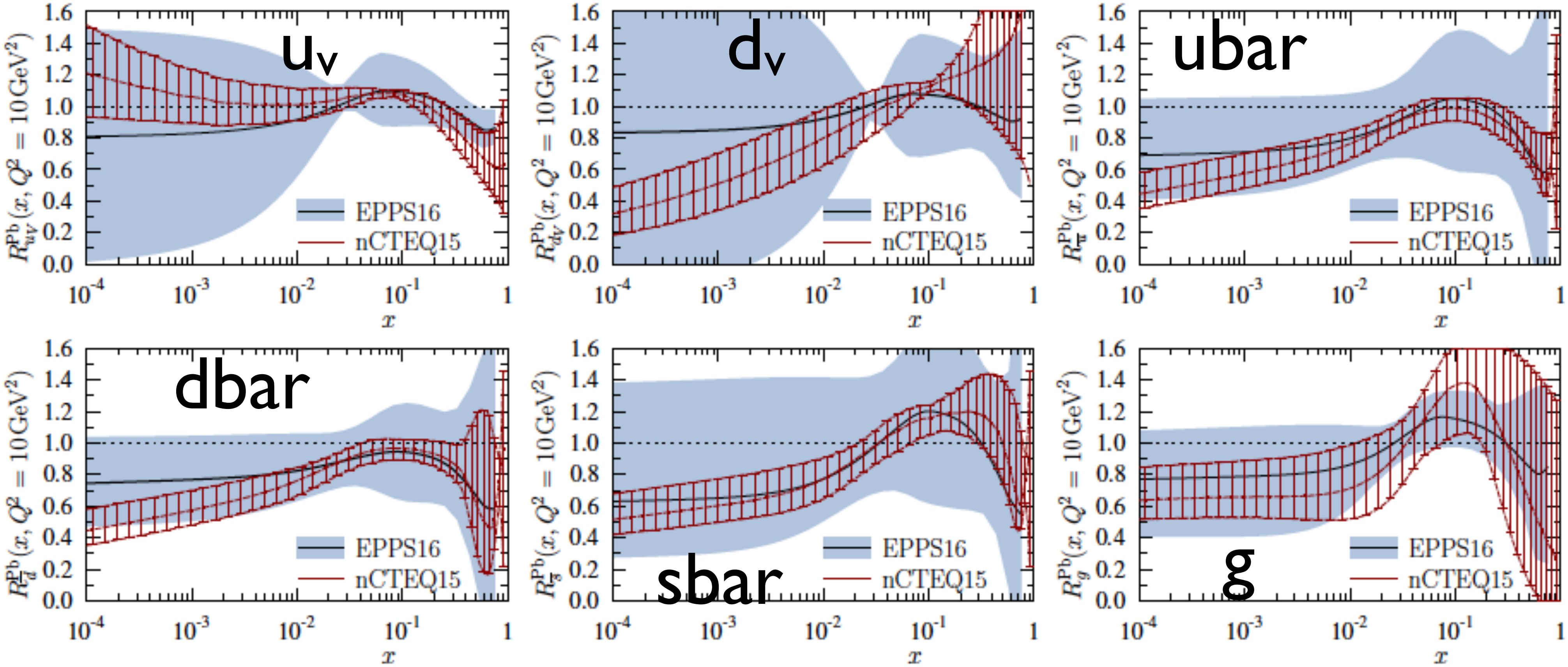

- Presently available LHC data seem not to have a large effect.

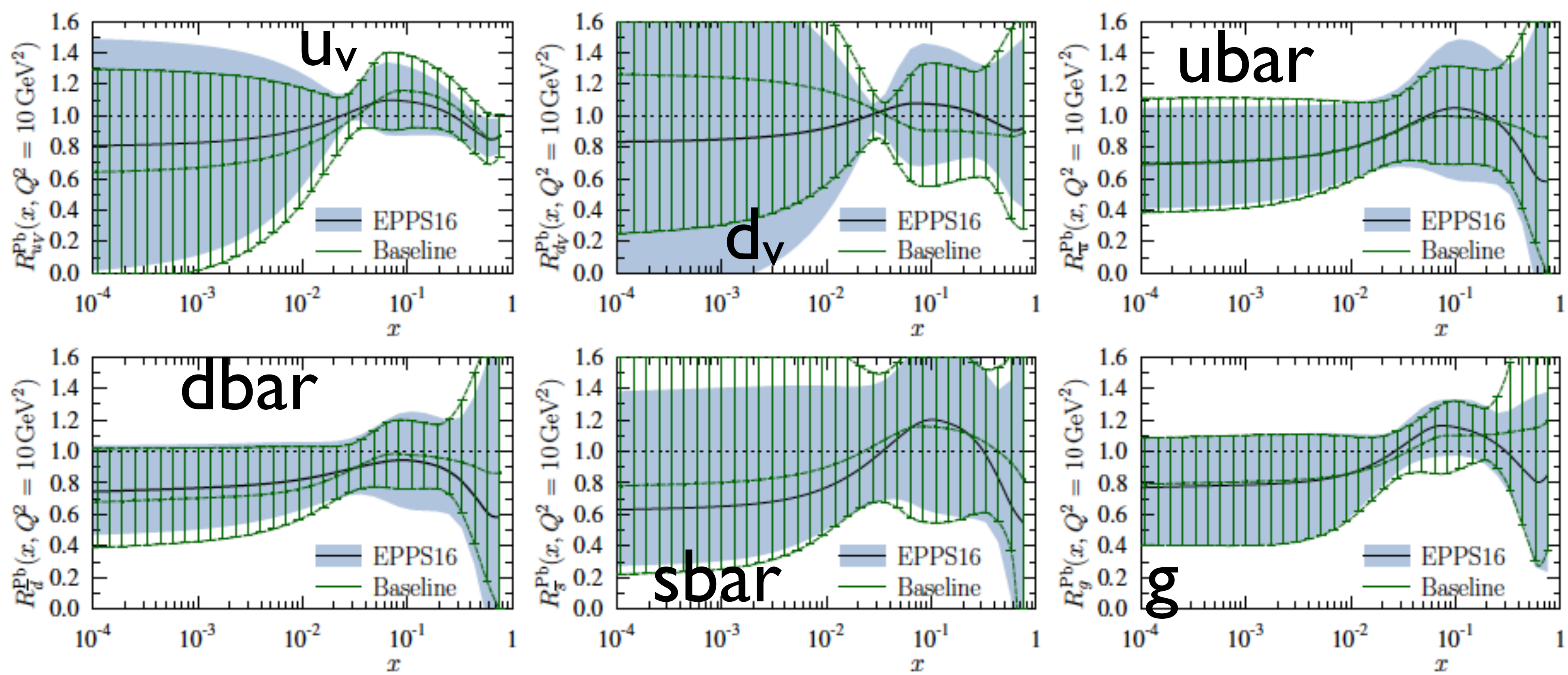

nPDFs at present:

- nCTEQ15 vs. EPPS16: beware of the parametrisation bias.

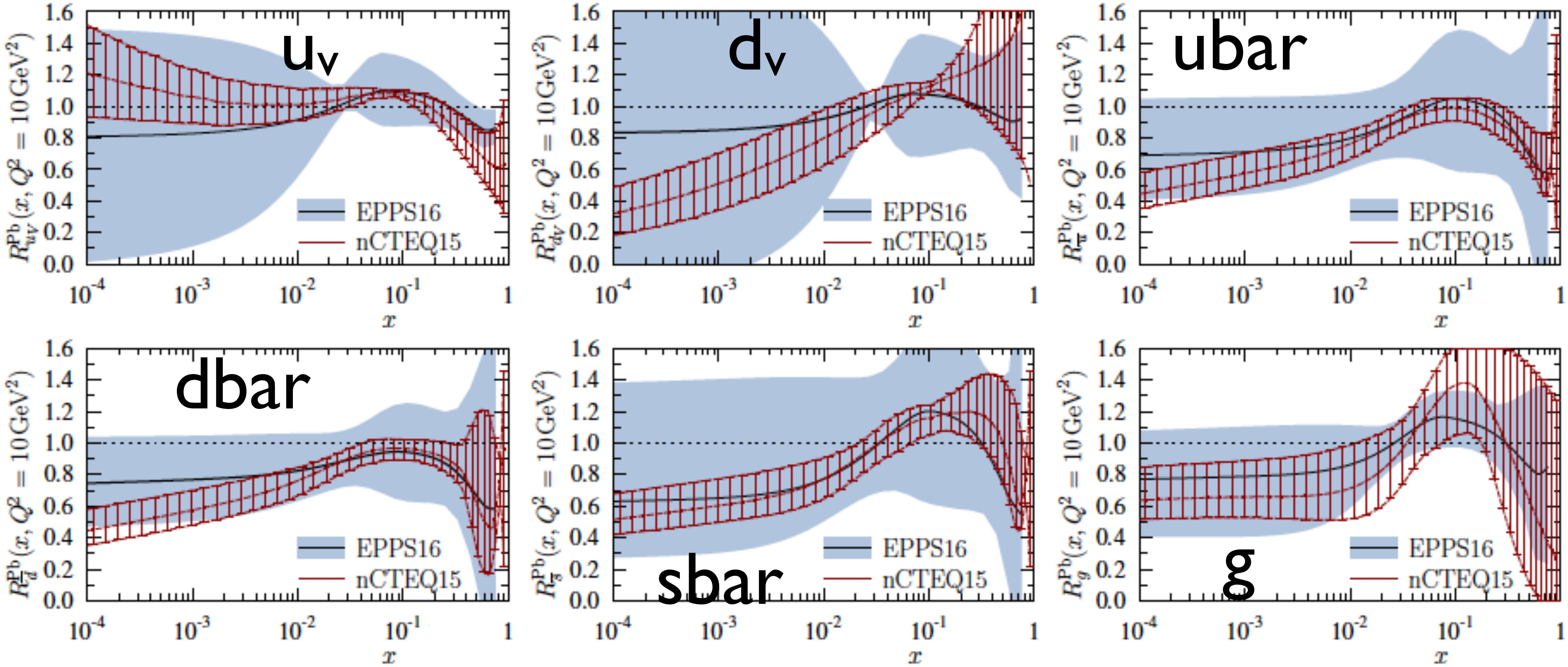

- P
ava
data seem not to have a large effect.

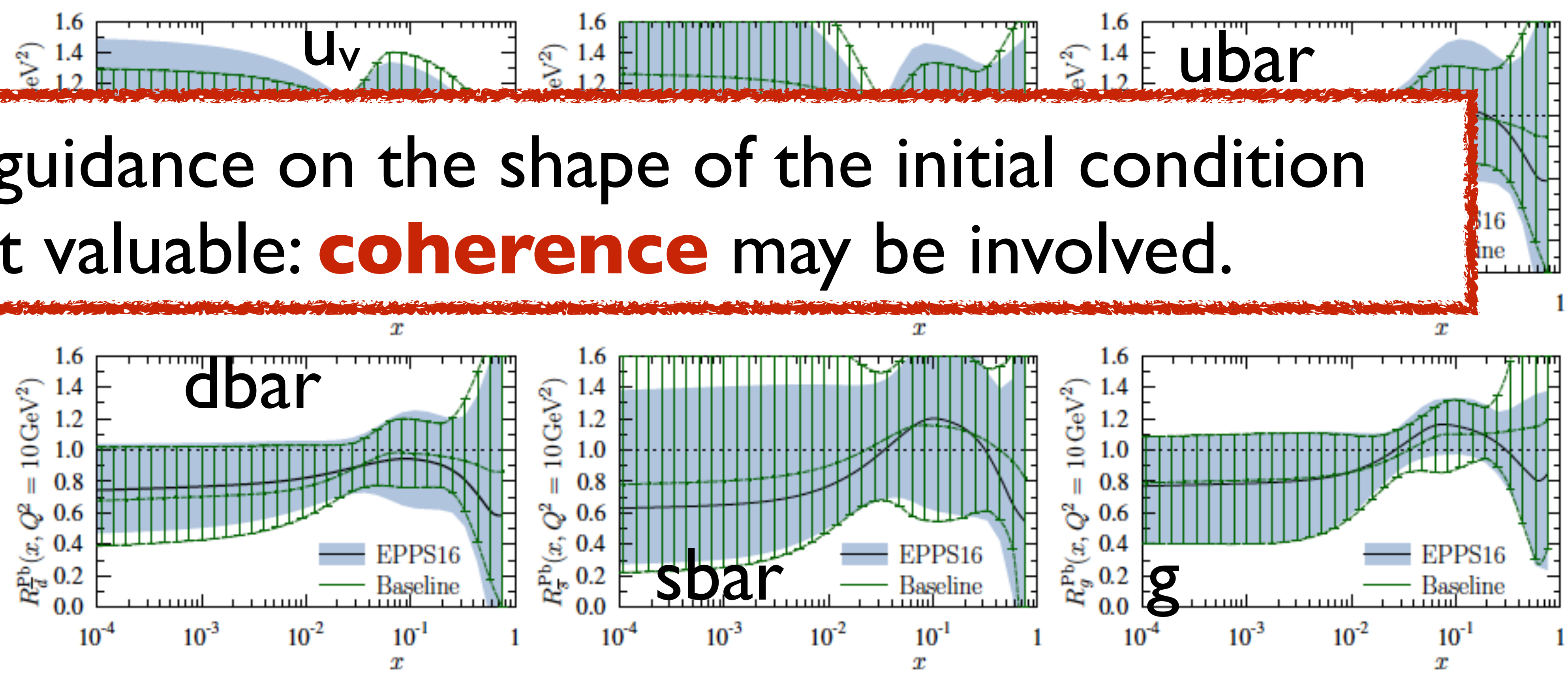

- Theoretical guidance on the shape of the initial condition would be most valuable: **coherence** may be involved.

Coherence: two scattering case

$$\mathrm{i}t\,(q=0)=\mathrm{i}t_{\mathrm{forw}}=-\sigma$$

$$\mathrm{i}\mathcal{T}_n(q=0)=-\sigma_A^{(n)}$$

$$q=p'-p$$

$$T_A(x_T)=\int_{-\infty}^{+\infty}\mathrm{d}x_+\,\rho_A(x_+,x_T)$$

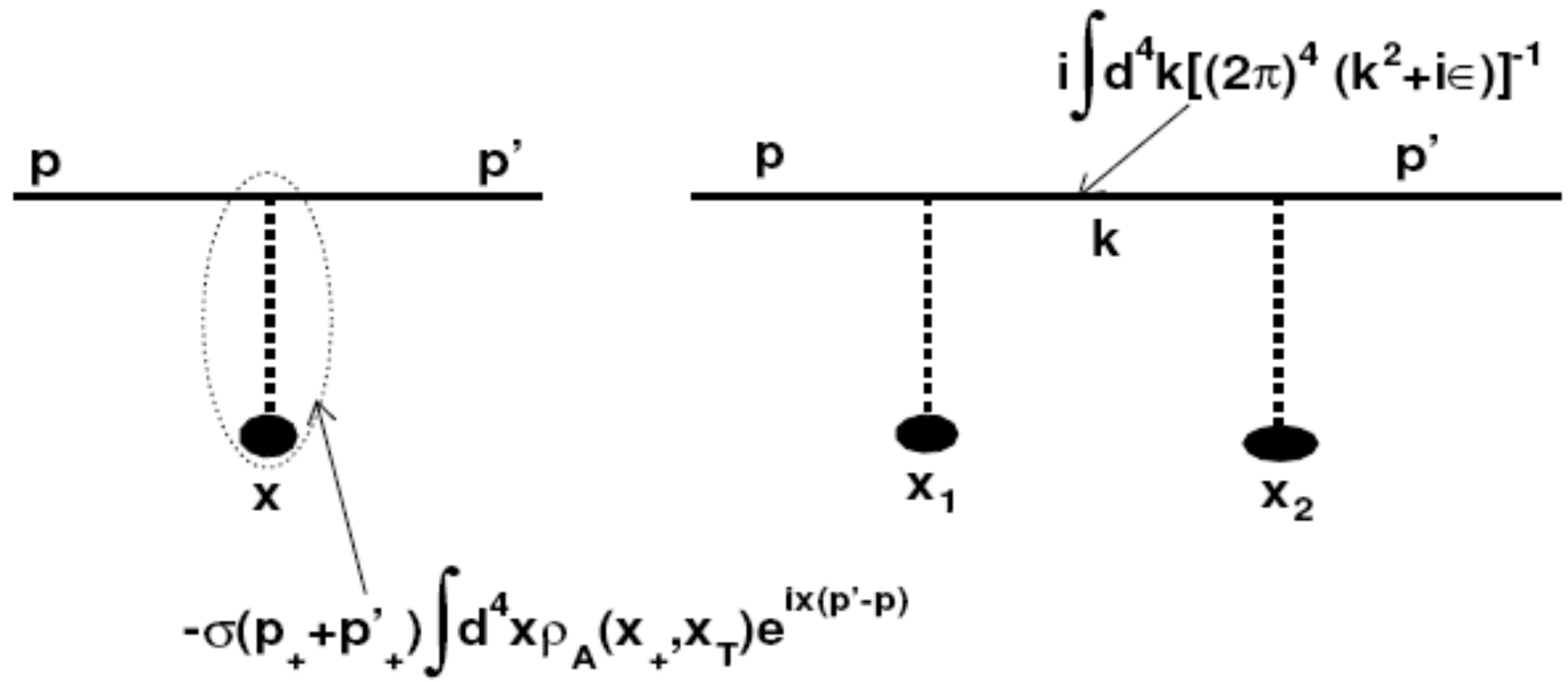

$$c(p_+,p'_+)\mathrm{i}\mathcal{T}_1(q)=\mathrm{i}t_{\mathrm{forw}}c(p_+,p'_+)A\int\mathrm{d}^2x_T\,T_A(x_T)\,\mathrm{e}^{-\mathrm{i}x_T\cdot(p'_T-p_T)}\quad\Rightarrow\quad\sigma_A^1=A\sigma$$

$$c(p_+,p'_+)\mathrm{i}\mathcal{T}_2(q)=c(p_+,p'_+)A(A-1)(\mathrm{i}t_{\mathrm{forw}})^2$$
$$\times\int\frac{\mathrm{d}^2k_T}{(2\pi)^2}\mathrm{d}x_{1+}\,\mathrm{d}x_{2+}\,\mathrm{d}^2x_{1T}\,\mathrm{d}^2x_{2T}\exp\left(-\mathrm{i}k_T^2(x_{2+}-x_{1+})/(2p_+)\right)$$
$$\times\exp(-\mathrm{i}[x_{1T}\cdot(k_T-p_T)+x_{2T}\cdot(p'_T-k_T)])\rho_A(x_{1+},x_{1T})$$
$$\times\rho_A(x_{2+},x_{2T})\theta(x_{2+}-x_{1+})$$

Coherence: two scattering case

$$it(q=0) = it_{\text{forw}} = -\sigma$$

$$i\mathcal{T}_n(q=0) = -\sigma_A^{(n)}$$

$$q = p' - p$$

$$T_A(x_T) = \int_{-\infty}^{+\infty} dx_+ \, \rho_A(x_+, x_T)$$

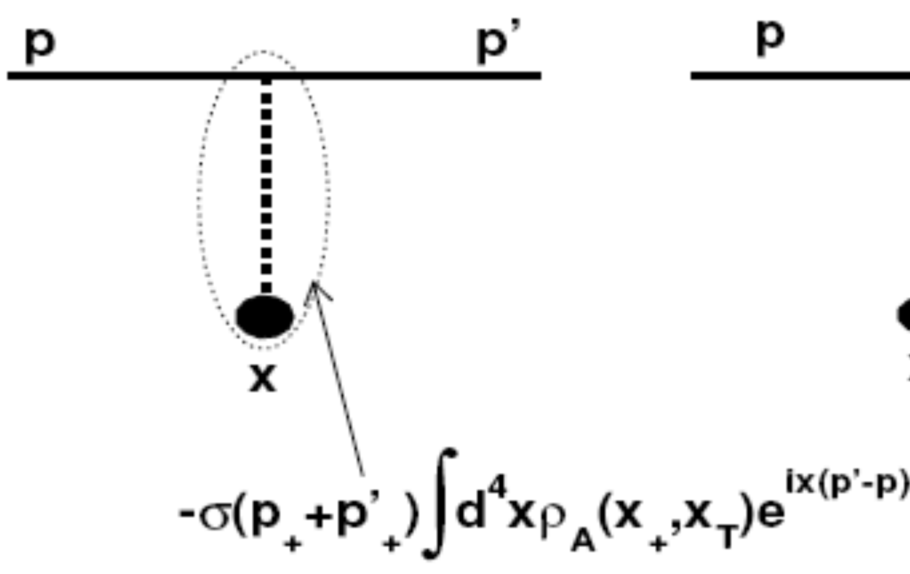

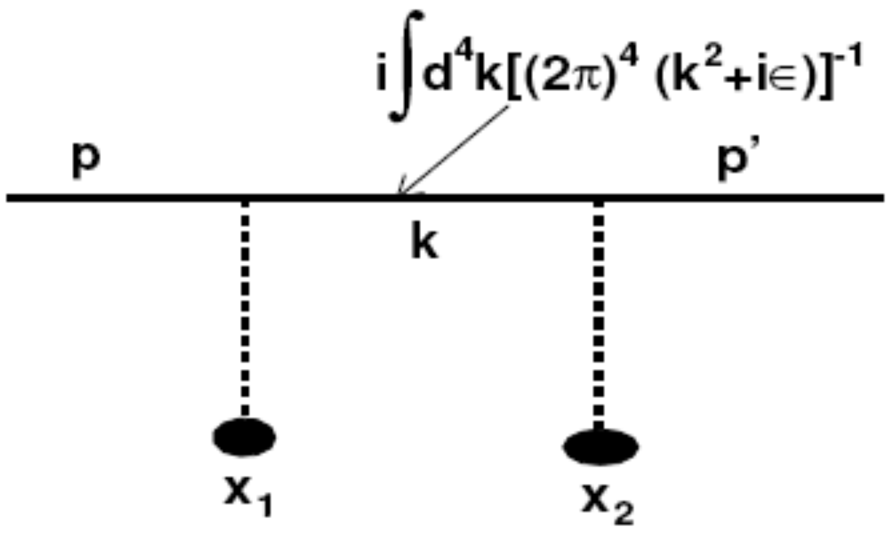

$$c(p_+, p'_+) i\mathcal{T}_1(q) = it_{\text{forw}} c(p_+, p'_+) A \int d^2x_T \, T_A(x_T) \, e^{-ix_T\cdot(p'_T - p_T)} \quad \Rightarrow \quad \sigma_A^1 = A\sigma$$

non-eikonal phase

$$\begin{aligned} c(p_+, p'_+) i\mathcal{T}_2(q) = &\; c(p_+, p'_+) A(A-1)(it_{\text{forw}})^2 \\ &\times \int \frac{d^2k_T}{(2\pi)^2} dx_{1+} \, dx_{2+} \, d^2x_{1T} \, d^2x_{2T} \exp\left(-ik_T^2(x_{2+} - x_{1+})/(2p_+)\right) \\ &\times \exp(-i[x_{1T}\cdot(k_T - p_T) + x_{2T}\cdot(p'_T - k_T)]) \rho_A(x_{1+}, x_{1T}) \\ &\times \rho_A(x_{2+}, x_{2T}) \theta(x_{2+} - x_{1+}) \end{aligned}$$

Coherence length, shadowing:

$$\exp\left[-\mathrm{i}k_T^2(x_{2+}-x_{1+})/(2p_+)\right] = \exp\left[-\mathrm{i}(x_{2+}-x_{1+})/l_c\right], \text{ with } l_c = 2p_+/k_T^2$$

A) $p_+ \to 0$ $\qquad \mathrm{i}\mathcal{T}_2(q) \to 0$

B) $p_+ \to \infty, \exp\left[-\mathrm{i}(x_{2+}-x_{1+})/l_c\right] \to 1$

$$\mathrm{i}\mathcal{T}_2(q) = \frac{A(A-1)}{2}(\mathrm{i}t_{\mathrm{forw}})^2 \int \mathrm{d}^2x_T\, \mathrm{e}^{-\mathrm{i}x_T\cdot(p'_T-p_T)} T_A^2(x_T),$$

$$\sigma_A^{(2)} = -\frac{A(A-1)}{2}\int \mathrm{d}^2x_T [T_A(x_T)\sigma]^2$$

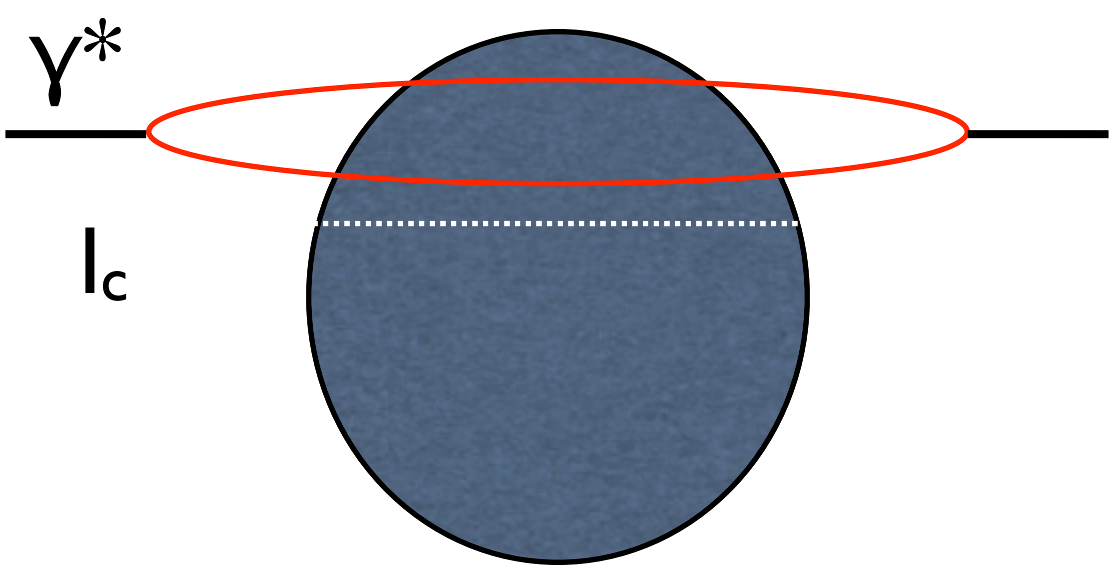

The lifetime of the qqbar fluctuation is $\geq R_A$ for $x \leq 0.1A^{-1/3}$.

$$\tau \sim \frac{1}{Q}\times\frac{E_{\mathrm{lab}}}{Q} \simeq \frac{W^2}{2m_{\mathrm{nucleon}}Q^2} \simeq \frac{1}{2m_{\mathrm{nucleon}}x}$$

Coherence length, shadowing:

$$\exp\left[-ik_T^2(x_{2+}-x_{1+})/(2p_+)\right] = \exp\left[-i(x_{2+}-x_{1+})/l_c\right], \text{ with } l_c = 2p_+/k_T^2$$

- This simple example leads to shadowing at small x, and to no nuclear effects when the situation becomes incoherent.
- Its generalisation for many scattering in the coherent case leads to the Glauber model; if done for coloured partons, to the Wilson line (with additional high-energy approximation).

$$\sigma_A^{(2)} = -\frac{A(A-1)}{2}\int d^2x_T\,[T_A(x_T)\sigma]^2$$

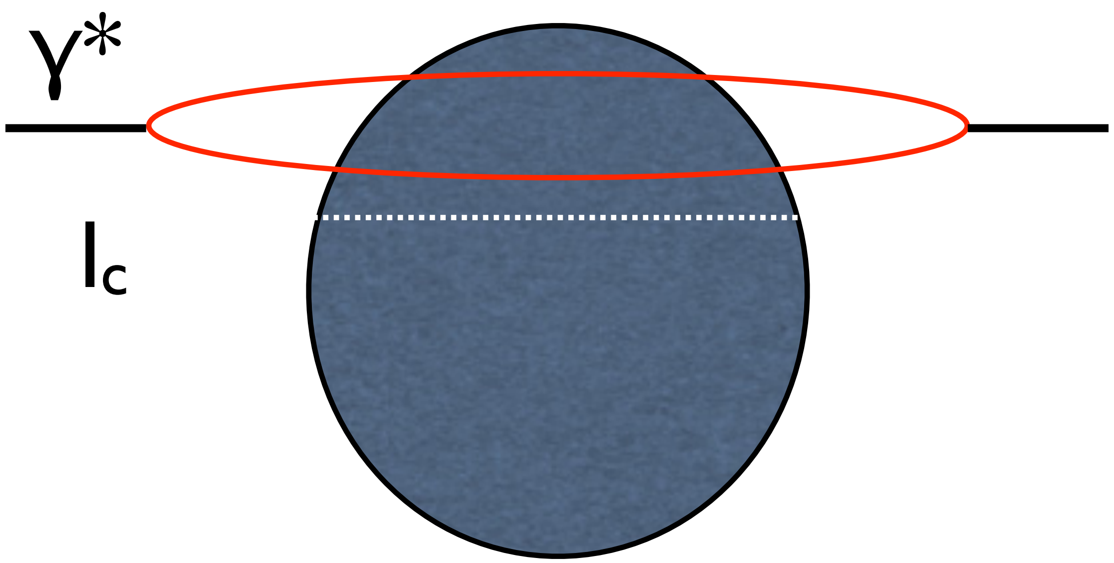

The lifetime of the qqbar fluctuation is $\geq R_A$ for $x \leq 0.1A^{-1/3}$.

$$\tau \sim \frac{1}{Q}\times\frac{E_{\rm lab}}{Q} \simeq \frac{W^2}{2m_{\rm nucleon}Q^2} \simeq \frac{1}{2m_{\rm nucleon}x}$$

Glauber-like rescatterings:

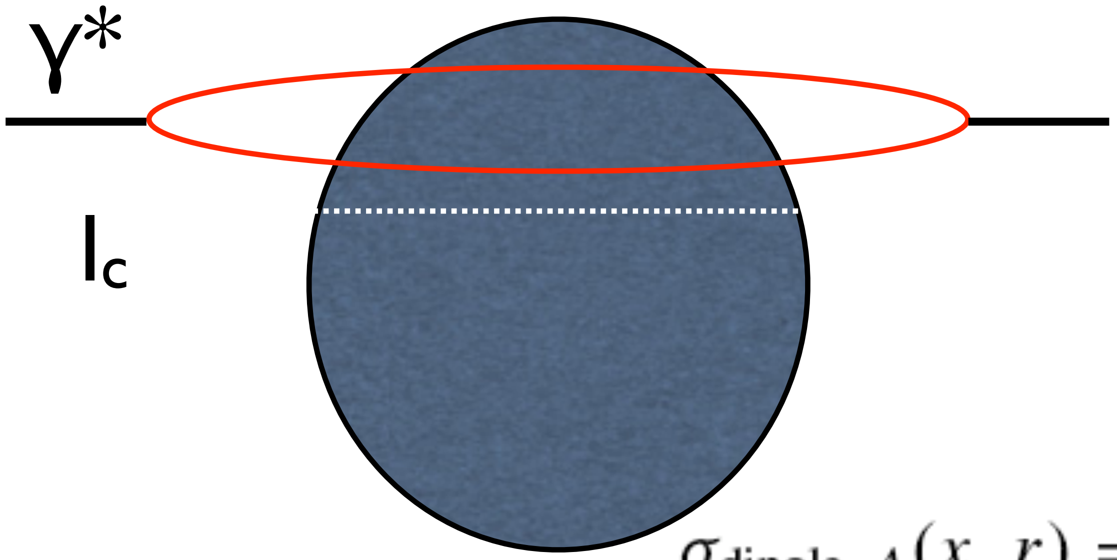

$$\sigma_{\gamma^*\text{-}A}(x, Q^2) = \int d^2r\, \rho(r, Q^2)\sigma_{\text{dipole}-A}(x, r)$$

$$\sigma_{\text{dipole-}A}(x, r) = \int d^2b\, 2\left[1 - \exp\left(-\frac{1}{2}AT_A(b)\sigma_{\text{dipole-nucleon}}(x, r)\right)\right]$$

- This relation is provided by the Glauber model: at fixed impact parameter, total cross section as twice [1 - the S-matrix].

- Almost any model which is successful for the proton works for the nuclear case!!!

Glauber-like rescatterings:

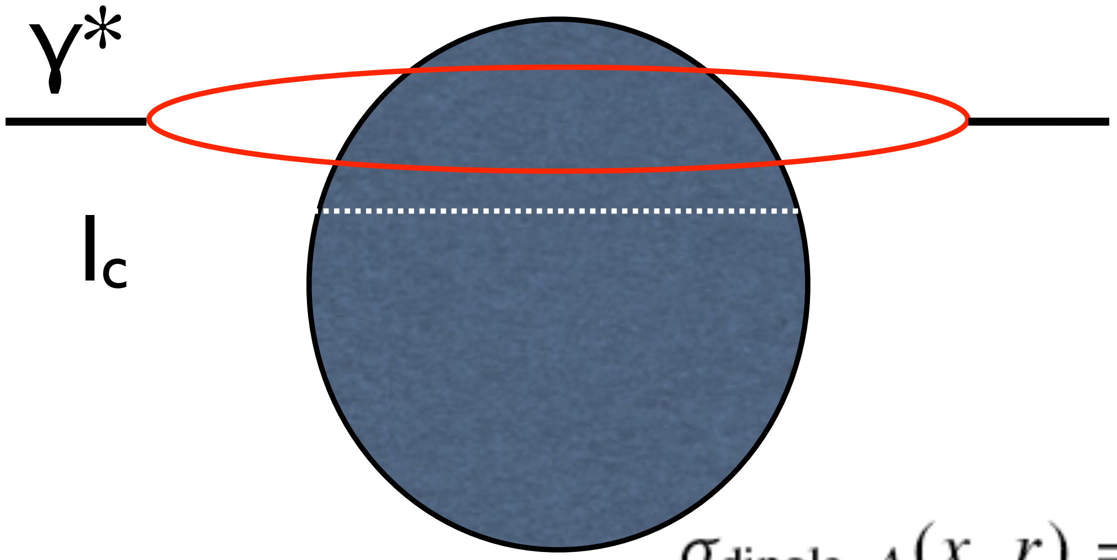

$$\sigma_{\gamma^*\text{-}A}(x,Q^2)=\int d^2r\,\rho(r,Q^2)\sigma_{\text{dipole}-A}(x,r)$$

$$\sigma_{\text{dipole-}A}(x,r)=\int d^2b\,2\left[1-\exp\left(-\frac{1}{2}AT_A(b)\sigma_{\text{dipole-nucleon}}(x,r)\right)\right]$$

- This relation is provided by the Glauber model: at fixed impact parameter, total cross section as twice [1 - the S-matrix].

- Almost any model which is successful for the proton works for the nuclear case!!!

Glauber-like rescatterings:

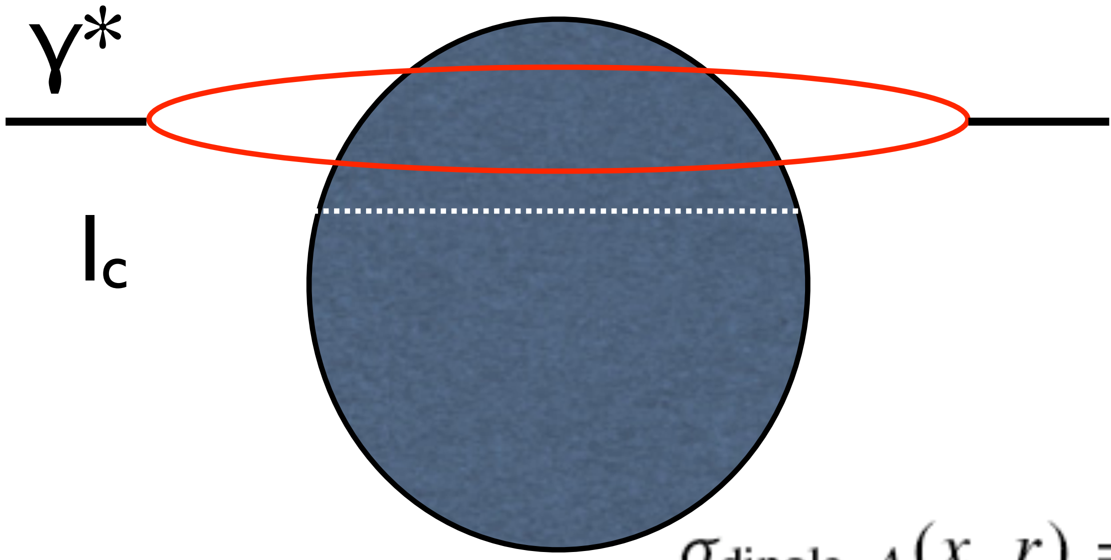

$$\sigma_{\gamma^*\text{-}A}(x, Q^2) = \int d^2r\, \rho(r, Q^2)\sigma_{\mathrm{dipole}-A}(x, r)$$

$$\sigma_{\mathrm{dipole}\text{-}A}(x, r) = \int d^2b\, 2\left[1 - \exp\left(-\frac{1}{2}AT_A(b)\sigma_{\mathrm{dipole}\text{-}\mathrm{nucleon}}(x, r)\right)\right]$$

- This relation is provided by the Glauber model: at fixed impact parameter, total cross section as twice [1 - the S-matrix].

- Almost any model which is successful for the proton works for the nuclear case!!!

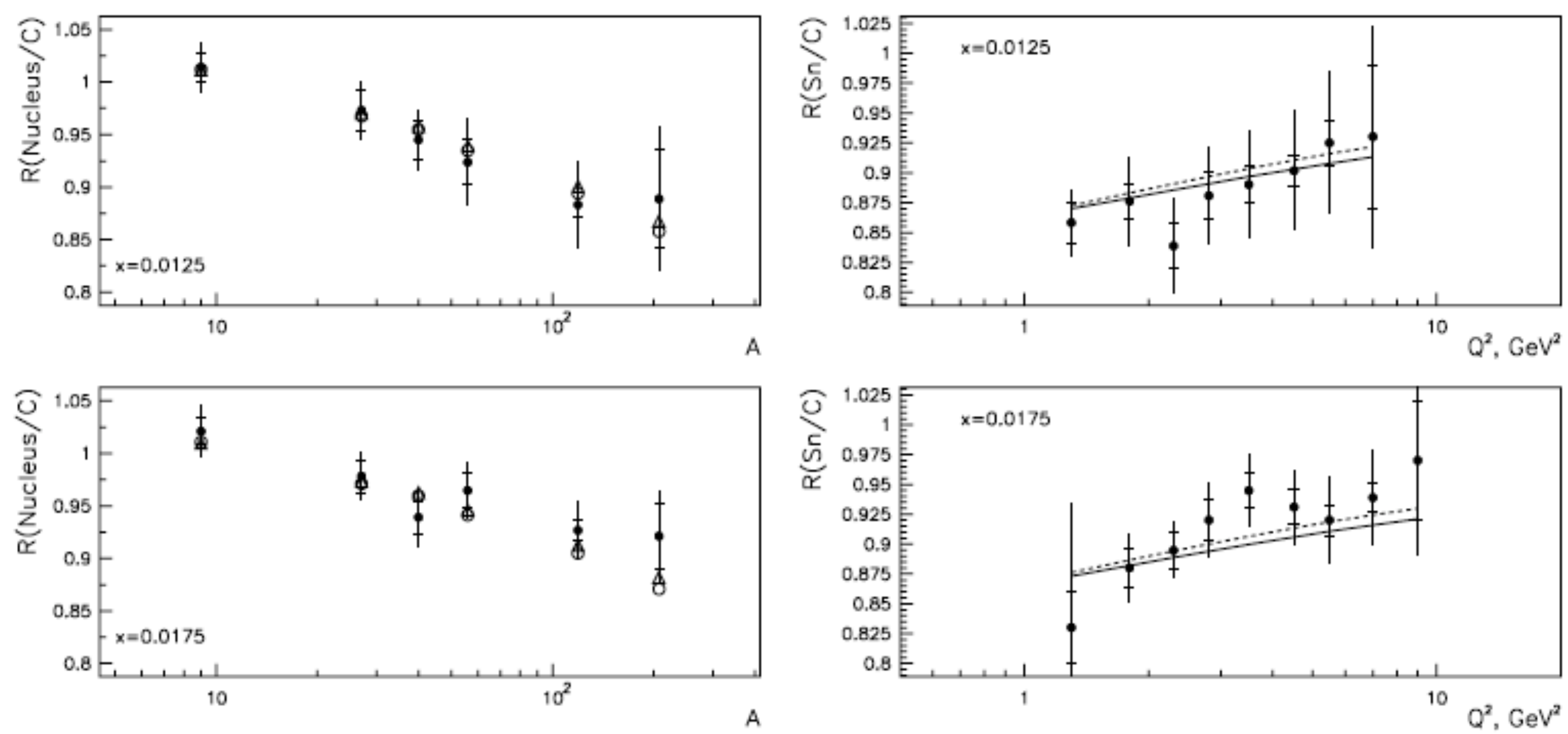

Gribov inelastic shadowing:

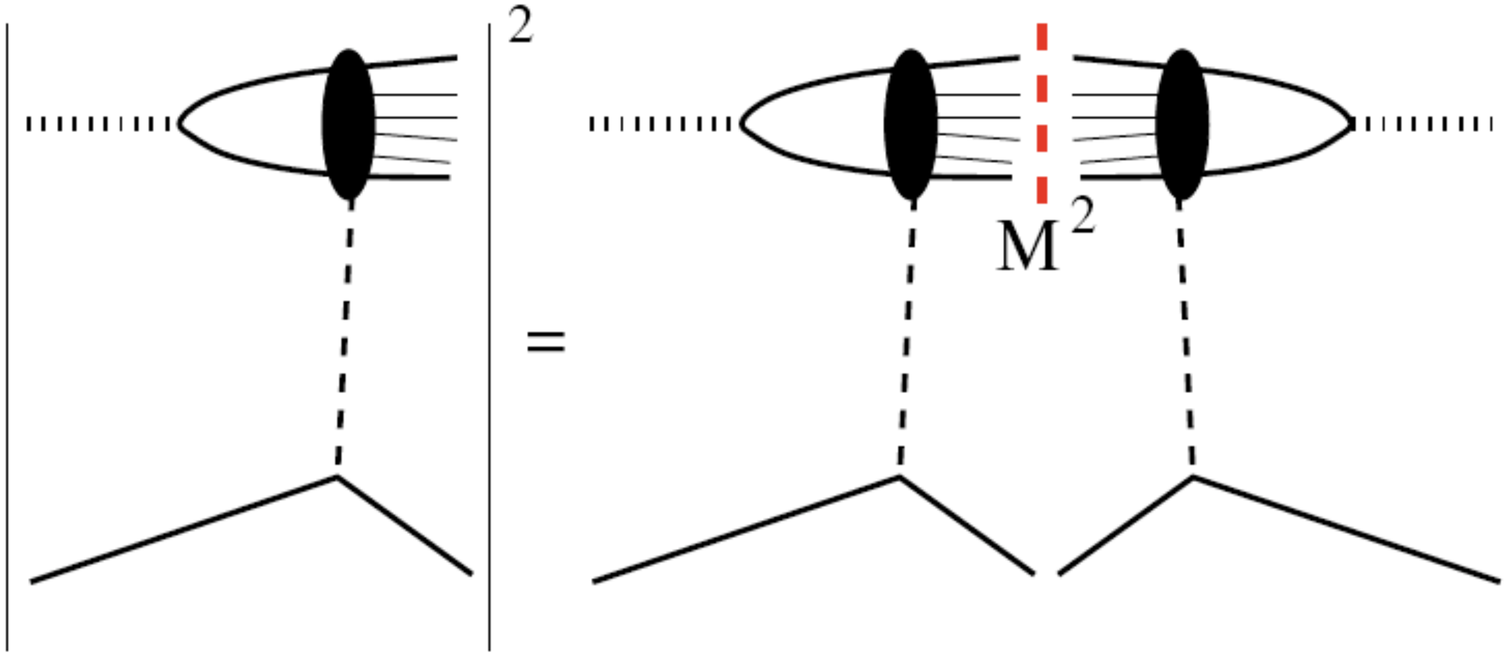

$$\sigma_A^2 = -4\pi A(A-1)\int d^2b\, T_A^2(b)\int_{M^2_{min}}^{M^2_{max}} dM^2 \frac{d\sigma^{\mathcal{D}}_{\gamma^*-p}}{dM^2 dt}\Big|_{t=0} F_A^2(t_{min}) \qquad F_A(t_{min}) = \int d^2b\, J_0(b\sqrt{-t_{min}})T_A(b)$$

coherent length of the qqbar pair

- Different groups use different implementations of this idea: they include real parts (FGS), use models for diffraction (AACKS) or parametrizations from HERA data (FGS, BCKTZ),... to be checked in eD collisions.
- The extension to more than 2 scatterings is model-dependent.

Gribov inelastic shadowing:

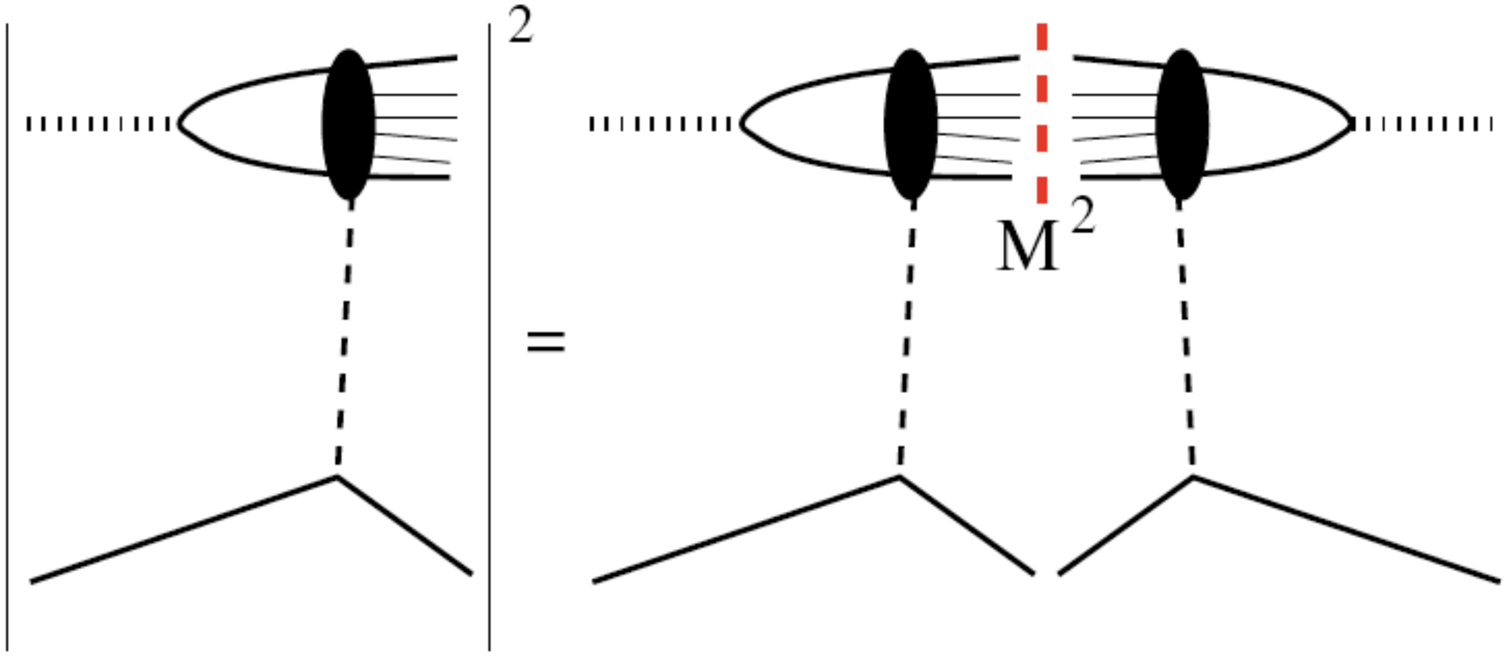

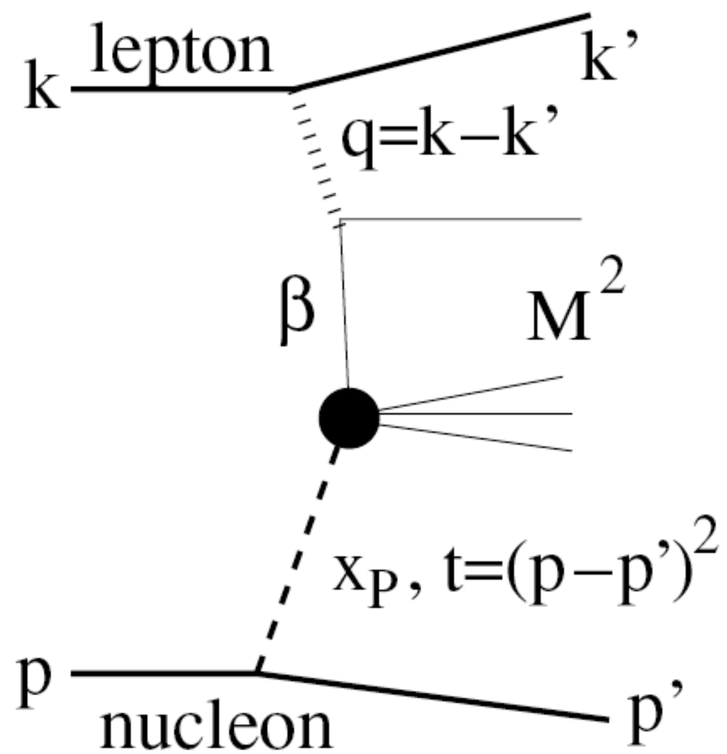

$$\sigma_A^2 = -4\pi A(A-1) \int d^2b\, T_A^2(b) \int_{M^2_{\rm min}}^{M^2_{\rm max}} dM^2 \left. \frac{d\sigma^{\mathcal{D}}_{\gamma^*-p}}{dM^2 dt} \right|_{t=0} F_A^2(t_{\rm min}) \qquad F_A(t_{\rm min}) = \int d^2b\, J_0(b\sqrt{-t_{\rm min}})\, T_A(b)$$

coherent length of the qqbar pair

- Different groups use different implementations of this idea: they include real parts (FGS), use models for diffraction (AACKS) or parametrizations from HERA data (FGS, BCKTZ),… to be checked in eD collisions.
- The extension to more than 2 scatterings is model-dependent.

Gribov inelastic shadowing:

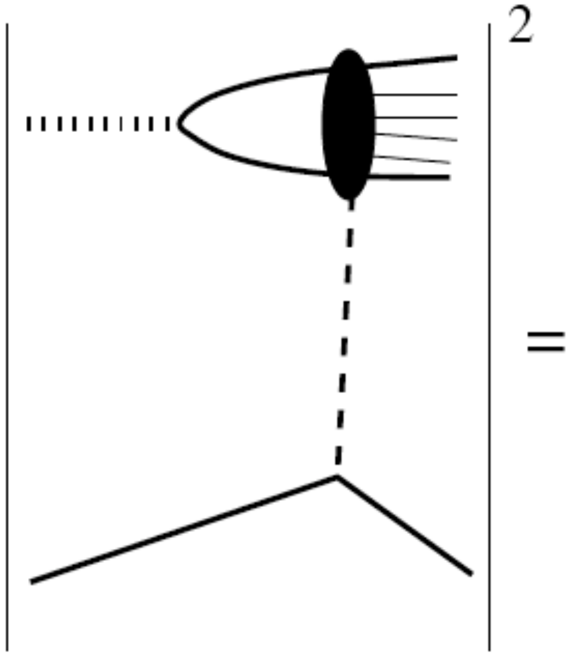

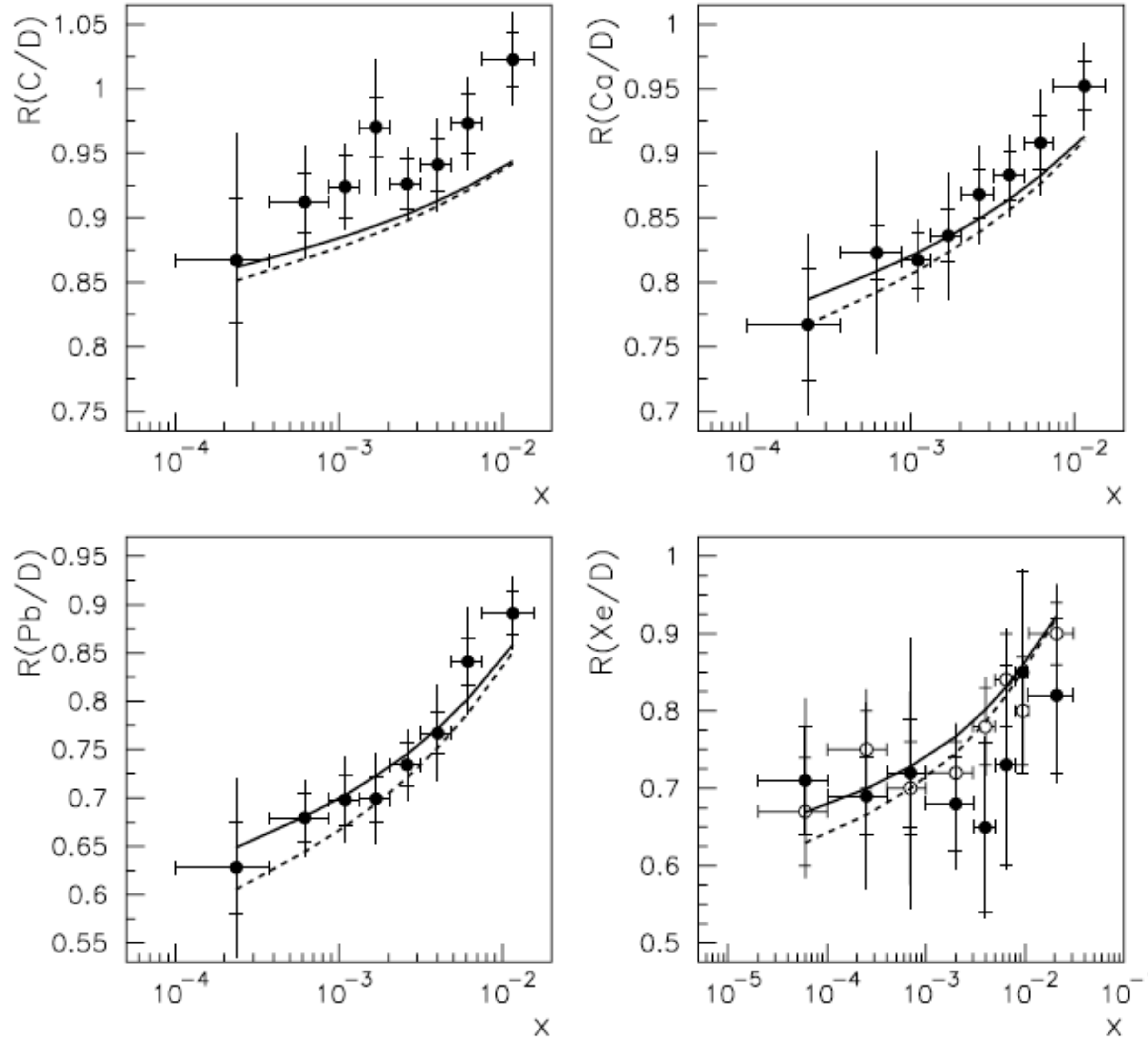

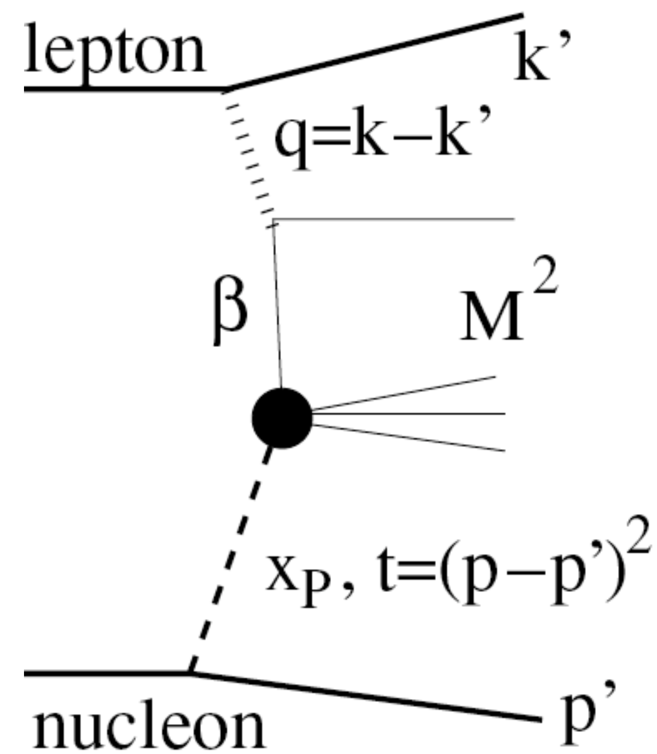

$$\sigma_A^2 = -4\pi A(A-1)\int d^2 \ldots = \int d^2b\, J_0(b\sqrt{-t_{\min}})T_A(b)$$

coherent length of the qqbar pair

- Different groups use different implementations of this idea: they include real parts (FGS), use models for diffraction (AACKS) or parametrizations from HERA data (FGS, BCKTZ),… to be checked in eD collisions.
- The extension to more than 2 scatterings is model-dependent.

Two-particle correlations:

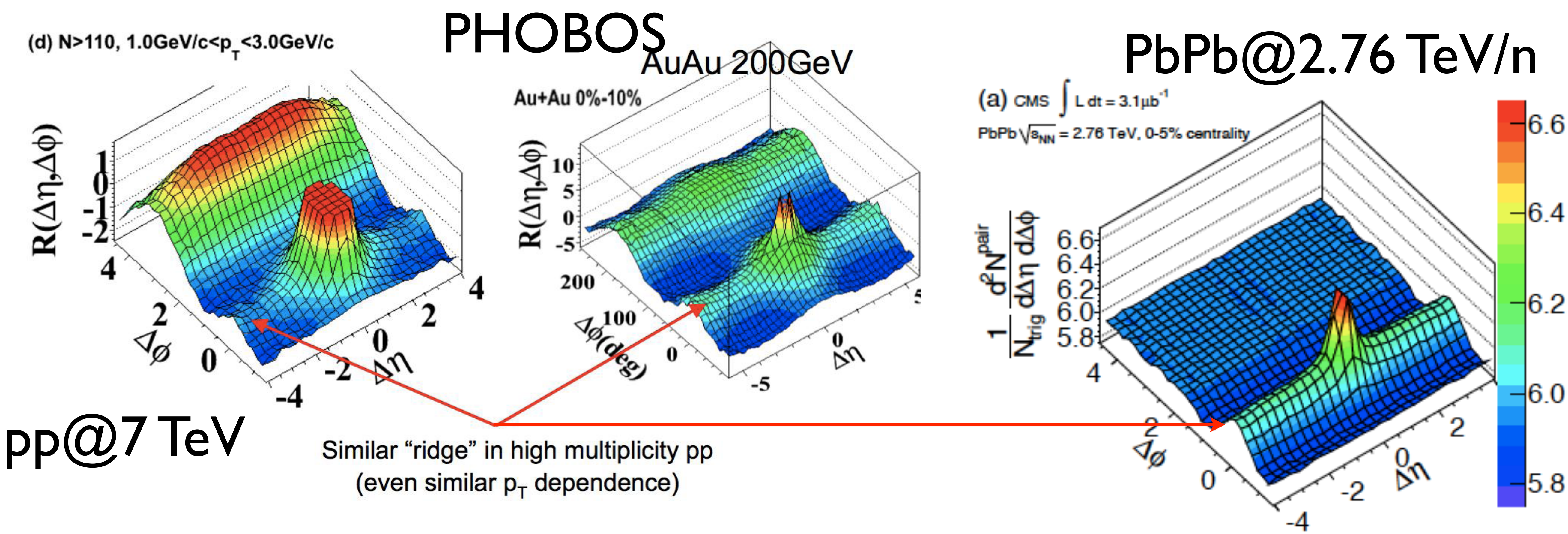

- η-elongated structure in the two-particle correlation in the near and away side regions.
- Long range rapidity correlations in particle production provide information on the early stages and appear naturally in several models: string models with a varying number of them, CGC,...
- Origin unsettled yet: coupling fragmentation ↔ flowing medium, ISR, flow itself (v_3),...

Two-particle correlations:

pp@7 TeV

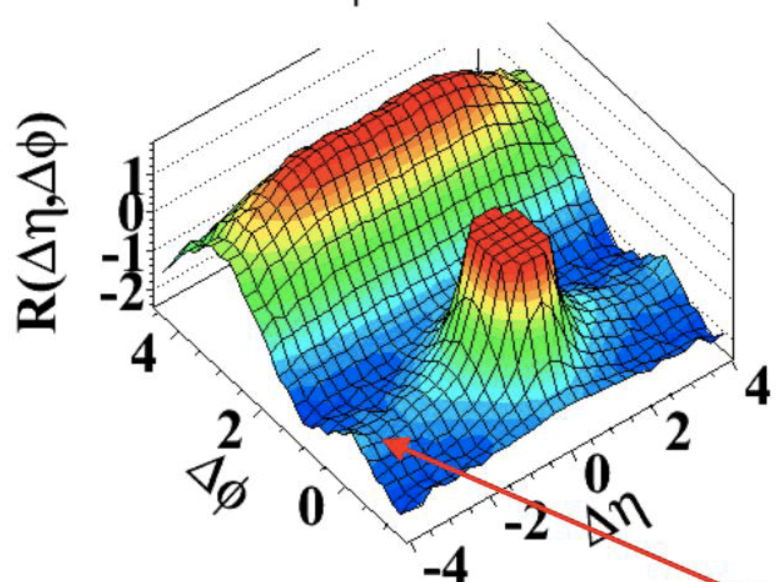

PHOBOS AuAu 200GeV

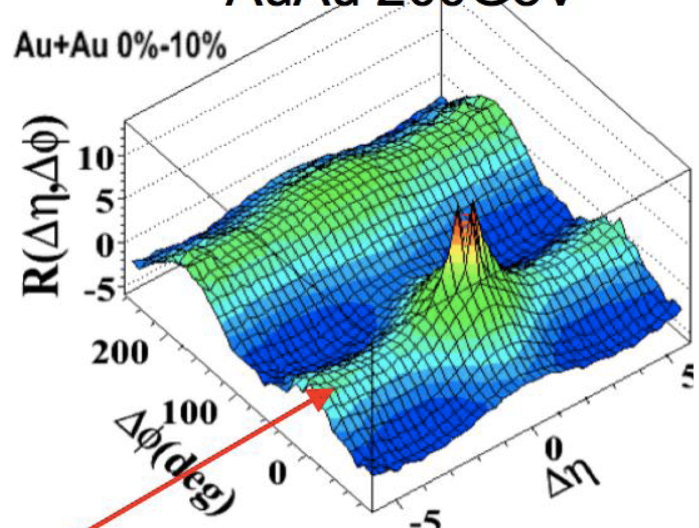

PbPb@2.76 TeV/n

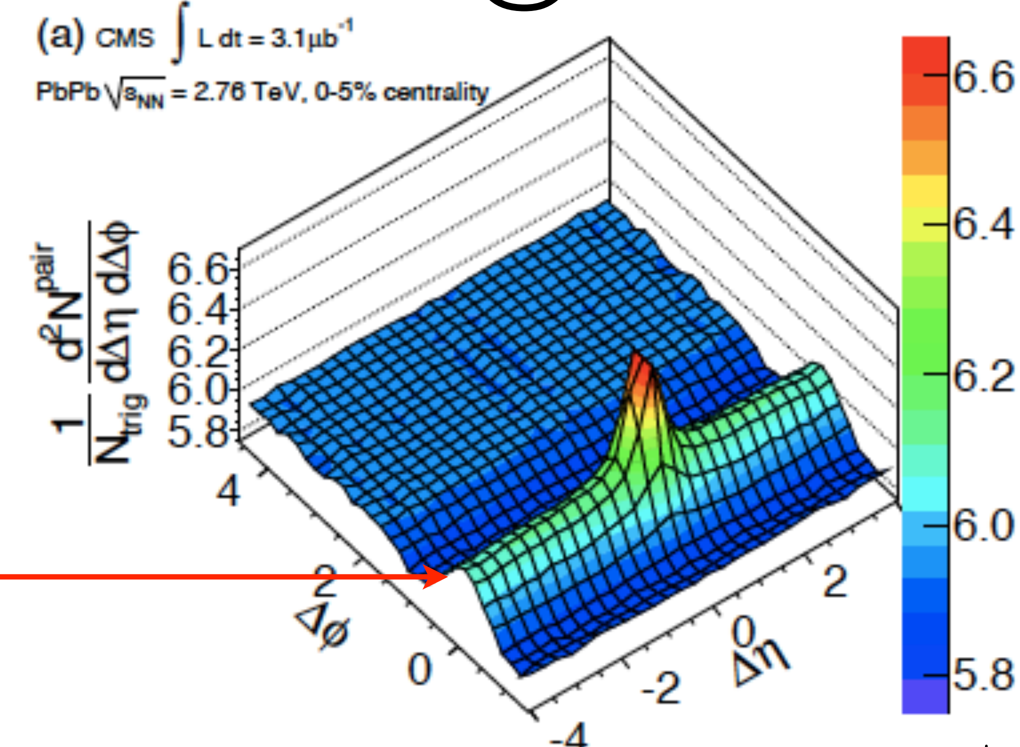

Similar "ridge" in high multiplicity pp
(even similar p_T dependence)

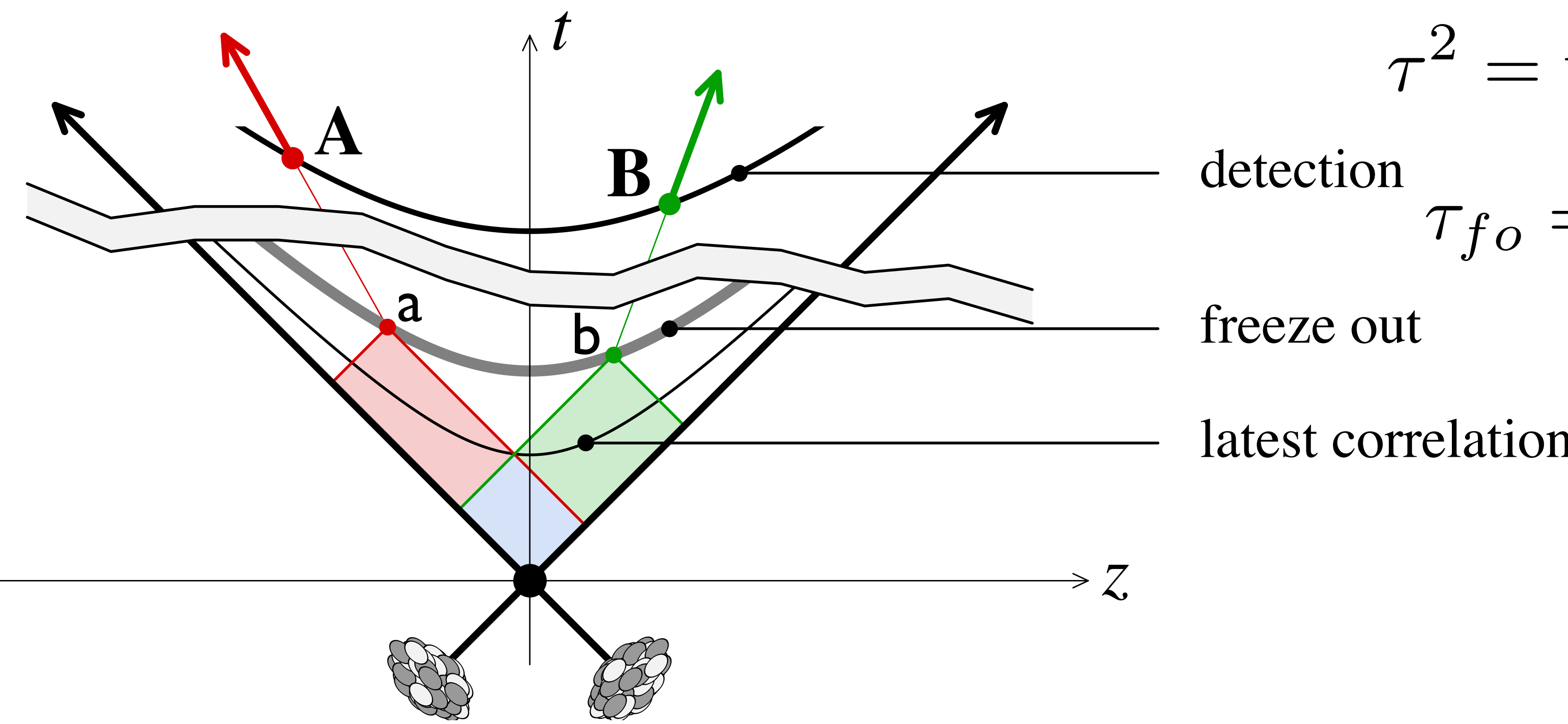

$$\tau^2 = t^2 - z^2 = x^+ x^-, \quad \eta = \frac{1}{2} \ln \frac{x^+}{x^-}$$

$$\tau_{fo} = x_a^+ x_a^- = x_b^+ x_b^-, \quad \tau_{lc} = x_a^+ x_b^-$$

$$\eta_a = \ln \frac{x_a^+}{\tau_{fo}}, \quad \eta_b = \ln \frac{\tau_{fo}}{x_b^-}$$

$$\Delta\eta = \eta_b - \eta_a = 2 \ln \frac{\tau_{fo}}{\tau_{lc}}$$

$$\tau_{lc} \leq \tau_{fo} e^{-\Delta\eta/2}$$

The ridge:

- Two-particle correlations in pp and pPb at the LHC show features that in AA are attributed to final state interactions describable by hydro and interpreted as a signal of equilibration.
- EKT, AdS/CFT: hydro works for large momentum anisotropies.

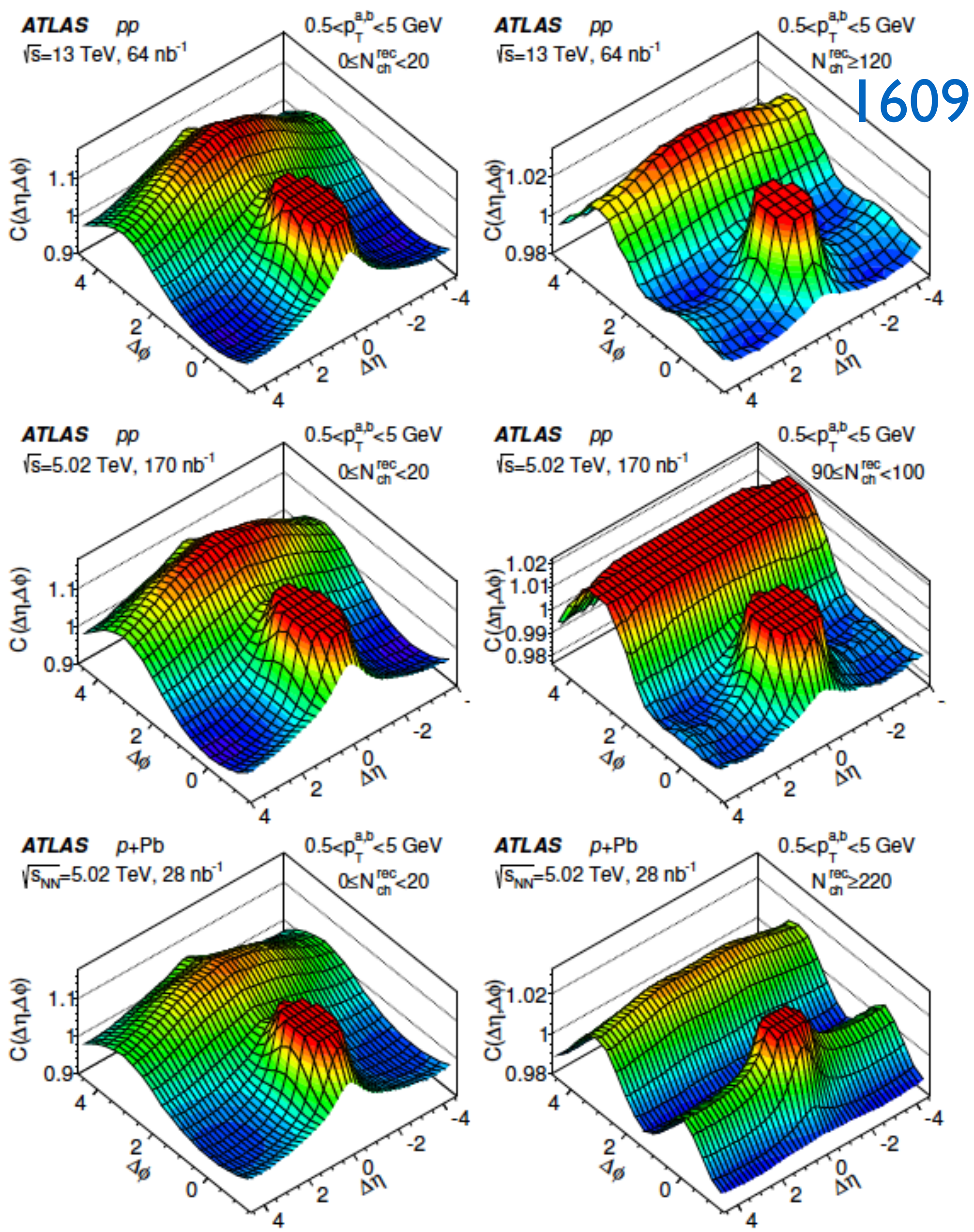

1609.06213

$$\frac{dN}{d\phi} = \left\langle \frac{dN}{d\phi} \right\rangle \left(1 + \sum_n 2v_n \cos\left[n\left(\phi - \Psi_n\right)\right]\right) \qquad Y^{\mathrm{ridge}}(\Delta\phi) = G\left(1 + \sum_{n=2}^{\infty} 2v_{n,n}\cos\left(n\Delta\phi\right)\right)$$

$$v_{n,n}(p_T^a, p_T^b) = v_n(p_T^a)\, v_n(p_T^b)$$

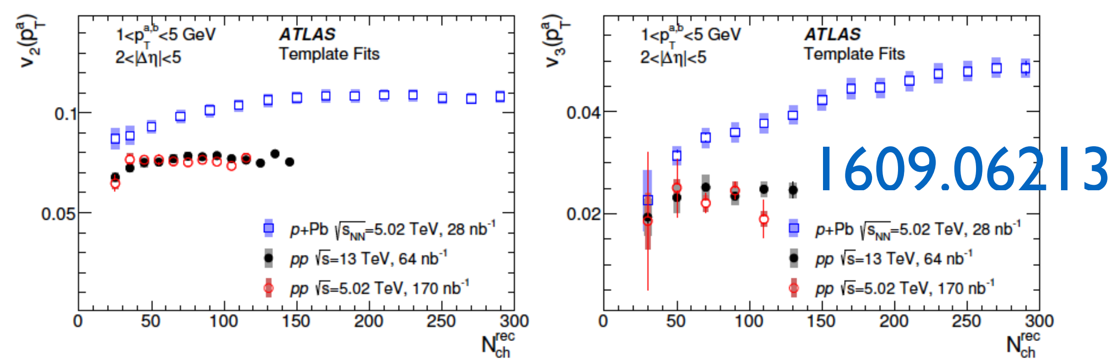

1609.06213

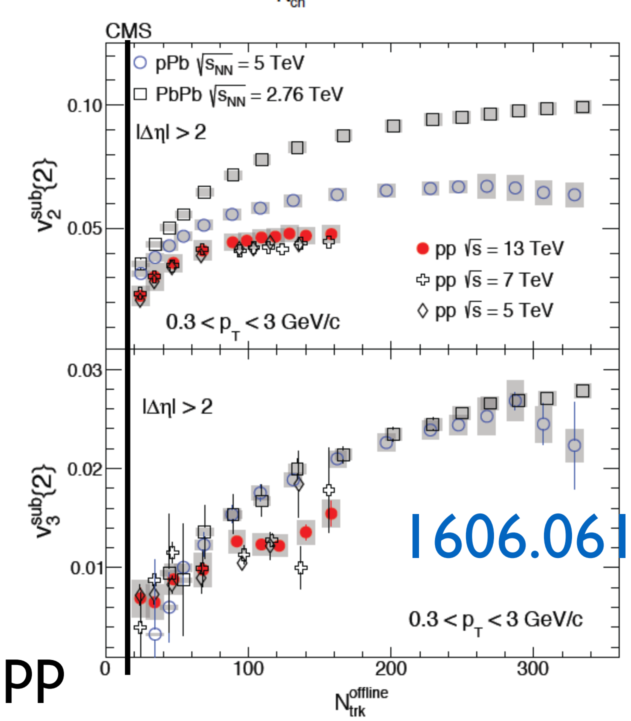

1606.06198

MB in pp

The ridge:

- Two-particle correlations in pp and pPb at the LHC show features that in AA are attributed to final state interactions describable by hydro and interpreted as a signal of equilibration.
- EKT, AdS/CFT: hydro works for large momentum anisotropies.

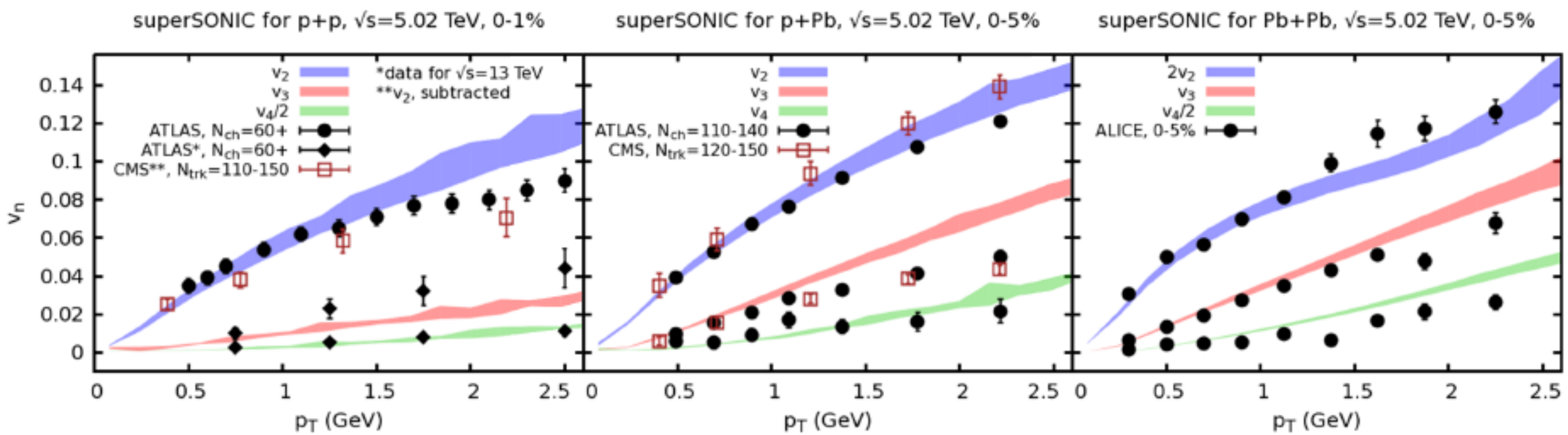

1701.07145, proton as 3 hot spots

FIG. 2. Elliptic (v_2), triangular (v_3) and quadrupolar (v_4) flow coefficients from superSONIC simulations (bands) compared to experimental data from ATLAS, CMS and ALICE (symbols) for p+p (left panel), p+Pb (center panel) and Pb+Pb (right panel) collisions at $\sqrt{s} = 5.02$ TeV [58–62]. Simulation parameters used were $\frac{\eta}{s} = 0.08$ and $\frac{\zeta}{s} = 0.01$ for all systems. Note that ATLAS results for v_3, v_4 are only available for $\sqrt{s} = 13$ TeV, while all simulation results are for $\sqrt{s} = 5.02$ TeV.

The ridge:

- Two-particle correlations in pp and pPb at the LHC show features that in AA are attributed to final state interactions describable by hydro and interpreted as a signal of equilibration.
- EKT, AdS/CFT: hydro works for large momentum anisotropies.

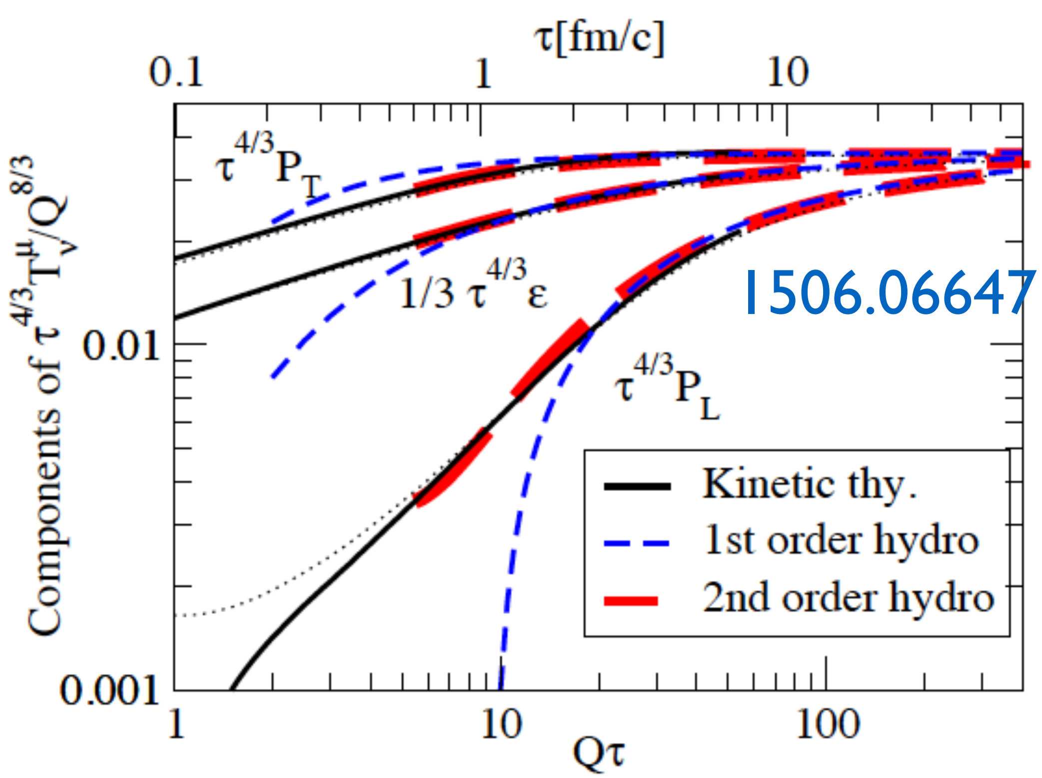

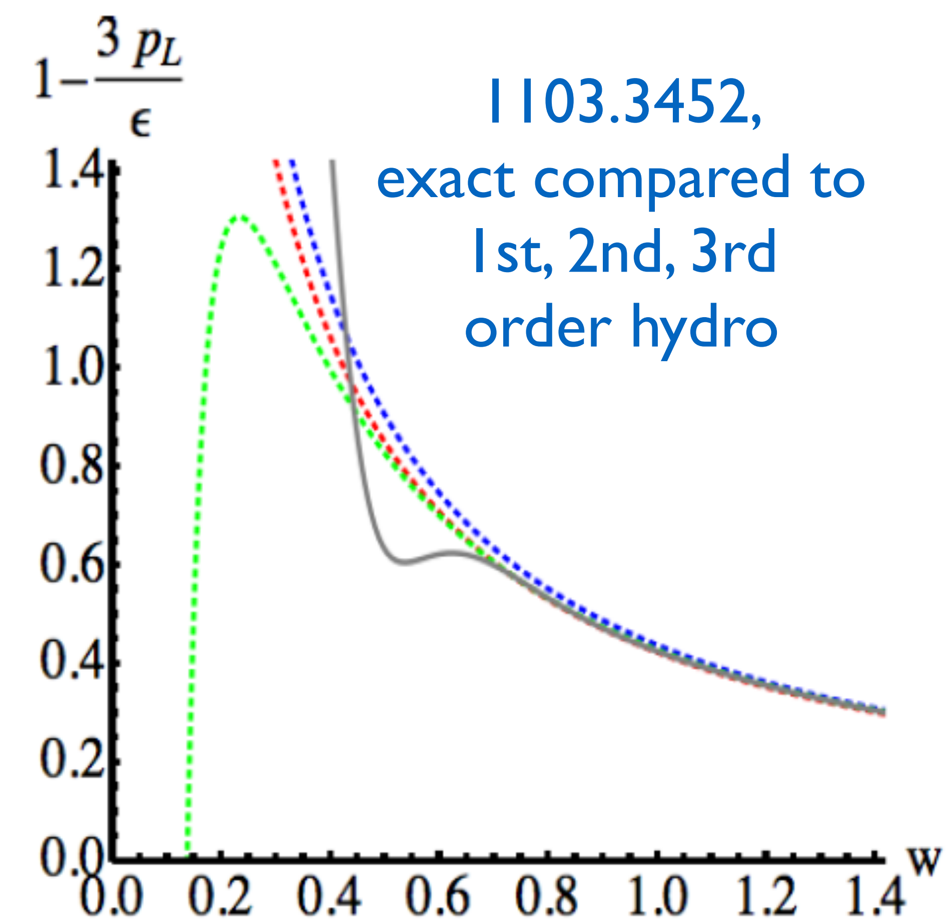

The ridge:

- Two-particle correlations in pp and pPb at the LHC show features that in AA are attributed to final state interactions describable by hydro and interpreted as a signal of equilibration.
- EKT, AdS/CFT: hydro works for large momentum anisotropies.

- The statement of the success of hydro as a signal of equilibration is moving to the statement of what this success is telling us about the non-equilibrium evolution of a partonic system in QCD: the ubiquitous emergence problem (1609.02820).

- What about a non-hydro initial-state explanation? (anyway long range rapidity correlations must come from the very early times…). We need to compute multiparticle amplitudes.

Alternatives to pure hydro:

- Several explanations have been proposed in the CGC: assume that the final state carry the imprint of initial-state correlations, and use that the CGC wave function is rapidity invariant over $Y \propto 1/\alpha_s$.

Alternatives to pure hydro:

- Several explanations have been proposed in the CGC: assume that the final state carry the imprint of initial-state correlations, and use that the CGC wave function is rapidity invariant over $Y \propto 1/\alpha_s$.

➜ Local anisotropy of target fields (Kovner-Lublinsky, Dumitru-McLerran-Skokov).

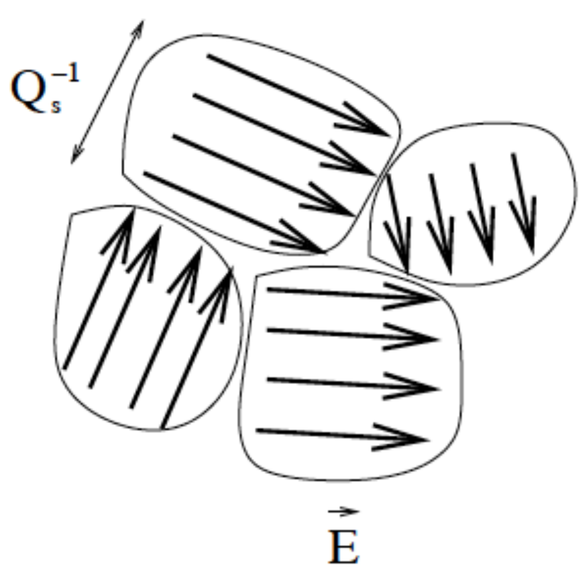

➜ "Glasma graphs": succesful phenomenology (Dusling-Gelis-Jalilian-Marian-Lappi-McLerran-Venugopalan, Kovchegov-Werpteny).

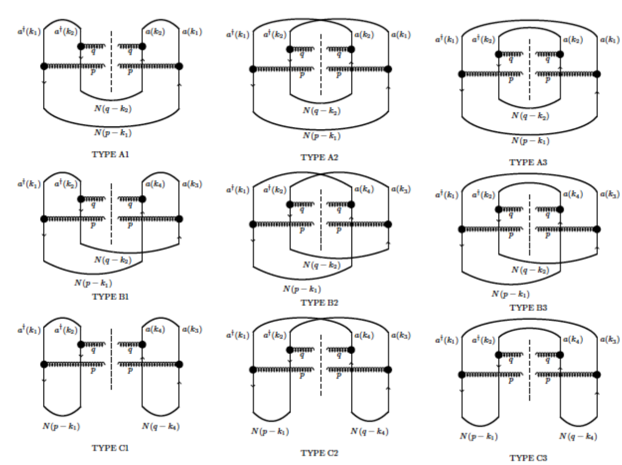

➜ Spatial variation of partonic density (Levin-Rezaeian).

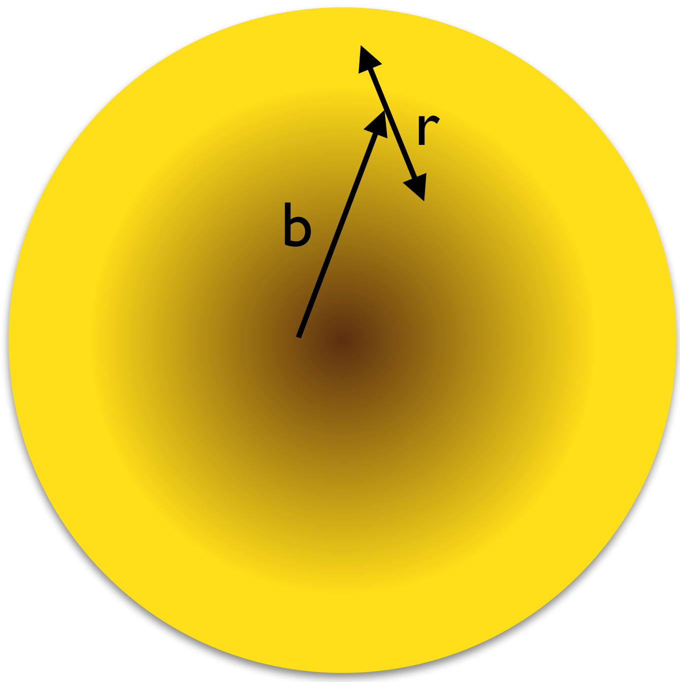

Alternatives to pure hydro:

- Several explanations have been proposed in the CGC: assume that the final state carry the imprint of initial-state correlations, and use that the CGC wave function is rapidity invariant over $Y \propto 1/\alpha_s$.

➜ Local anisotropy of target fields (Kovner-Lublinsky, Dumitru-McLerran-Skokov).

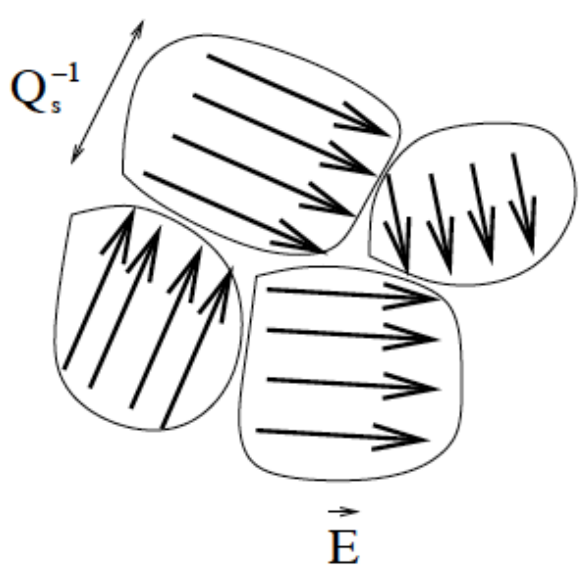

➜ "Glasma graphs": succesful phenomenology (Dusling-Gelis-Jalilian-Marian-Lappi-McLerran-Venugopalan, Kovchegov-Werpteny).

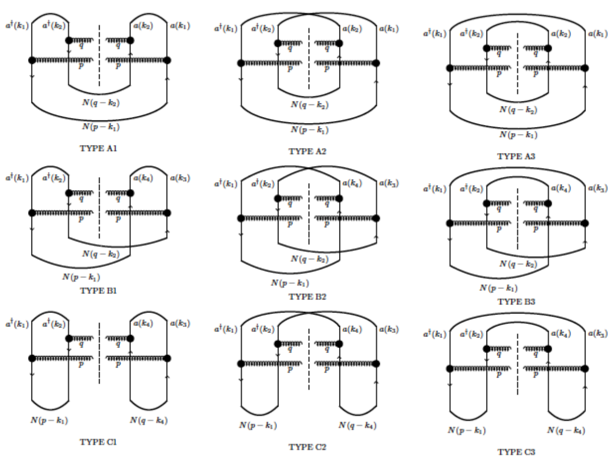

➜ Spatial variation of partonic density (Levin-Rezaeian).

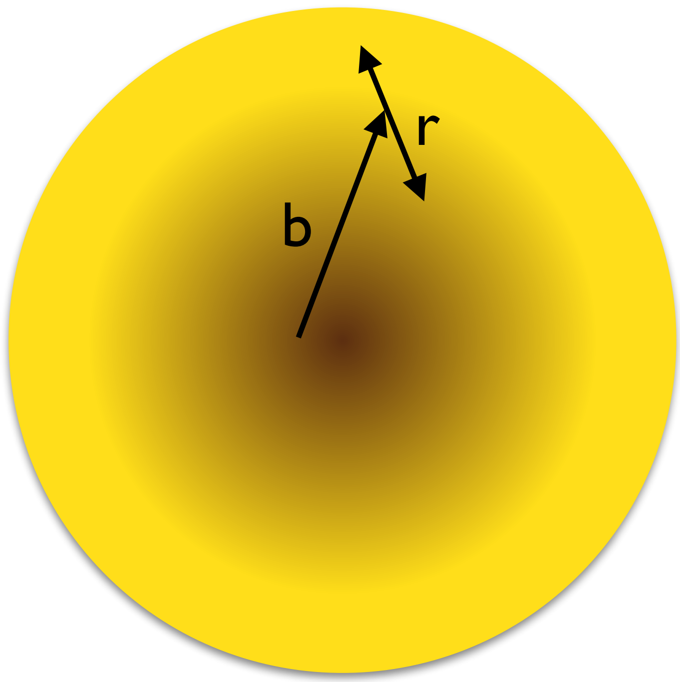

- Work undergoing to explain n-particle correlations, n>2, and odd harmonics: multiple scattering, density corrections,…

Alternatives to pure hydro:

- Several explanations have been proposed in the CGC: assume that the final state carry the imprint of initial-state correlations, and use that the CGC wave function is rapidity invariant over $Y \propto 1/\alpha_s$.

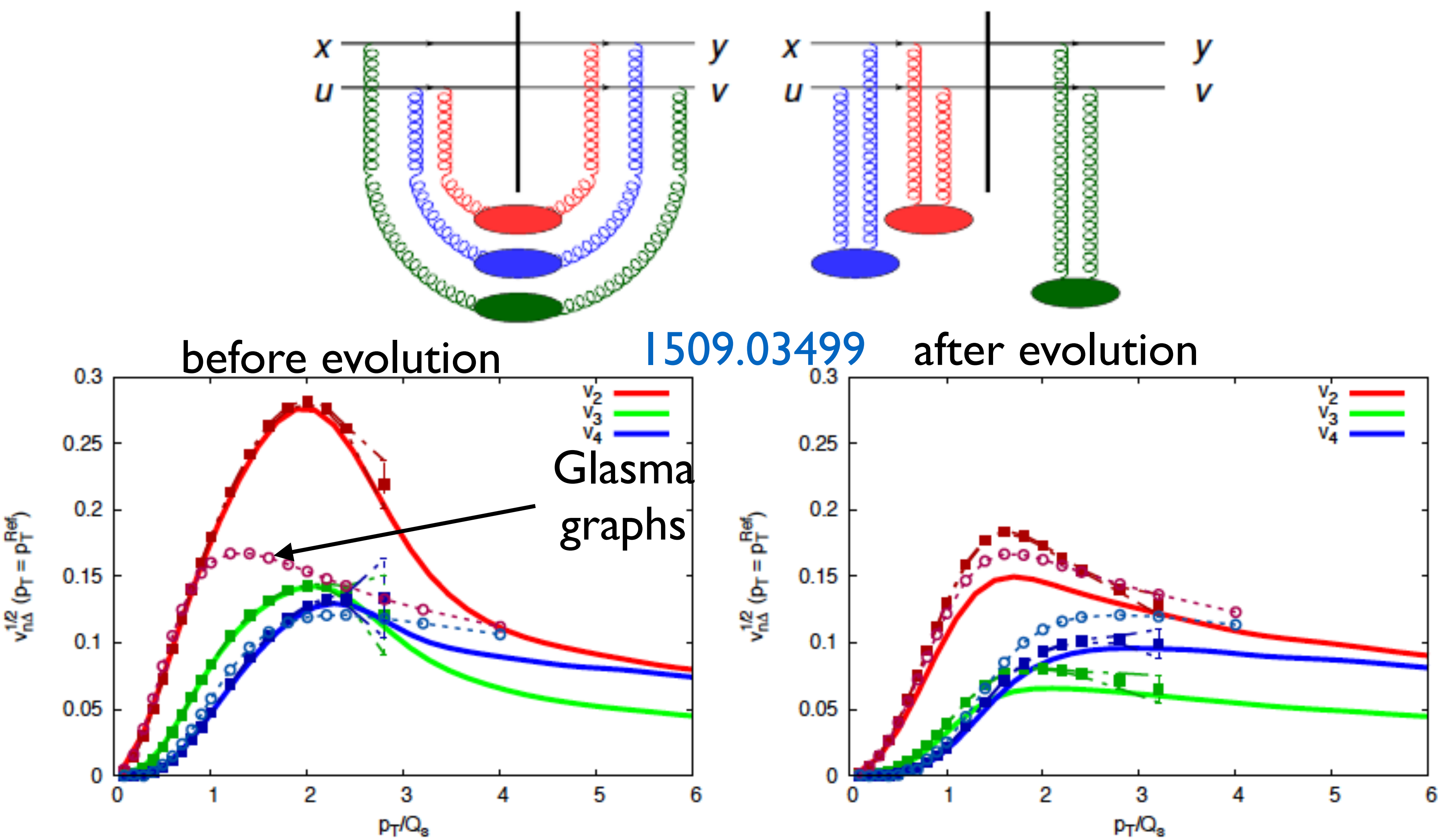

- Work undergoing to explain n-particle correlations, n>2, and odd harmonics: multiple scattering, density corrections,…

Coherence in the high-energy WF:

- Low energies: short-lived fluctuations of the components of the wave function when compared with the size of the target.

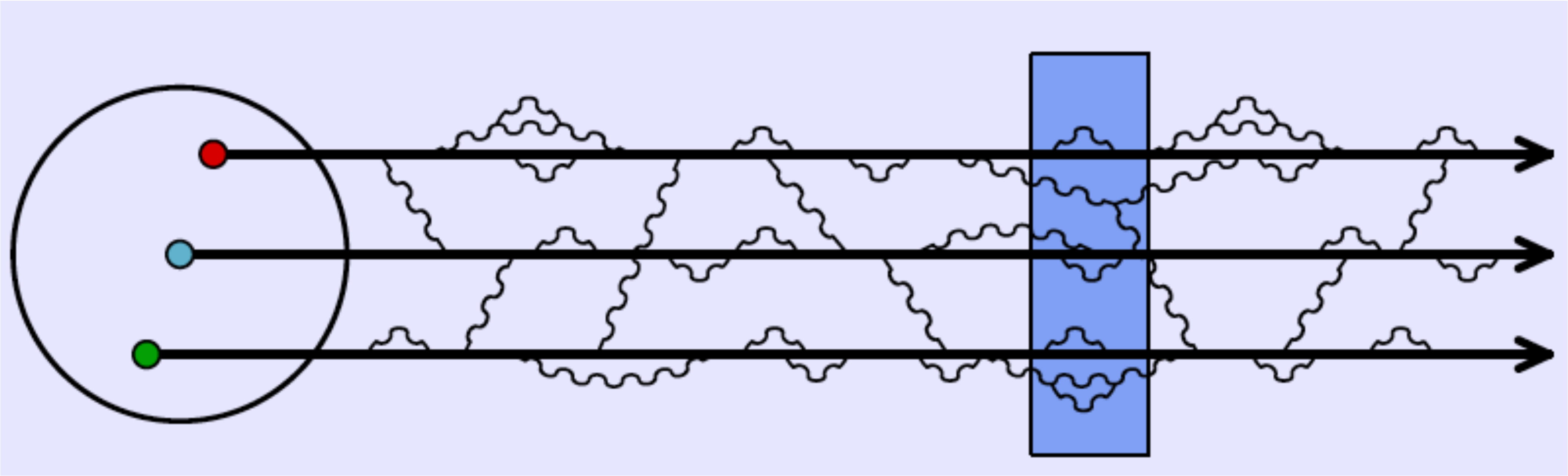

- High energies: many long lived fluctuations (small-x gluons) that do not interact during the scattering time, frozen configuration.

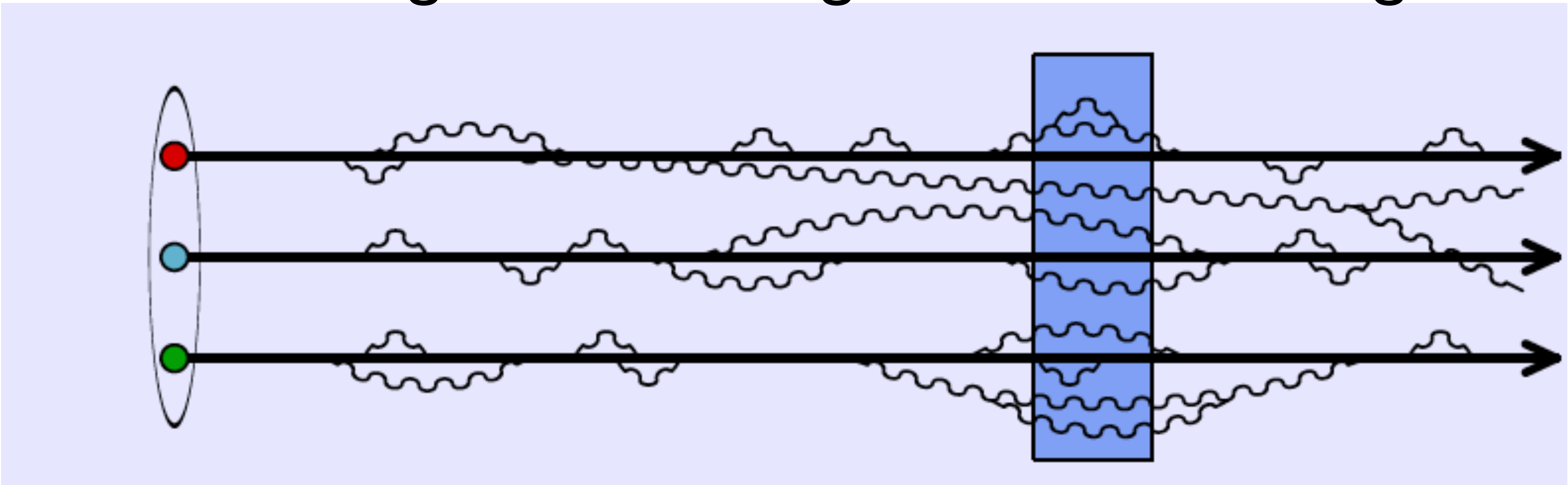

Coherence in the high-energy WF:

• Interaction of a frozen configuration of partons through a shock wave, the S-matrix is given by a Wilson line:

$$W(x_\perp) = S(x_\perp) = \mathcal{P}\exp\left[ig\int dx^+ A^-(x^+, x_\perp)\right]$$

• High energies: many long lived fluctuations (small-x gluons) that do not interact during the scattering time, frozen configuration.

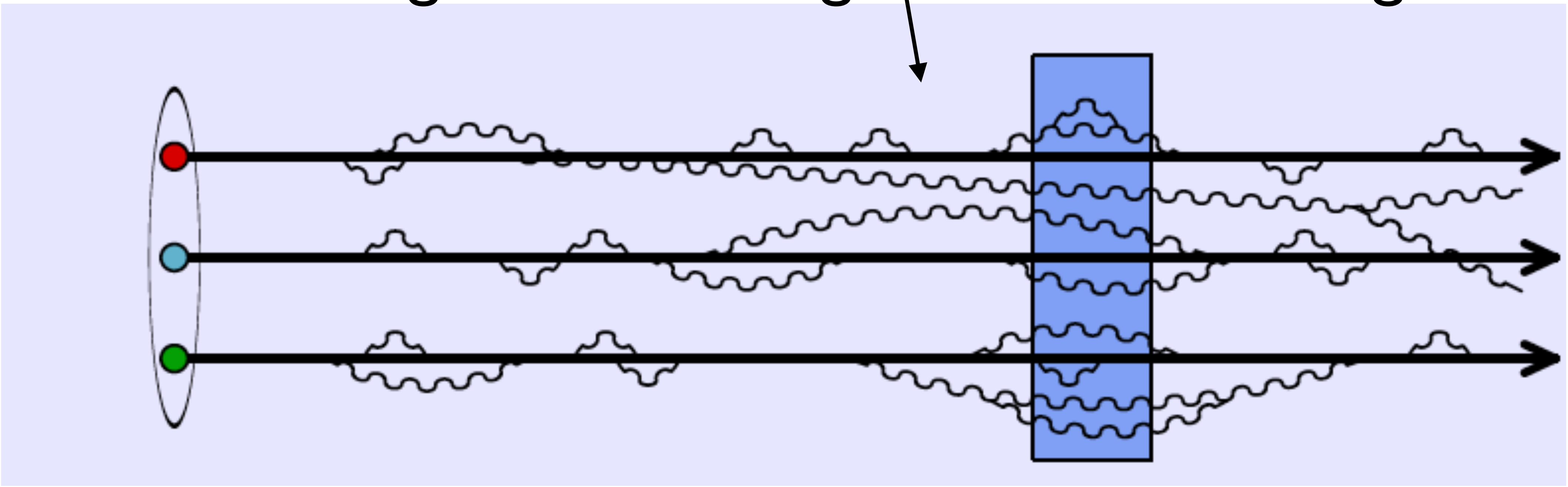

Bose enhancement for gluons:

- The appearance of the ridge in the final state, within the glasma graph approach, can be traced to the Bose enhancement of gluons in the (rapidity invariant) wave function:

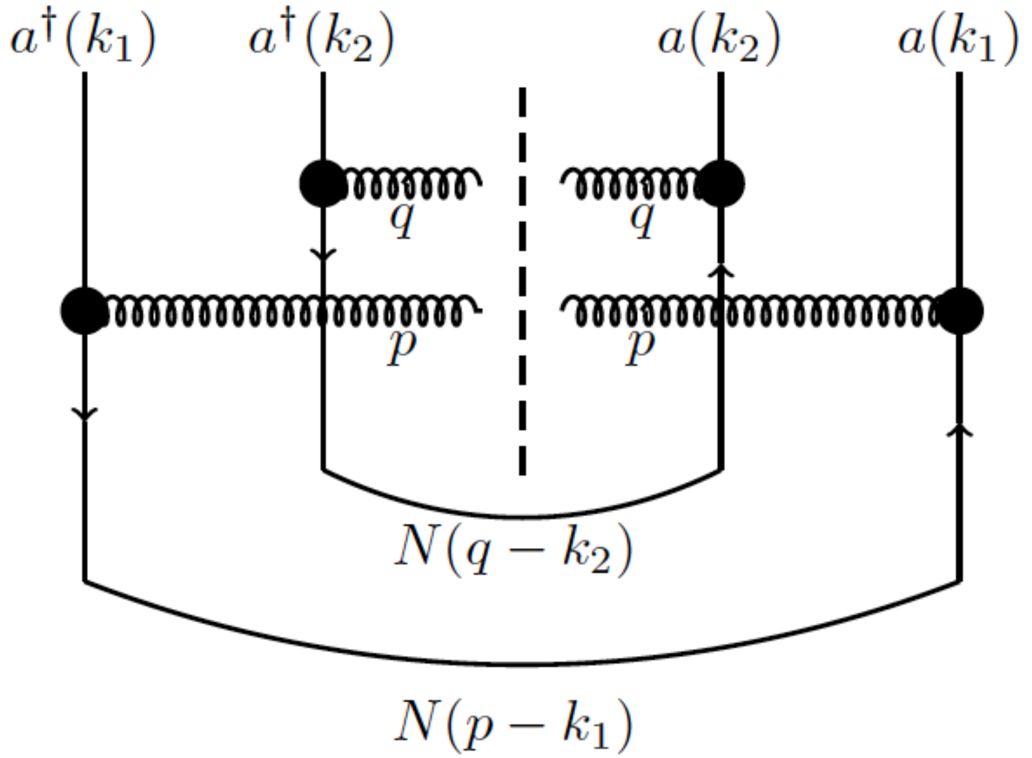

1503.07126, 1509.03223

Bose enhancement for gluons:

- The appearance of the ridge in the final state, within the glasma graph approach, can be traced to the Bose enhancement of gluons in the (rapidity invariant) wave function:

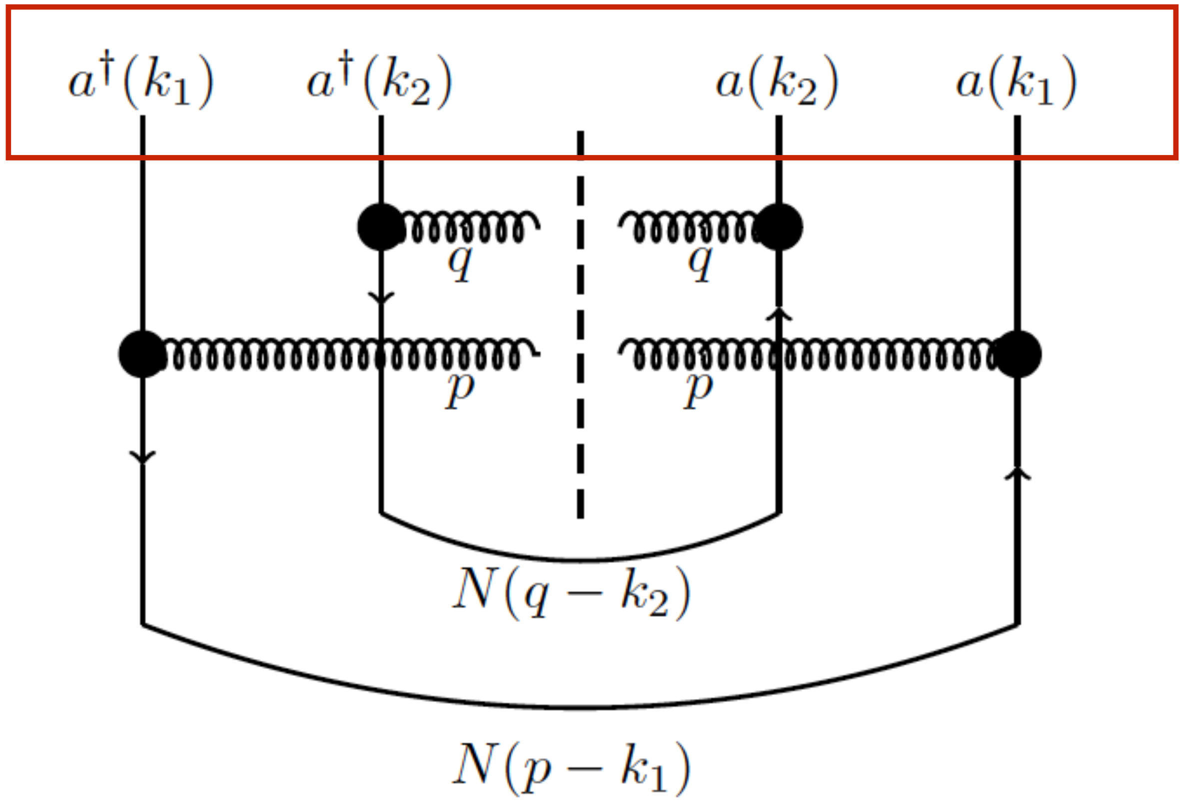

gluons in the WF

1503.07126, 1509.03223

$$[a_a^i(k), a_b^{\dagger j}(p)] = (2\pi)^2 \delta_{ab}\delta^{ij}\delta^{(2)}(k-p)$$

$$a_a^i(k) \equiv \frac{1}{\sqrt{Y}} \int_{|\eta<Y/2|} \frac{d\eta}{2\pi}\, a_a^i(\eta, k)$$

Bose enhancement for gluons:

- The appearance of the ridge in the final state, within the glasma graph approach, can be traced to the Bose enhancement of gluons in the (rapidity invariant) wave function:

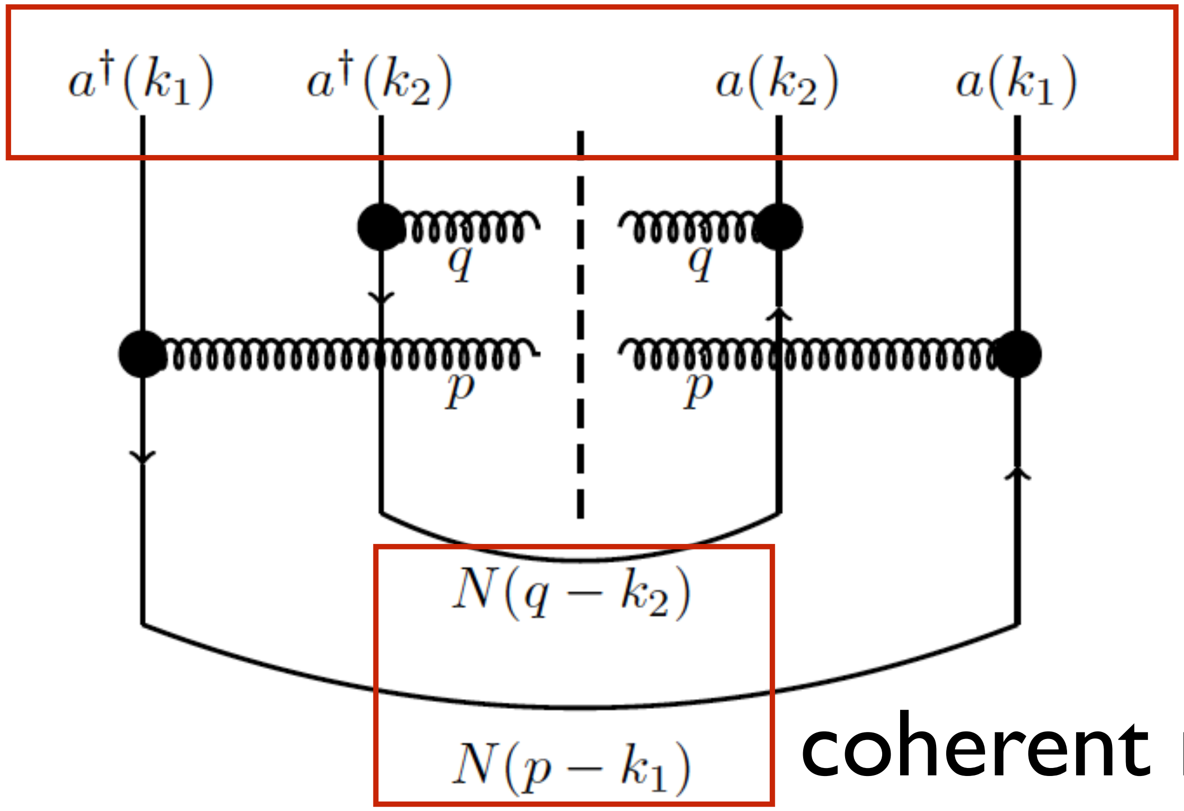

gluons in the WF

1503.07126, 1509.03223

$$[a_a^i(k), a_b^{\dagger j}(p)] = (2\pi)^2 \delta_{ab}\delta^{ij}\delta^{(2)}(k-p)$$

$$a_a^i(k) \equiv \frac{1}{\sqrt{Y}} \int_{|\eta<Y/2|} \frac{d\eta}{2\pi}\, a_a^i(\eta, k)$$

coherent rescattering on the target

Bose enhancement for gluons:

- The appearance of the ridge in the final state, within the glasma graph approach, can be traced to the Bose enhancement of gluons in the (rapidity invariant) wave function:

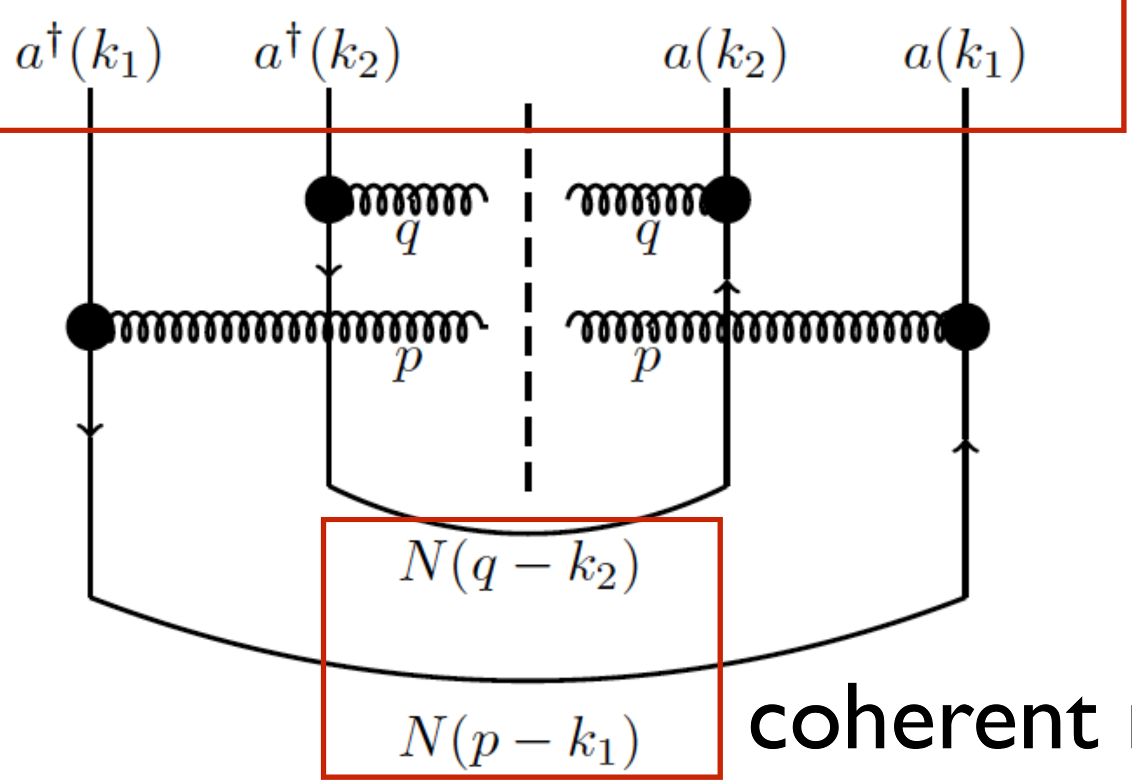

gluons in the WF

coherent rescattering on the target

1503.07126, 1509.03223

$$[a_a^i(k), a_b^{\dagger j}(p)] = (2\pi)^2 \delta_{ab} \delta^{ij} \delta^{(2)}(k-p)$$

$$a_a^i(k) \equiv \frac{1}{\sqrt{Y}} \int_{|\eta<Y/2|} \frac{d\eta}{2\pi}\, a_a^i(\eta, k)$$

$$C \int_{k_1,k_2} \langle in | a_a^{\dagger i}(k_1) a_b^{\dagger j}(k_2) a_a^k(k_1) a_b^l(k_2) | in \rangle \left[\delta^{ik} - \frac{k_1^i k_1^k}{p^2}\right] \left[\delta^{jl} - \frac{k_2^j k_2^l}{q^2}\right] N(p-k_1) N(q-k_2)$$

Bose enhancement for gluons:

- The appearance of the ridge in the final state, within the glasma graph approach, can be traced to the Bose enhancement of gluons in the (rapidity invariant) wave function:

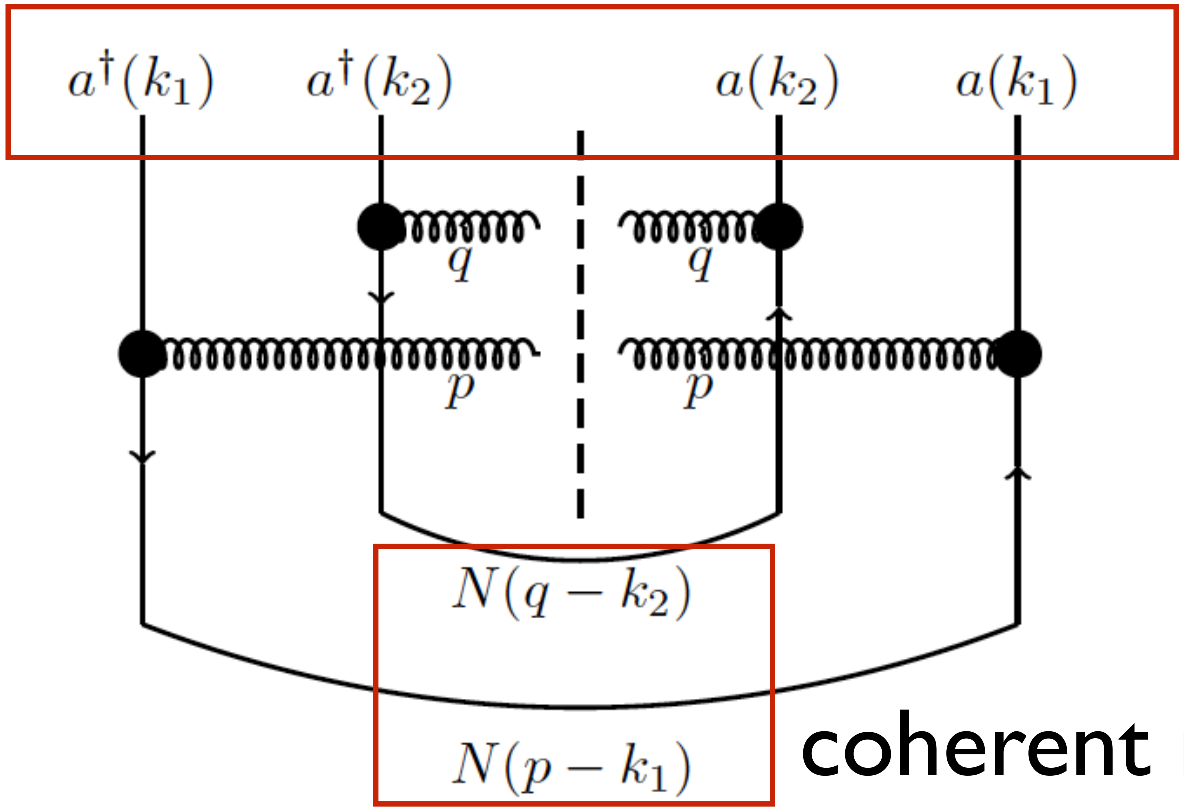

gluons in the WF

1503.07126, 1509.03223

$$[a_a^i(k), a_b^{\dagger j}(p)] = (2\pi)^2\delta_{ab}\delta^{ij}\delta^{(2)}(k-p)$$

$$a_a^i(k) \equiv \frac{1}{\sqrt{Y}}\int_{|\eta<Y/2|}\frac{d\eta}{2\pi}\, a_a^i(\eta, k)$$

coherent rescattering on the target

$$C\int_{k_1,k_2}\langle in|a_a^{\dagger i}(k_1)a_b^{\dagger j}(k_2)a_a^k(k_1)a_b^l(k_2)|in\rangle\left[\delta^{ik}-\frac{k_1^ik_1^k}{p^2}\right]\left[\delta^{jl}-\frac{k_2^jk_2^l}{q^2}\right]N(p-k_1)N(q-k_2)$$

$$D(k_1,k_2) = S^2(N_c^2-1)^2\frac{k_1^ik_1^kk_2^jk_2^l}{k_1^2k_2^2}\frac{g^4\mu^2(k_1)\mu^2(k_2)}{k_1^2k_2^2}\left\{1+\frac{1}{S(N_c^2-1)}\left[\delta^{(2)}(k_1-k_2)+\delta^{(2)}(k_1+k_2)\right]\right\}$$

$$a^*(k) = a(-k)$$

Bose enhancement for gluons:

- Obvious question: is there Pauli blocking for quarks in the CGC wave function and, if so, is it short or long range in rapidity?

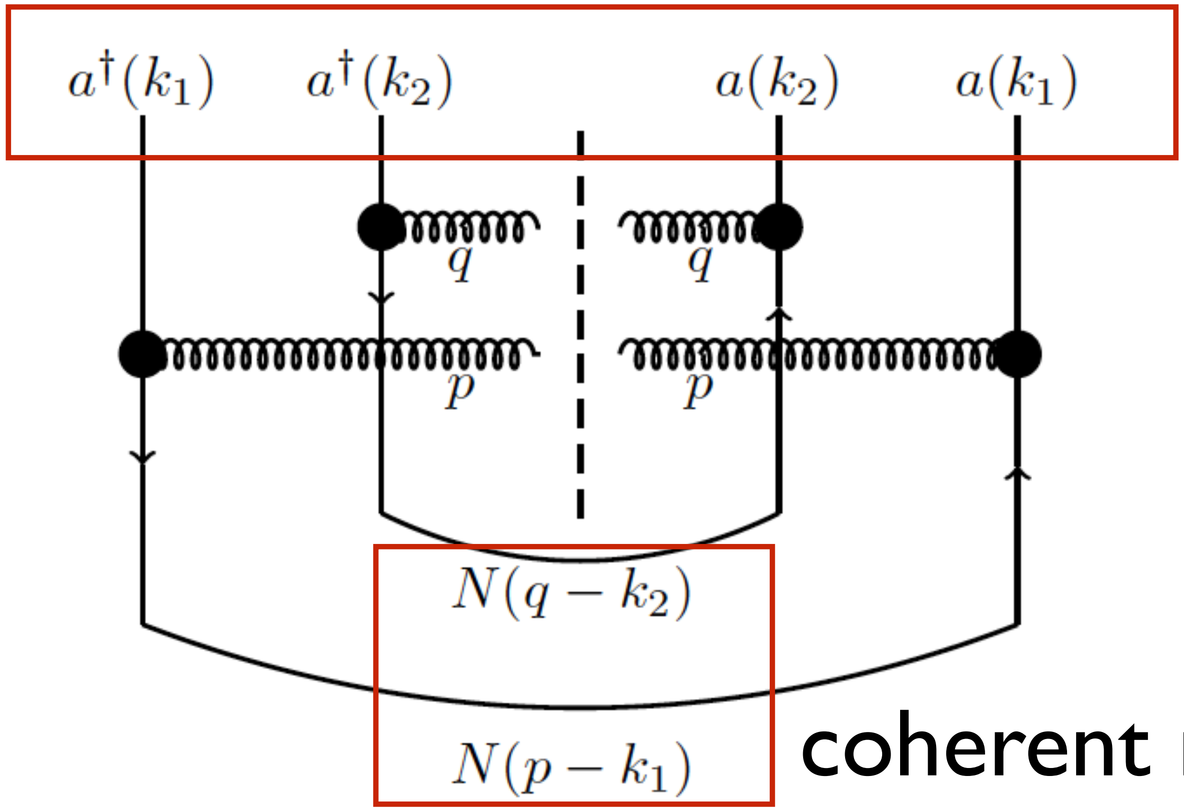

gluons in the WF

1503.07126, 1509.03223

$$[a_a^i(k), a_b^{\dagger j}(p)] = (2\pi)^2 \delta_{ab} \delta^{ij} \delta^{(2)}(k-p)$$

$$a_a^i(k) \equiv \frac{1}{\sqrt{Y}} \int_{|\eta<Y/2|} \frac{d\eta}{2\pi}\, a_a^i(\eta, k)$$

coherent rescattering on the target

$$C \int_{k_1,k_2} \langle in | a_a^{\dagger i}(k_1) a_b^{\dagger j}(k_2) a_a^k(k_1) a_b^l(k_2) | in \rangle \left[\delta^{ik} - \frac{k_1^i k_1^k}{p^2}\right] \left[\delta^{jl} - \frac{k_2^j k_2^l}{q^2}\right] N(p-k_1) N(q-k_2)$$

$$D(k_1, k_2) = S^2 (N_c^2 - 1)^2 \frac{k_1^i k_1^k k_2^j k_2^l}{k_1^2 k_2^2} \frac{g^4 \mu^2(k_1) \mu^2(k_2)}{k_1^2 k_2^2} \left\{ 1 + \frac{1}{S(N_c^2-1)} \left[\delta^{(2)}(k_1 - k_2) + \delta^{(2)}(k_1 + k_2)\right] \right\}$$

$$a^*(k) = a(-k)$$

Quark correlations: 1610.03020

- The two-particle inclusive cross section reads:

$$\frac{d\sigma}{dp^+d^2pdq^+d^2q} = \frac{1}{(2\pi)^6} \langle v|\Omega\,\hat{S}^\dagger\,\Omega^\dagger\ \left[d^\dagger_{\alpha,s_1}(p^+,p)\,d^\dagger_{\beta,s_2}(q^+,q)d_{\beta,s_2}(q^+,q)\,d_{\alpha,s_1}(p^+,p)\right]\,\Omega\,\hat{S}\,\Omega^\dagger|v\rangle$$

Quark correlations: 1610.03020

- The two-particle inclusive cross section reads:

$$\frac{d\sigma}{dp^+d^2p\,dq^+d^2q} = \frac{1}{(2\pi)^6}\langle v|\Omega\,\hat{S}^\dagger\,\Omega^\dagger\ \left[d^\dagger_{\alpha,s_1}(p^+,p)\,d^\dagger_{\beta,s_2}(q^+,q)d_{\beta,s_2}(q^+,q)\,d_{\alpha,s_1}(p^+,p)\right]\,\Omega\,\hat{S}\,\Omega^\dagger|v\rangle$$

operator that diagonalises perturbatively the Light Cone QCD Hamiltonian

Quark correlations: 1610.03020

- The two-particle inclusive cross section reads:

$$\frac{d\sigma}{dp^+d^2p\,dq^+d^2q} = \frac{1}{(2\pi)^6}\langle v|\Omega\,\hat{S}^\dagger\,\Omega^\dagger\,\left[d^\dagger_{\alpha,s_1}(p^+,p)\,d^\dagger_{\beta,s_2}(q^+,q)d_{\beta,s_2}(q^+,q)\,d_{\alpha,s_1}(p^+,p)\right]\,\Omega\,\hat{S}\,\Omega^\dagger|v\rangle$$

operator that diagonalises perturbatively the Light Cone QCD Hamiltonian

eikonal S-matrix

Quark correlations: 1610.03020

- The two-particle inclusive cross section reads:

$$\frac{d\sigma}{dp^+d^2p\,dq^+d^2q} = \frac{1}{(2\pi)^6}\langle v|\Omega\,\hat{S}^\dagger\,\Omega^\dagger\;[d^\dagger_{\alpha,s_1}(p^+,p)\,d^\dagger_{\beta,s_2}(q^+,q)\,d_{\beta,s_2}(q^+,q)\,d_{\alpha,s_1}(p^+,p)]\;\Omega\,\hat{S}\,\Omega^\dagger|v\rangle$$

operator that diagonalises perturbatively the Light Cone QCD Hamiltonian

eikonal S-matrix

$$\{d^{\omega}_{s_1}(k^+,k), d^{\dagger\zeta}_{s_2}(q^+,q)\} = (2\pi)^3\delta^{\omega\zeta}\delta_{s_1s_2}\delta(k^+-q^+)\delta^{(2)}(k-q)$$

quark creation operator

Quark correlations: 1610.03020

- The two-particle inclusive cross section reads:

valence state

$$\frac{d\sigma}{dp^+d^2p\,dq^+d^2q} = \frac{1}{(2\pi)^6}\langle v|\Omega\,\hat{S}^\dagger\,\Omega^\dagger\,\left[d^\dagger_{\alpha,s_1}(p^+,p)\,d^\dagger_{\beta,s_2}(q^+,q)\,d_{\beta,s_2}(q^+,q)\,d_{\alpha,s_1}(p^+,p)\right]\,\Omega\,\hat{S}\,\Omega^\dagger|v\rangle$$

operator that diagonalises perturbatively the Light Cone QCD Hamiltonian

eikonal S-matrix

$$\{d^\omega_{s_1}(k^+,k),d^{\dagger\zeta}_{s_2}(q^+,q)\} = (2\pi)^3\delta^{\omega\zeta}\delta_{s_1s_2}\delta(k^+-q^+)\delta^{(2)}(k-q)$$ quark creation operator

ρ1

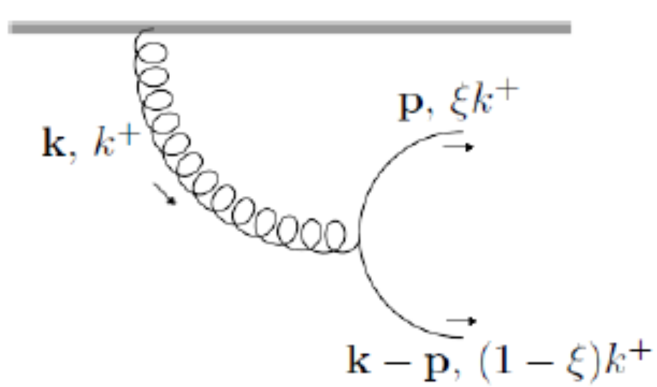

ρ2

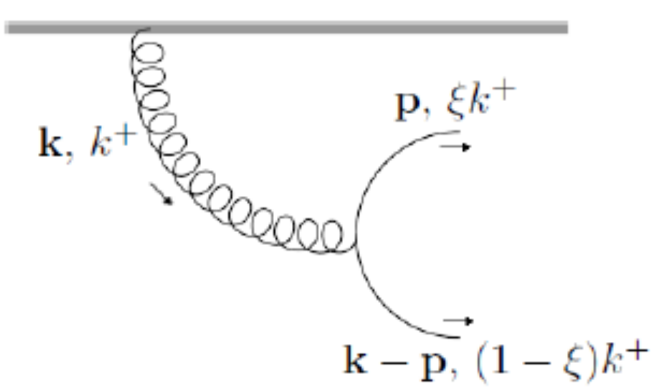

Quark correlations: 1610.03020

- The two-particle inclusive cross section reads:

valence state

$$\frac{d\sigma}{dp^+d^2p\,dq^+d^2q} = \frac{1}{(2\pi)^6}\langle v|\Omega\,\hat{S}^\dagger\,\Omega^\dagger\;[d^\dagger_{\alpha,s_1}(p^+,p)\,d^\dagger_{\beta,s_2}(q^+,q)\,d_{\beta,s_2}(q^+,q)\,d_{\alpha,s_1}(p^+,p)]\;\Omega\,\hat{S}\,\Omega^\dagger|v\rangle$$

operator that diagonalises perturbatively the Light Cone QCD Hamiltonian

eikonal S-matrix

$$\{d^\omega_{s_1}(k^+,k),d^{\dagger\zeta}_{s_2}(q^+,q)\} = (2\pi)^3\delta^{\omega\zeta}\delta_{s_1s_2}\delta(k^+-q^+)\delta^{(2)}(k-q)$$ quark creation operator

ρ1 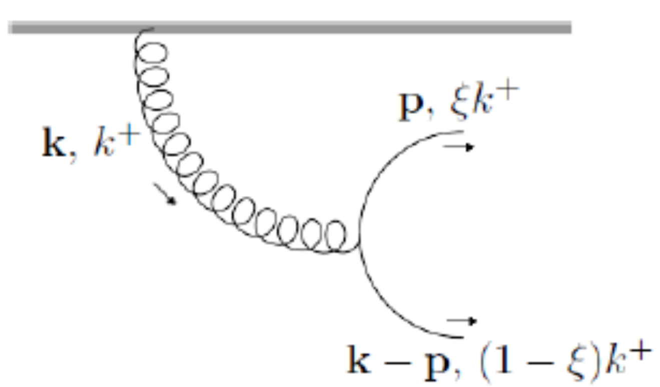

ρ2 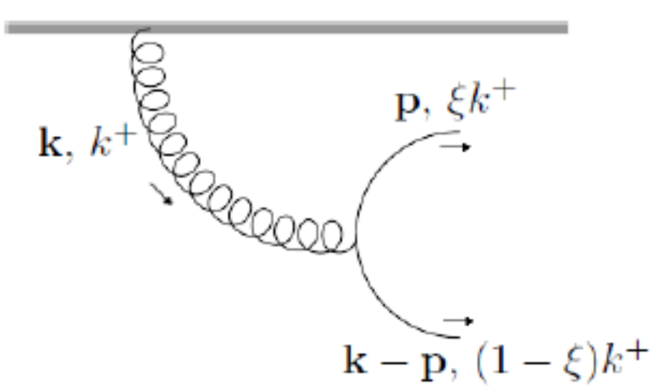

- ρg~1, so only density-enhanced contributions are taken i.e. NOT

ρ 

Quark correlations: 1610.03020

- The two-particle inclusive cross section reads:

valence state

$$\frac{d\sigma}{dp^+d^2p\,dq^+d^2q} = \frac{1}{(2\pi)^6}\langle v|\Omega\,\hat{S}^\dagger\,\Omega^\dagger\;[d^\dagger_{\alpha,s_1}(p^+,p)\,d^\dagger_{\beta,s_2}(q^+,q)\,d_{\beta,s_2}(q^+,q)\,d_{\alpha,s_1}(p^+,p)]\;\Omega\,\hat{S}\,\Omega^\dagger|v\rangle$$

operator that diagonalises perturbatively the Light Cone QCD Hamiltonian

eikonal S-matrix

$$\{d^\omega_{s_1}(k^+,k),d^{\dagger\zeta}_{s_2}(q^+,q)\} = (2\pi)^3\delta^{\omega\zeta}\delta_{s_1s_2}\delta(k^+-q^+)\delta^{(2)}(k-q)$$ quark creation operator

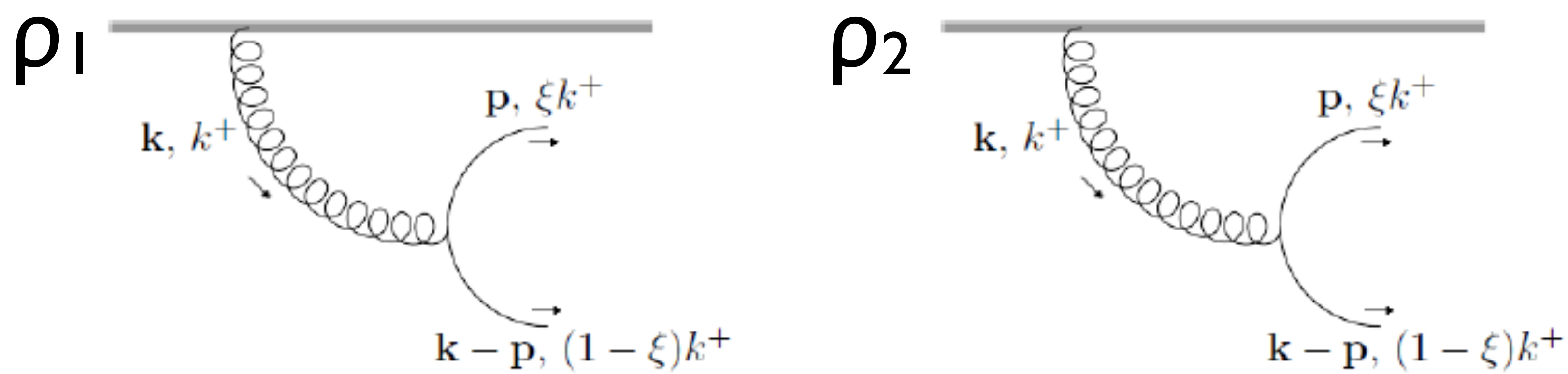

- Performing Gaussian (MV) averages of projectile and target colour charges, we get Pauli blocking ($\propto -\delta^{(2)}(p-q)$) that results short range in rapidity.

$$\left\langle \rho^a(k)\rho^b(p)\right\rangle_P = (2\pi)^2\mu^2(k)\;\delta^{ab}\;\delta^{(2)}(k+p)$$

To think about:

- Baryon-baryon correlations show features that seem suggestive of Pauli blocking; a similar effect seen [PRL57(1986)3140] in e^+e^- but there modifications of hadronisation reproduced the data.

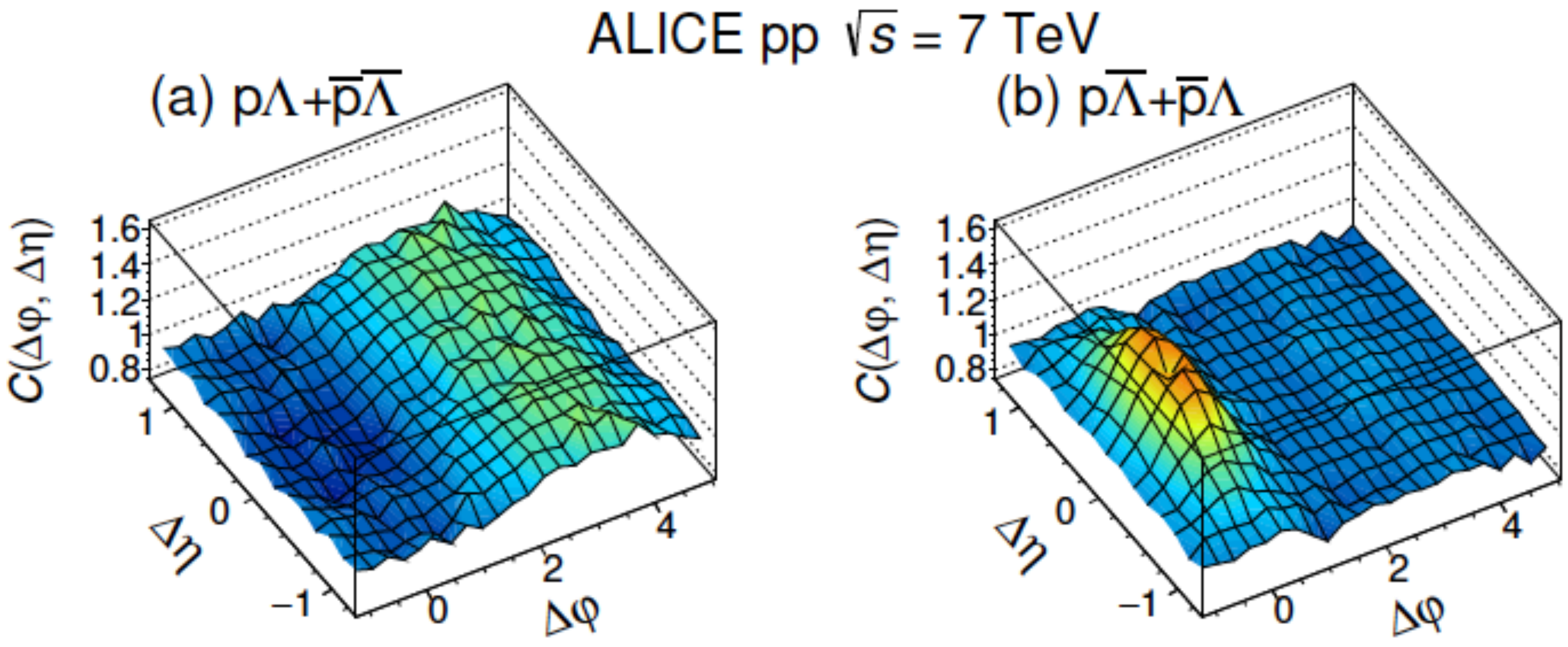

1612.08975

$$C(\varphi_1,\eta_1,\varphi_2,\eta_2)=\frac{P_{12}(\varphi_1,\eta_1,\varphi_2,\eta_2)}{P_1(\varphi_1,\eta_1)P_2(\varphi_2,\eta_2)}$$

To think about:

- Baryon-baryon correlations show features that seem suggestive of Pauli blocking; a similar effect seen [PRL57(1986)3140] in e^+e^- but there modifications of hadronisation reproduced the data.

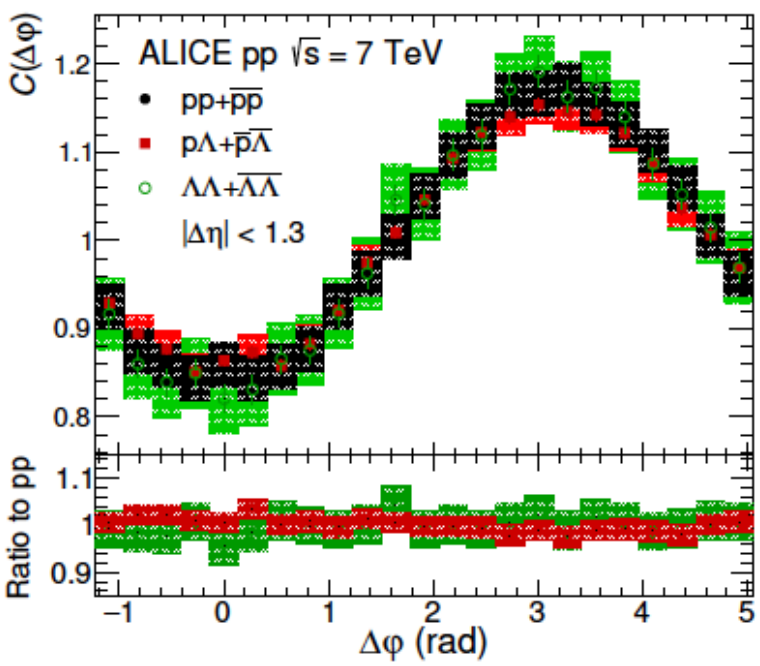

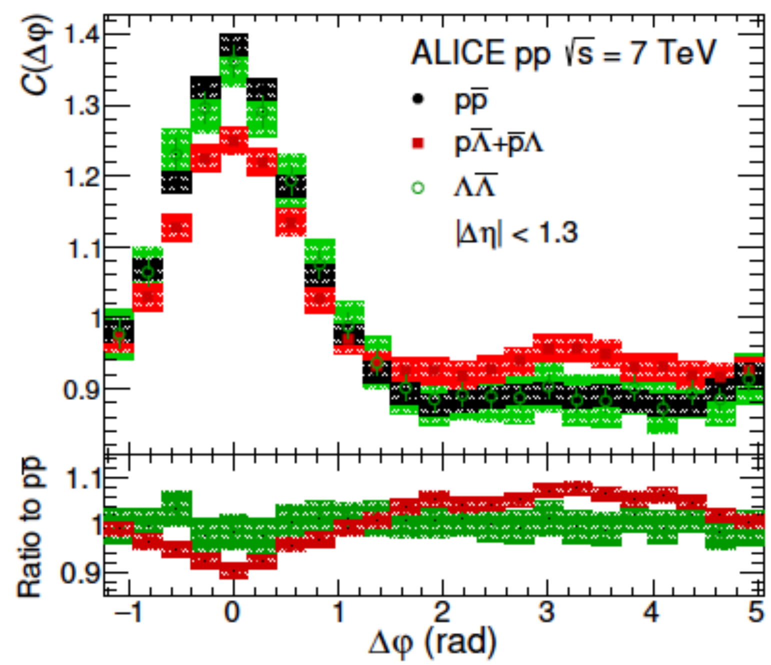

1612.08975

$$C(\varphi_1,\eta_1,\varphi_2,\eta_2) = \frac{P_{12}(\varphi_1,\eta_1,\varphi_2,\eta_2)}{P_1(\varphi_1,\eta_1)P_2(\varphi_2,\eta_2)}$$

To think about:

- Baryon-baryon correlations show features that seem suggestive of Pauli blocking; a similar effect seen [PRL57(1986)3140] in e^+e^- but there modifications of hadronisation reproduced the data.

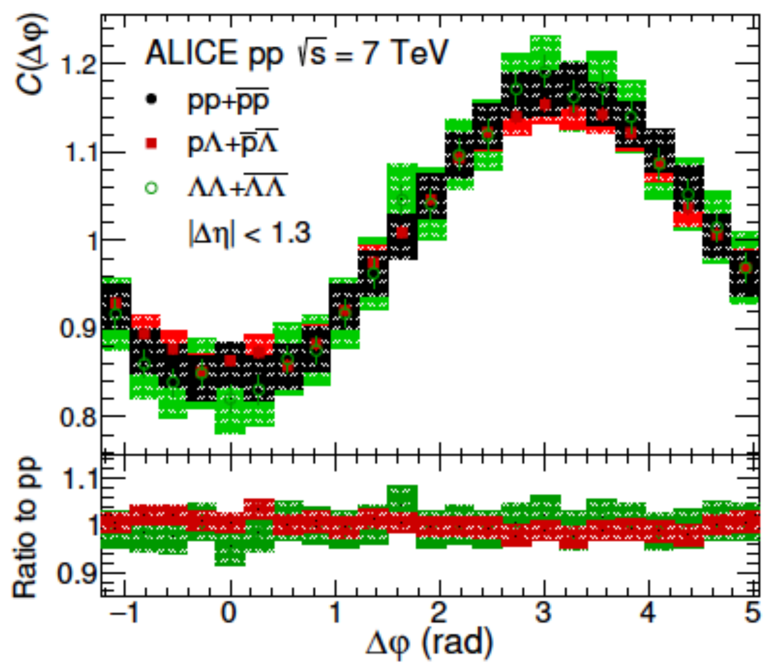

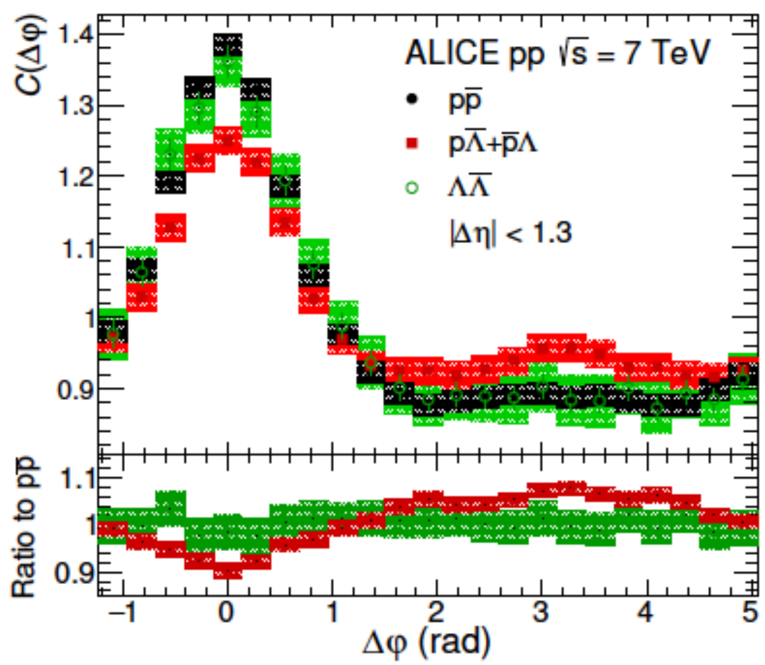

1612.08975

$$C(\varphi_1,\eta_1,\varphi_2,\eta_2)=\frac{P_{12}(\varphi_1,\eta_1,\varphi_2,\eta_2)}{P_1(\varphi_1,\eta_1)P_2(\varphi_2,\eta_2)}$$

- Quark correlations could contribute to charge correlations (proposed as signals of Chiral Magnetic Effect).

CMS, 1610.00263

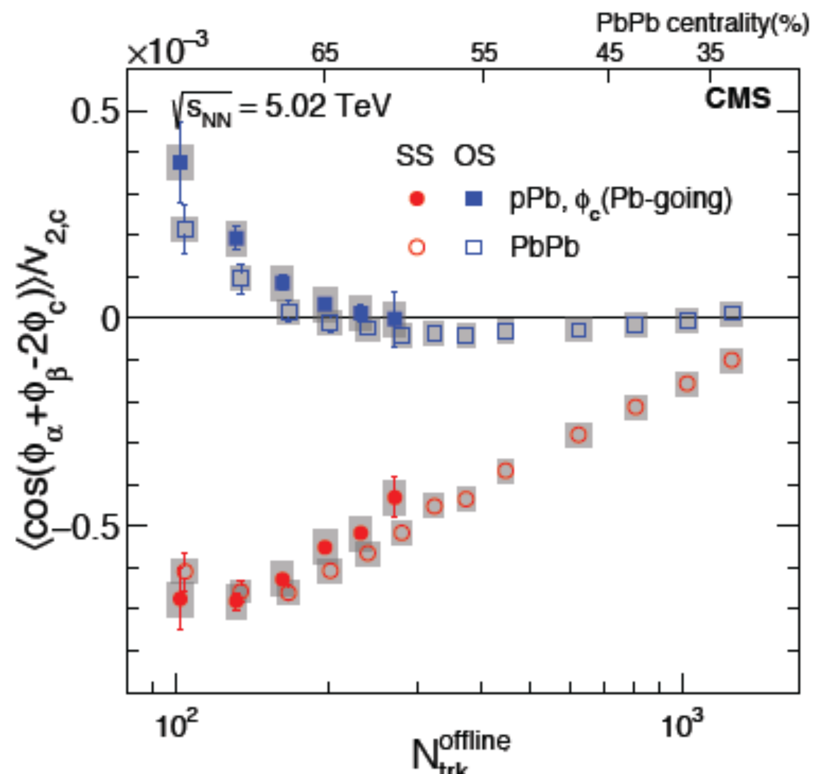

NLO particle production:

- Light and heavy production computed at NLO in the hybrid formalism: collinear parton through a dense target, forward η, yields LO DGLAP PDFs/FFs and LO BK dipoles. [Chirilli-Xiao-Yuan+Stasto-Zaslavsky-Wanatabe, Altinoluk-Kovner+Armesto-Beuf-Lublinsky, Kang-Vitev-Xing, Ducloue-Lappi-Mantysaari-Zhu]

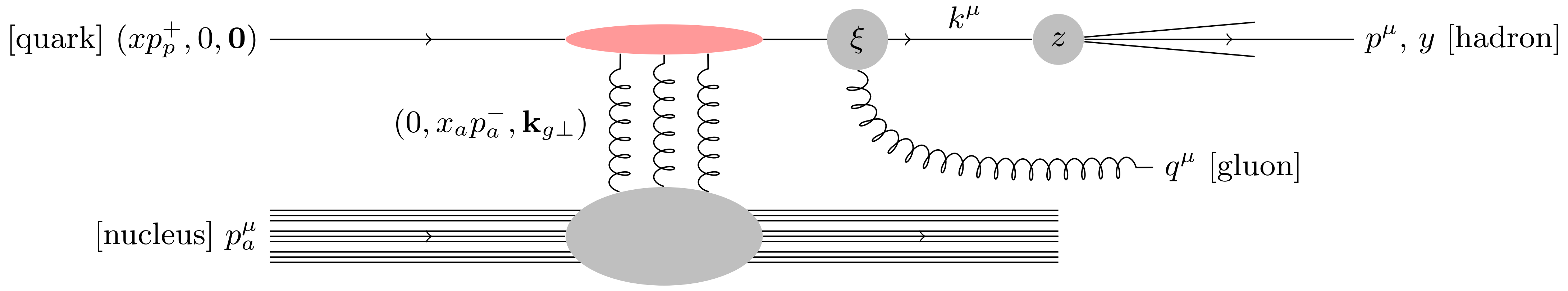

NLO particle production:

- Light and heavy production computed at NLO in the hybrid formalism: collinear parton through a dense target, forward η, yields LO DGLAP PDFs/FFs and LO BK dipoles. [Chirilli-Xiao-Yuan+Stasto-Zaslavsky-Wanatabe, Altinoluk-Kovner+Armesto-Beuf-Lublinsky, Kang-Vitev-Xing, Ducloue-Lappi-Mantysaari-Zhu]

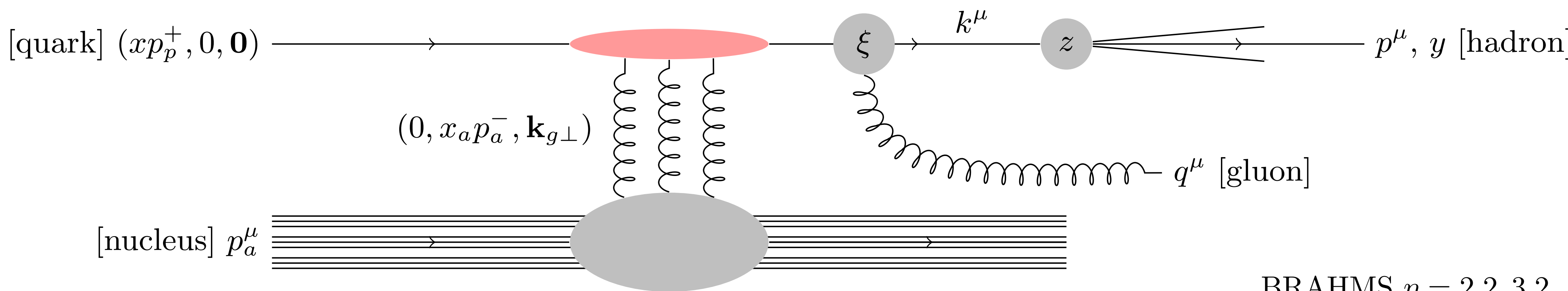

- Negative results at large rapidities from the original CXY calculation, with dependence on the choice of dipole.

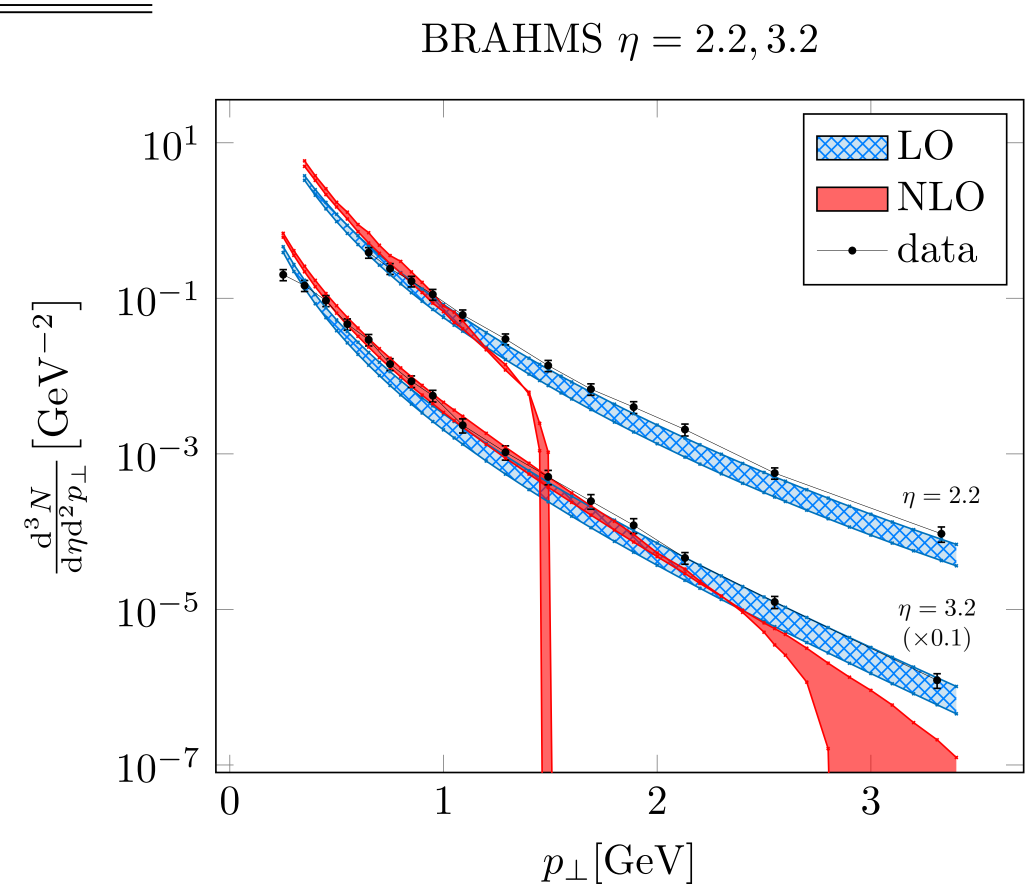

NLO particle production:

- Light and heavy production computed at NLO in the hybrid formalism: collinear parton through a dense target, forward η, yields LO DGLAP PDFs/FFs and LO BK dipoles. [Chirilli-Xiao-Yuan+Stasto-Zaslavsky-Wanatabe, Altinoluk-Kovner+Armesto-Beuf-Lublinsky, Kang-Vitev-Xing, Ducloue-Lappi-Mantysaari-Zhu]

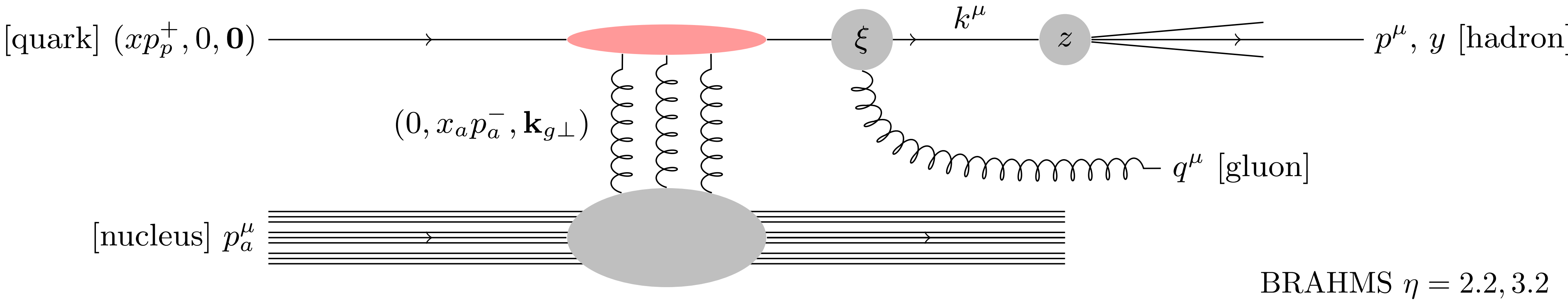

- Negative results at large rapidities from the original CXY calculation, with dependence on the choice of dipole.

➜ Note: hybrid valid for $p_T^2/s_0 << 1$.

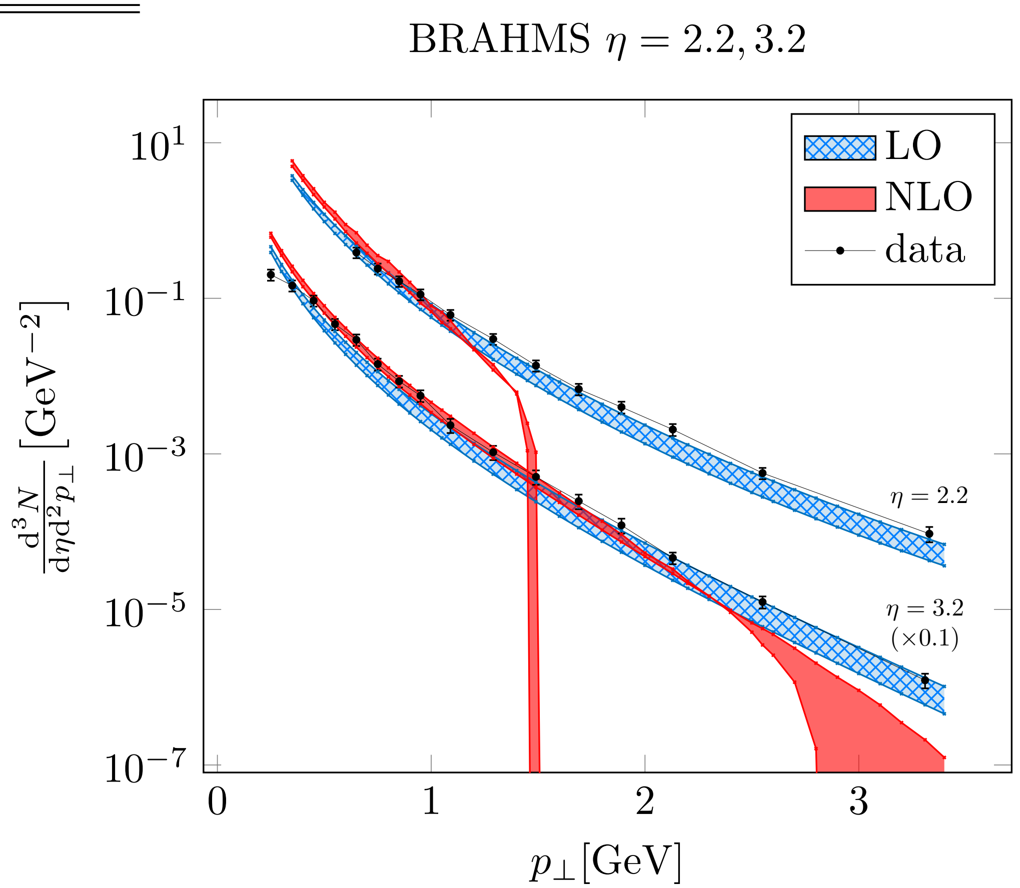

Restricting times:

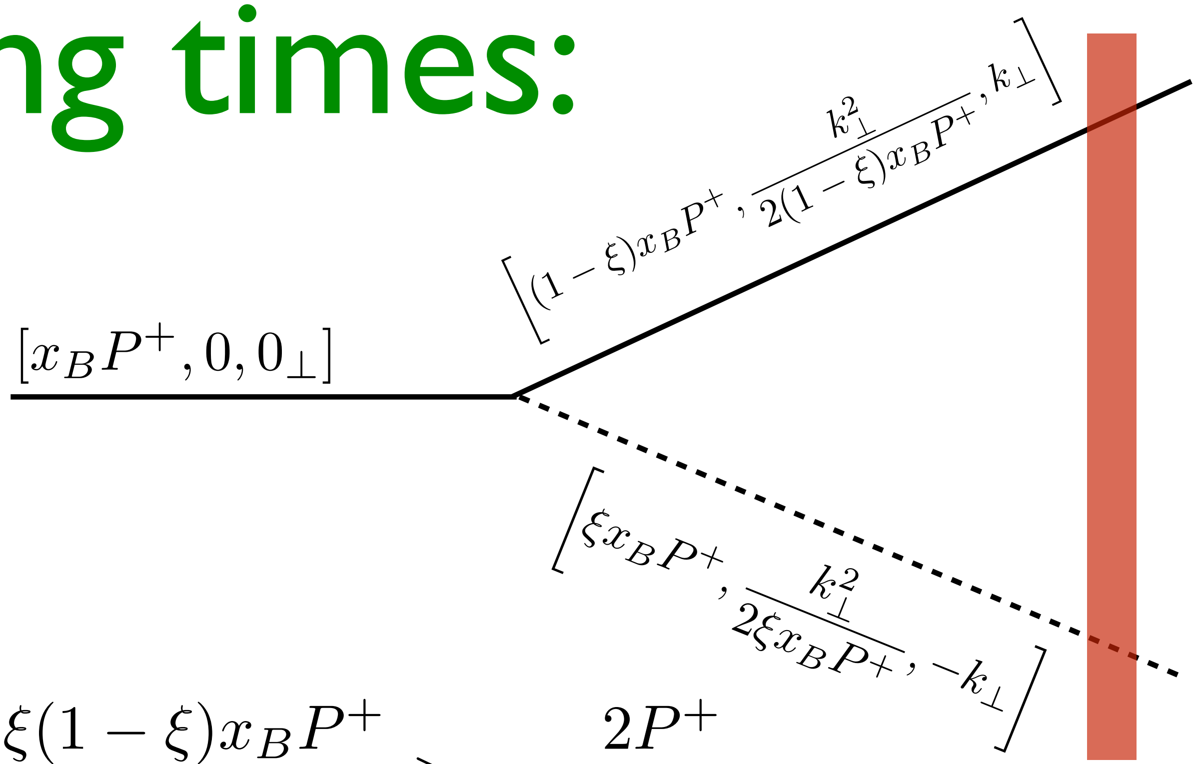

• Only fluctuations that are long lived are resolved coherently by the target: Ioffe time restriction, equivalent to P⁻ ordering from the target nucleus.

$$P^-_{pair} = \frac{k_\perp^2}{2\xi(1-\xi)x_B P^+} < P^-_T \Longrightarrow t_{Ioffe} = \frac{2\xi(1-\xi)x_B P^+}{k_\perp^2} > \tau = \frac{2P^+}{s_0}$$

Restricting times:

- Only fluctuations that are long lived are resolved coherently by the target: Ioffe time restriction, equivalent to P⁻ ordering from the target nucleus.

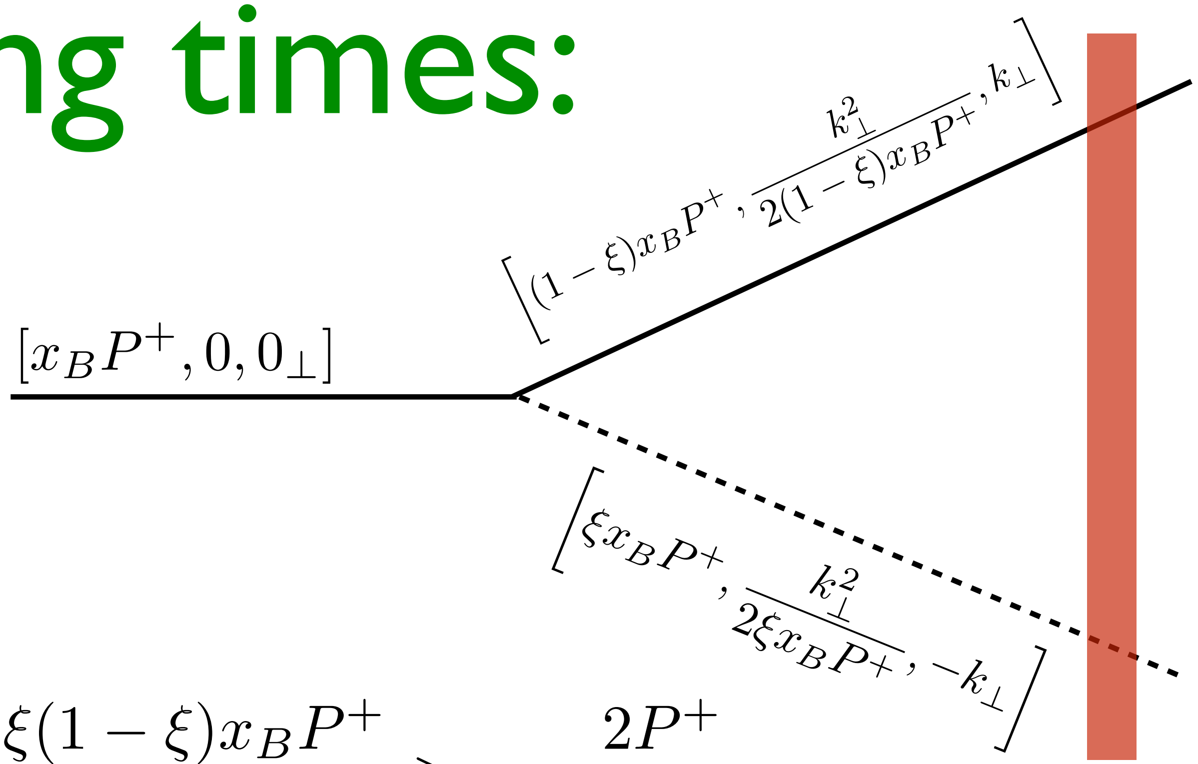

$$P^-_{pair} = \frac{k_\perp^2}{2\xi(1-\xi)x_B P^+} < P^-_T \Longrightarrow t_{Ioffe} = \frac{2\xi(1-\xi)x_B P^+}{k_\perp^2} > \tau = \frac{2P^+}{s_0}$$

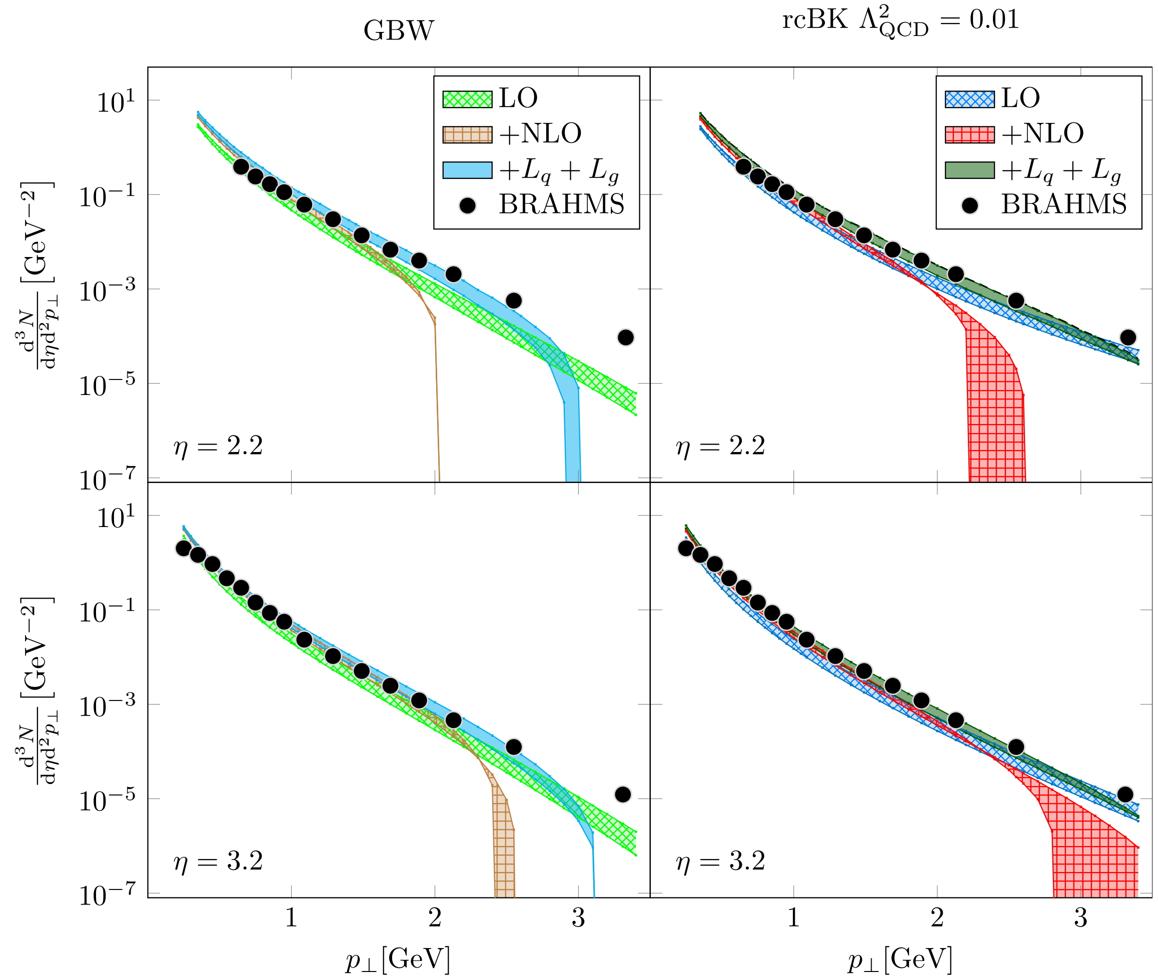

Restricting times:

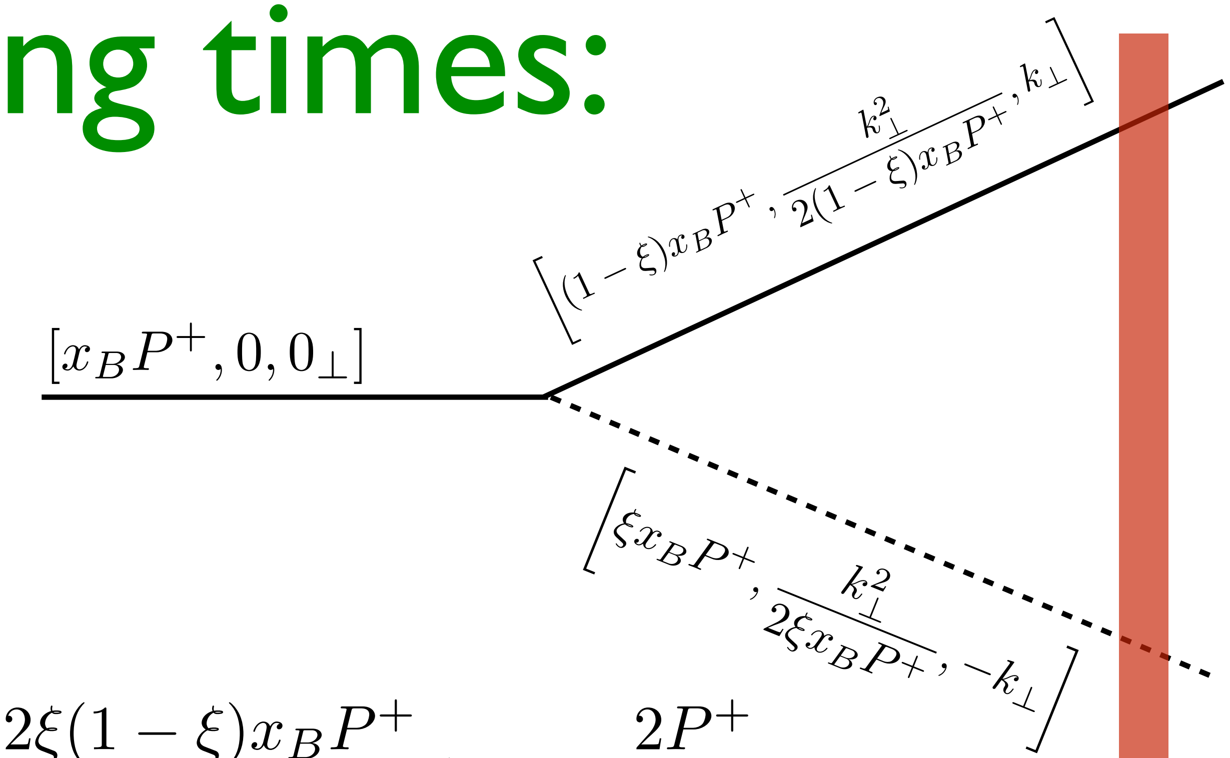

- Only fluctuations that are long lived are resolved coherently by the target: Ioffe time restriction, equivalent to P⁻ ordering from the target nucleus.

$$P^-_{pair} = \frac{k_\perp^2}{2\xi(1-\xi)x_B P^+} < P^-_T \Longrightarrow t_{Ioffe} = \frac{2\xi(1-\xi)x_B P^+}{k_\perp^2} > \tau = \frac{2P^+}{s_0}$$

- It offers a natural energy cutoff for regulating soft divergencies, leading to the non-linear LO BK evolution equation.

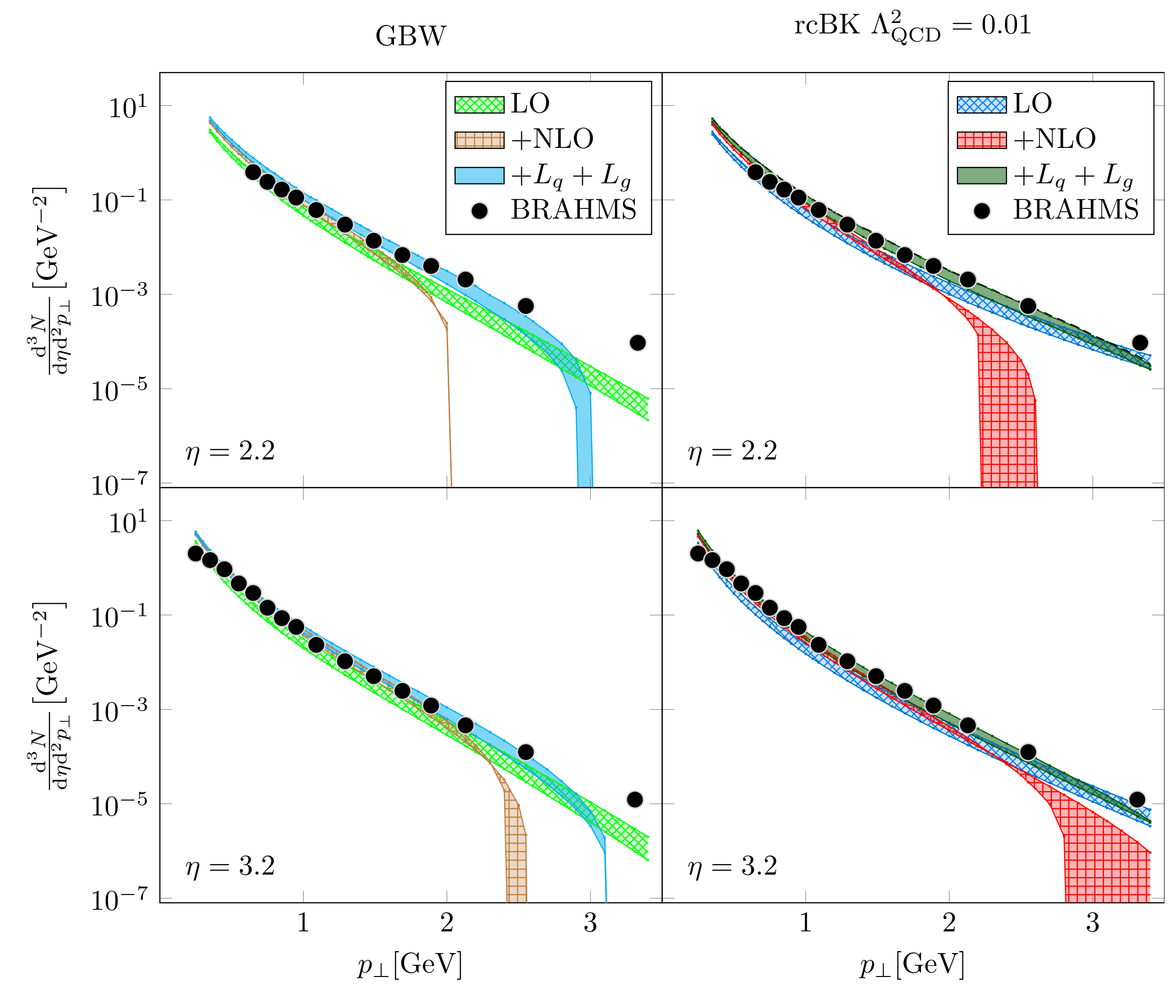

Restricting times:

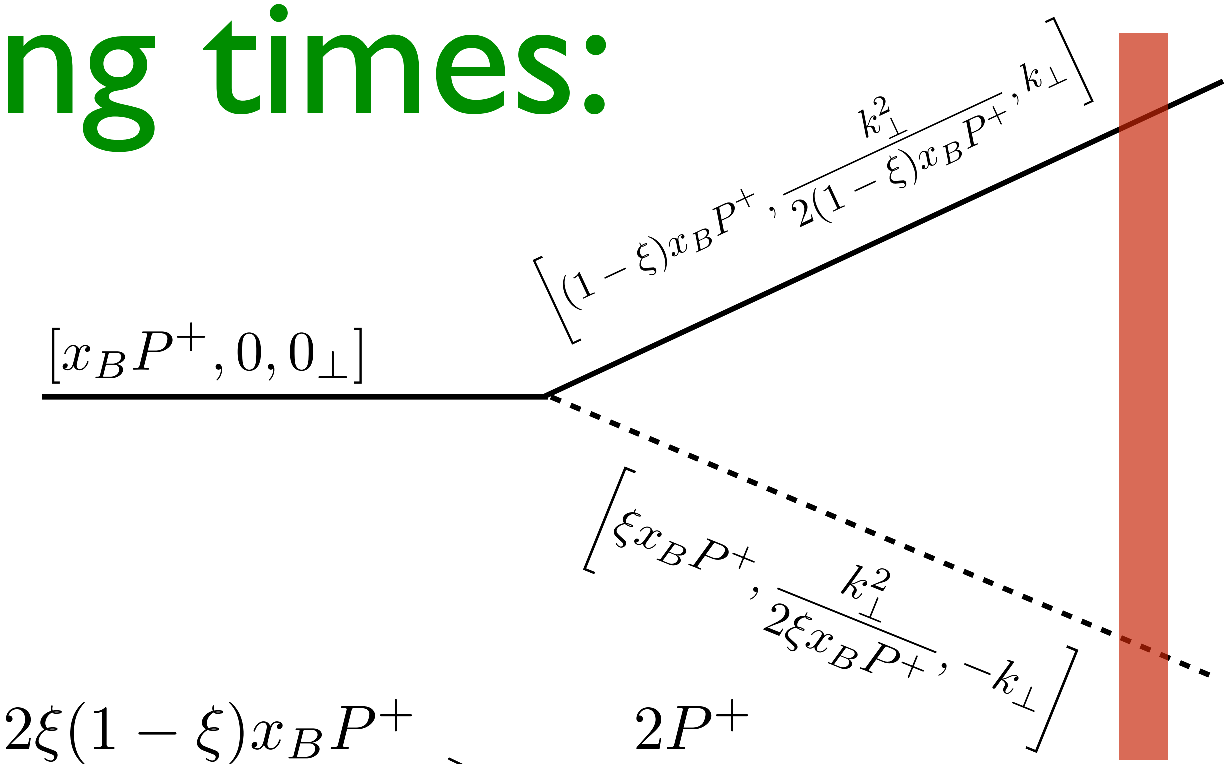

- Only fluctuations that are long lived are resolved coherently by the target: Ioffe time restriction, equivalent to P- ordering from the target nucleus.

$$P^-_{pair} = \frac{k_\perp^2}{2\xi(1-\xi)x_B P^+} < P^-_T \Longrightarrow t_{Ioffe} = \frac{2\xi(1-\xi)x_B P^+}{k_\perp^2} > \tau = \frac{2P^+}{s_0}$$

- It offers a natural energy cutoff for regulating soft divergencies, leading to the non-linear LO BK evolution equation.
- It lies at the root of present attempts to cure deficiencies of NLO BK and single particle production [Iancu-Mueller-Tryantafillopoulos, Lappi-Ducloue-Zhu].

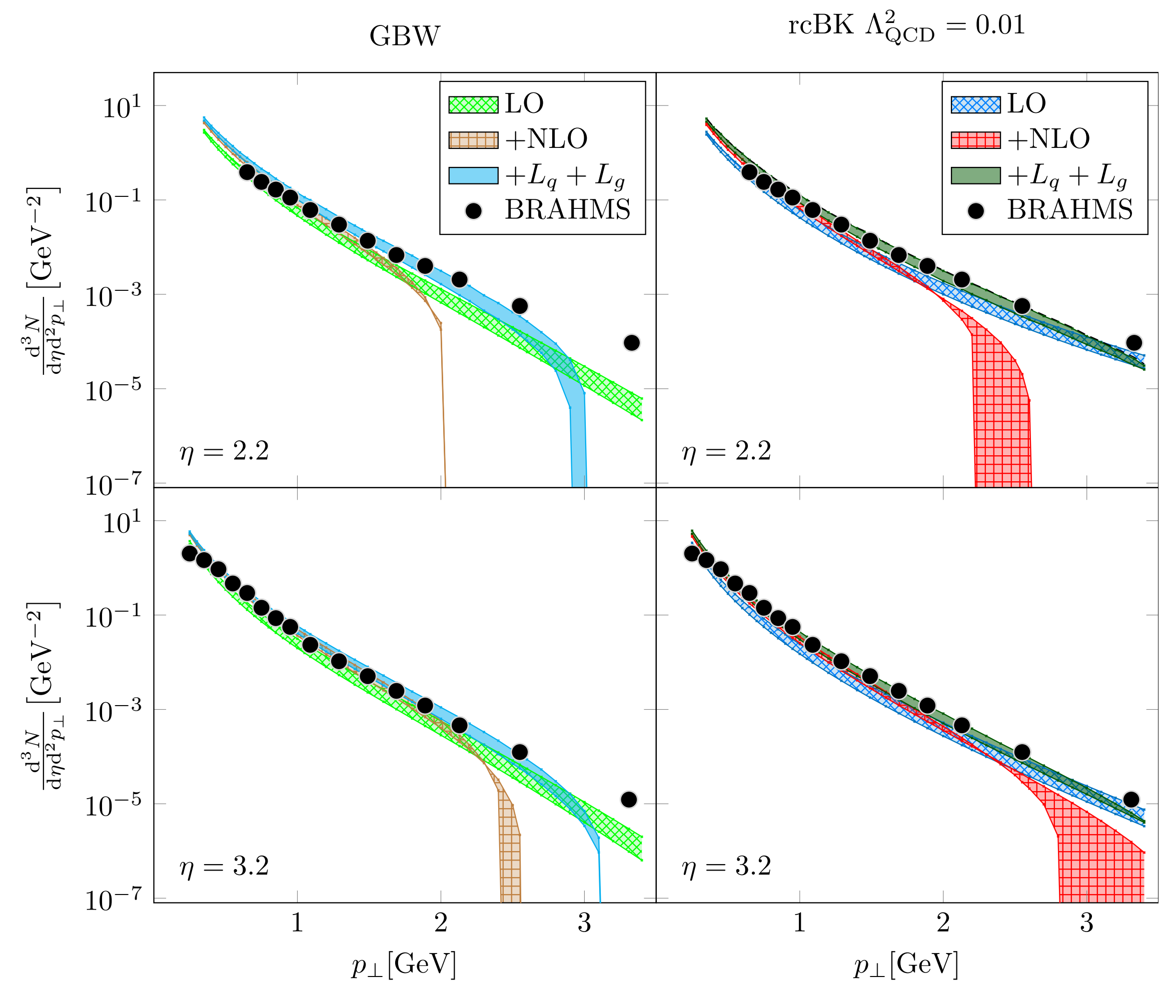

Contents:

See the talks by Jean-Paul Blaizot, Leticia Cunqueiro, Enrico Scomparin and Urs Wiedemann.

Disclaimer: this a personal selection of topics, not a comprehensive overview.

Hard probes:

- The collision provides self-generated probes with a large scale (pQCD): yield to be compared with that in pp and pA - benchmark.

- Hadronisation assumed to happen outside the medium (except for QQbar).

- I will discuss radiative energy loss (medium-induced gluon radiation) that is assumed to dominate for high parton energies.

[d'Enterria]

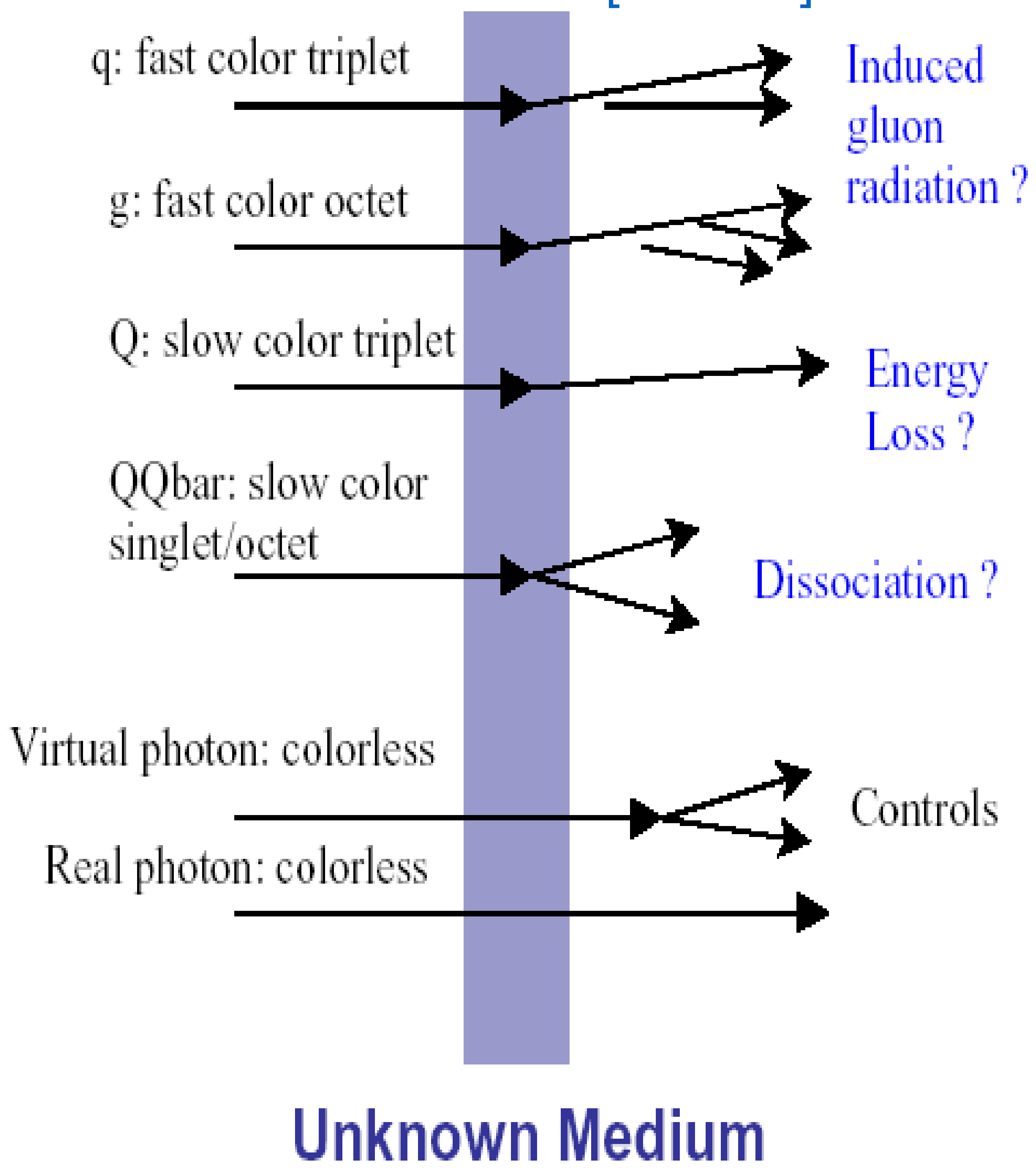

Hard probes:

$$R = \frac{\text{measured in pA, AA}}{\text{expected if no nuclear effects}}$$

- The collision provides self-generated probes with a large scale (pQCD): yield to be compared with that in pp and pA - benchmark.

- Hadronisation assumed to happen outside the medium (except for QQbar).

- I will discuss radiative energy loss (medium-induced gluon radiation) that is assumed to dominate for high parton energies.

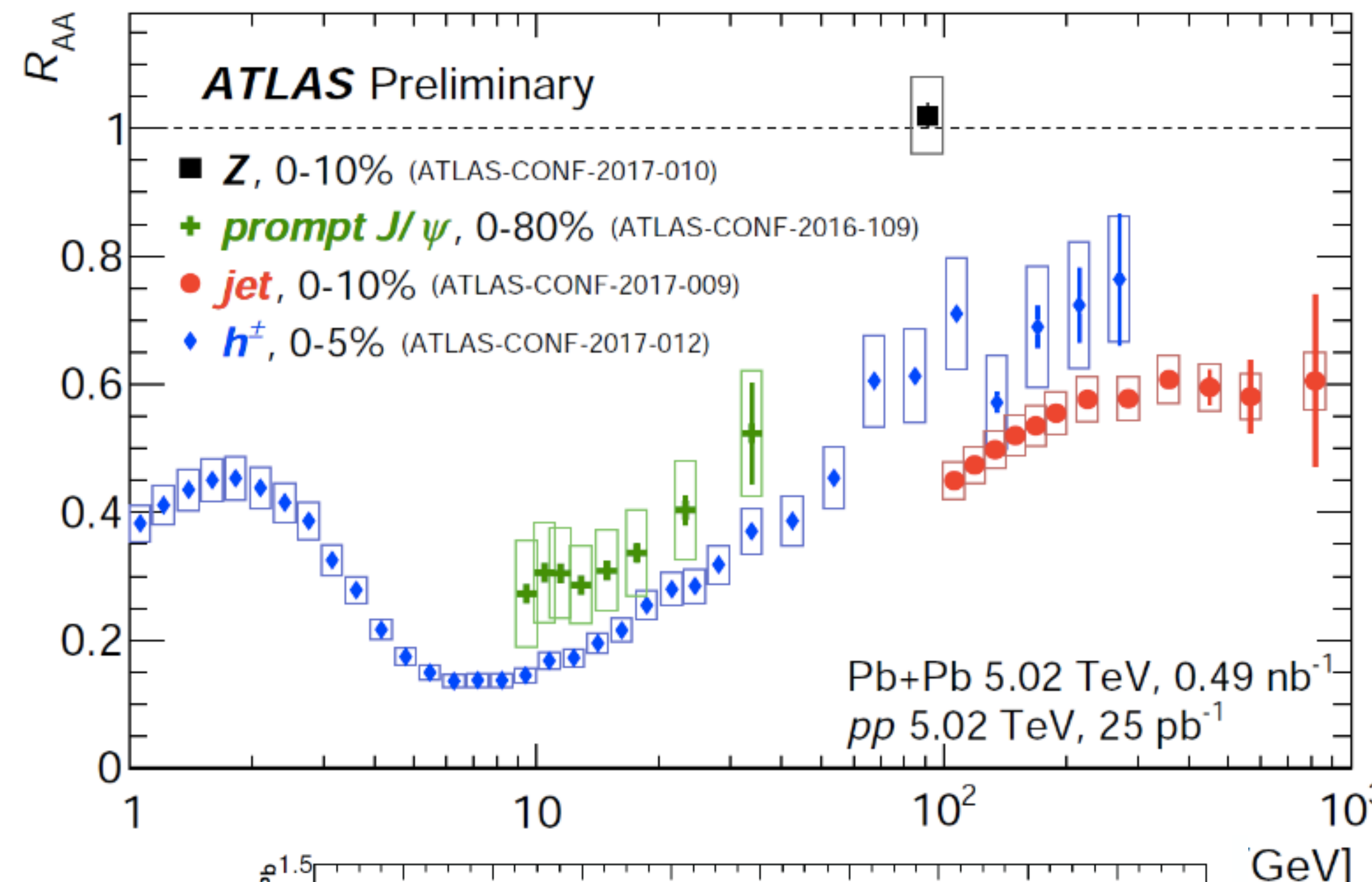

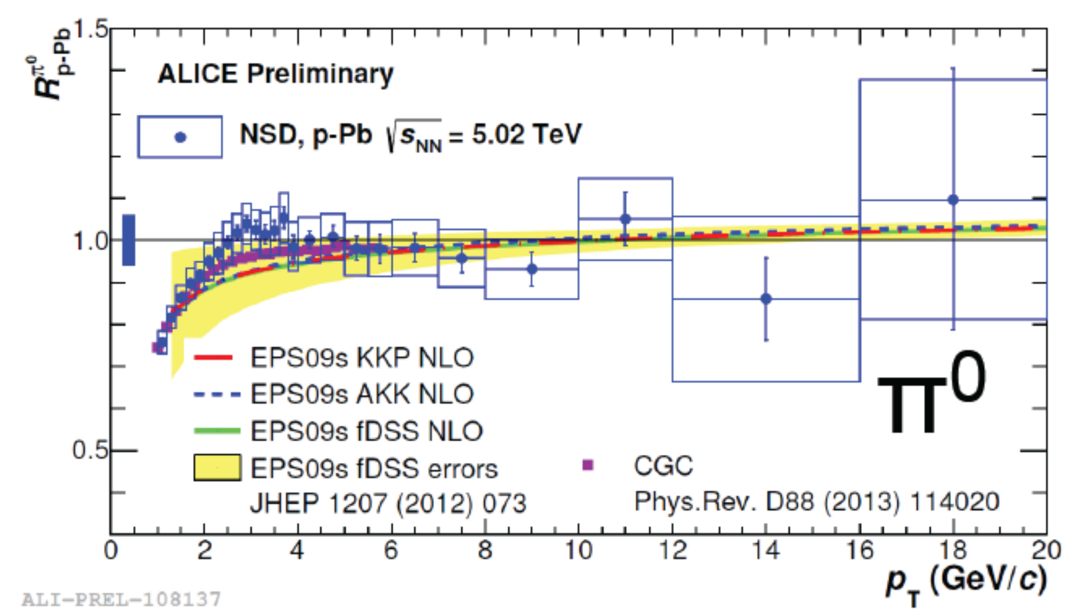

Single-source coherence (I):

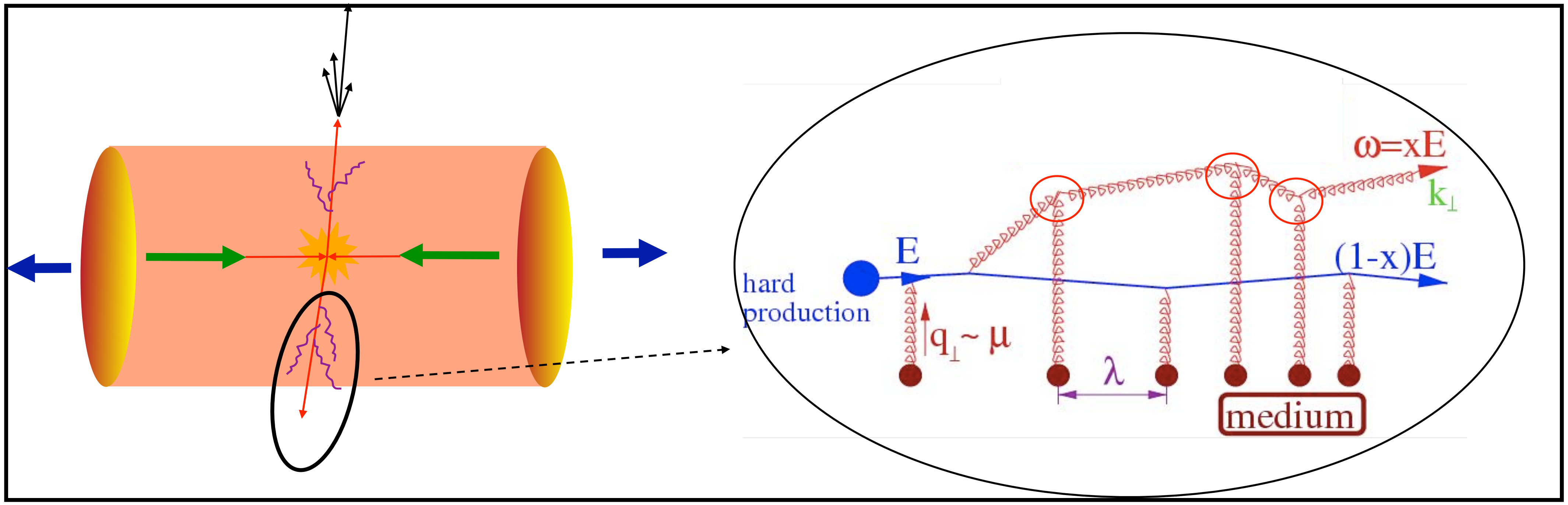

- Consider the de-coherence process |qg> → |q>+|g> and define the transport coefficient qhat=μ^2/λ.

- Remember the non-eikonal phase: $\exp\left[-ik_T^2(x_{2+}-x_{1+})/(2p_+)\right]$

$$\phi = \frac{k_T^2}{2\omega}\Delta z \sim 1 \Rightarrow \omega, k_T^2 \ll 1 \quad \text{suppressed}$$

$$\phi \sim \frac{\hat{q}L}{2\omega}L = \frac{\omega_c}{\omega} \sim 1 \Rightarrow \omega > \omega_c \quad \text{suppressed}$$

Single-source coherence (II):

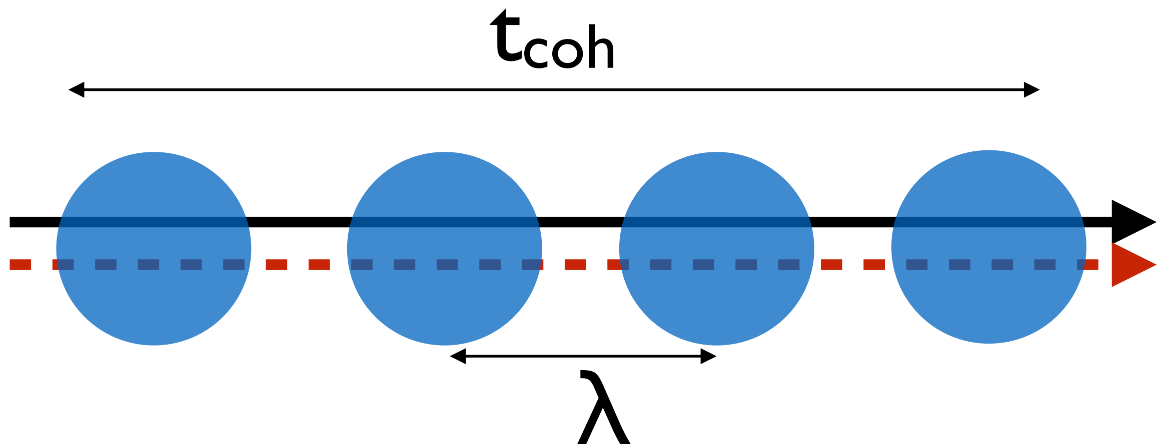

$$\omega \left.\frac{dI}{d\omega dz}\right|_{1\;scatt} \simeq \frac{\alpha_s}{\lambda}$$

$$\hat{q}t_{coh} \simeq \frac{\hat{q}\omega}{\langle k_T^2\rangle} \simeq \langle k_T^2\rangle, \quad \langle k_T^2\rangle \simeq \sqrt{\hat{q}\omega} \qquad t_{coh} = \sqrt{\frac{\omega}{\hat{q}}}, \quad N_{coh} = \frac{t_{coh}}{\lambda}$$

- The incoherent spectrum in the region ω_{GB}=qhatλ^2<<ω<<E is reduced by the number of incoherent scatterings during the coherence time of the pair (LPM effect in QED):

$$-\frac{dE}{dz} = \int d\omega \frac{1}{N_{coh}} \omega \left.\frac{dI}{d\omega dz}\right|_{1\;scatt} \simeq \alpha_s C_R \int_{\omega_{GB}}^{\omega_c} d\omega \sqrt{\frac{\hat{q}}{\omega}} \Longrightarrow -\Delta E \propto \alpha_s C_R \hat{q} L^2$$

- The final spectrum (BDPMS-Z-W/GLV) becomes infrared and collinear safe, to be constrasted with the vacuum.

Theory:

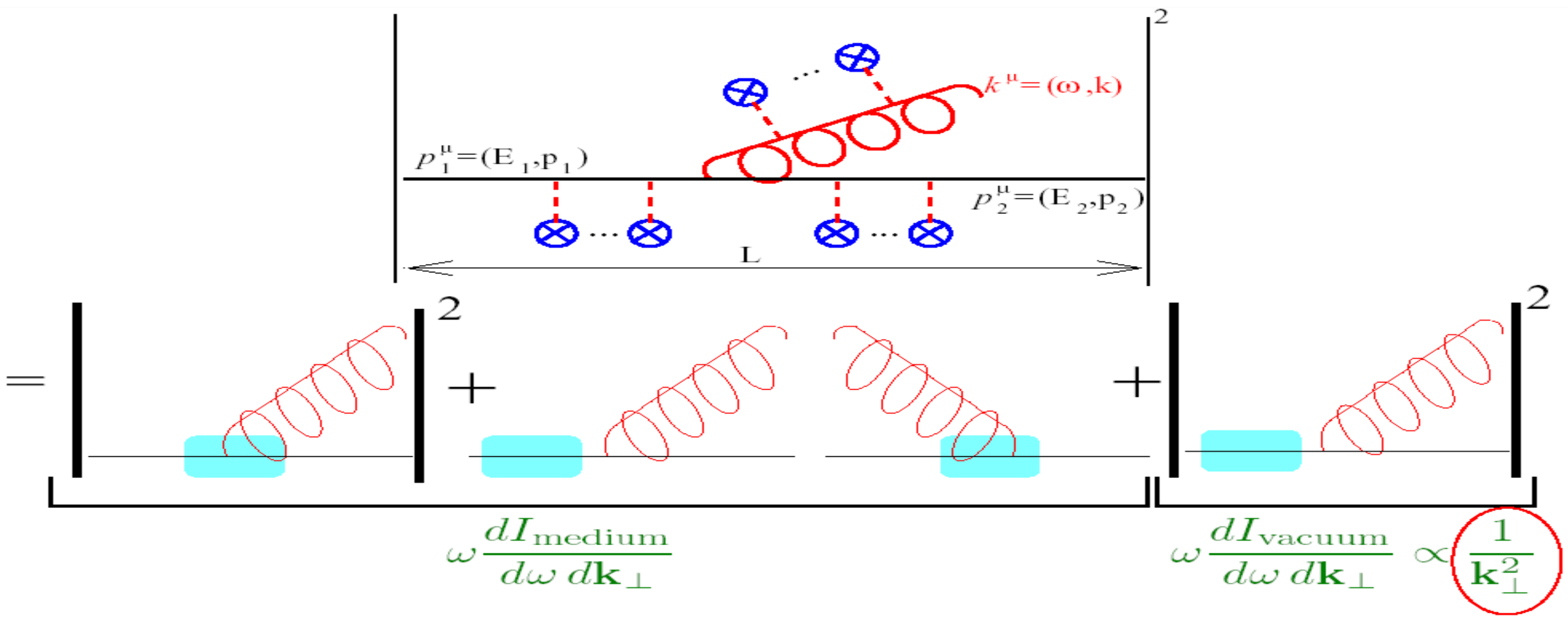

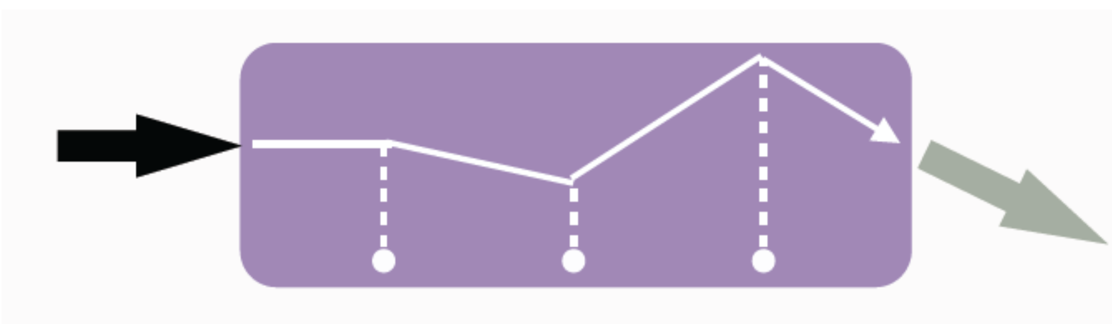

- Two parameters define the medium: one characterizing the density and strength of interactions with the medium, plus the length (geometry, dynamical expansion).
- You compute your diagrams using modified (non-eikonal propagators:

$$G(x_{0+},\mathbf{x_{0\perp}};L_+,\mathbf{x}_\perp|p_+)=\int_{\mathbf{r}_\perp(x_{0+})=\mathbf{x_{0\perp}}}^{\mathbf{r}_\perp(L_+)=\mathbf{x}_\perp}\mathcal{D}\mathbf{r}_\perp(\xi)\exp\left\{\frac{ip_+}{2}\int_{x_{0+}}^{L_+}d\xi\,\left(\frac{d\mathbf{r}_\perp}{d\xi}\right)^2\right\}$$
$$\times W(x_{0+},L_+;\mathbf{r}_\perp(\xi)),$$

Initial/Final coordinates

Theory:

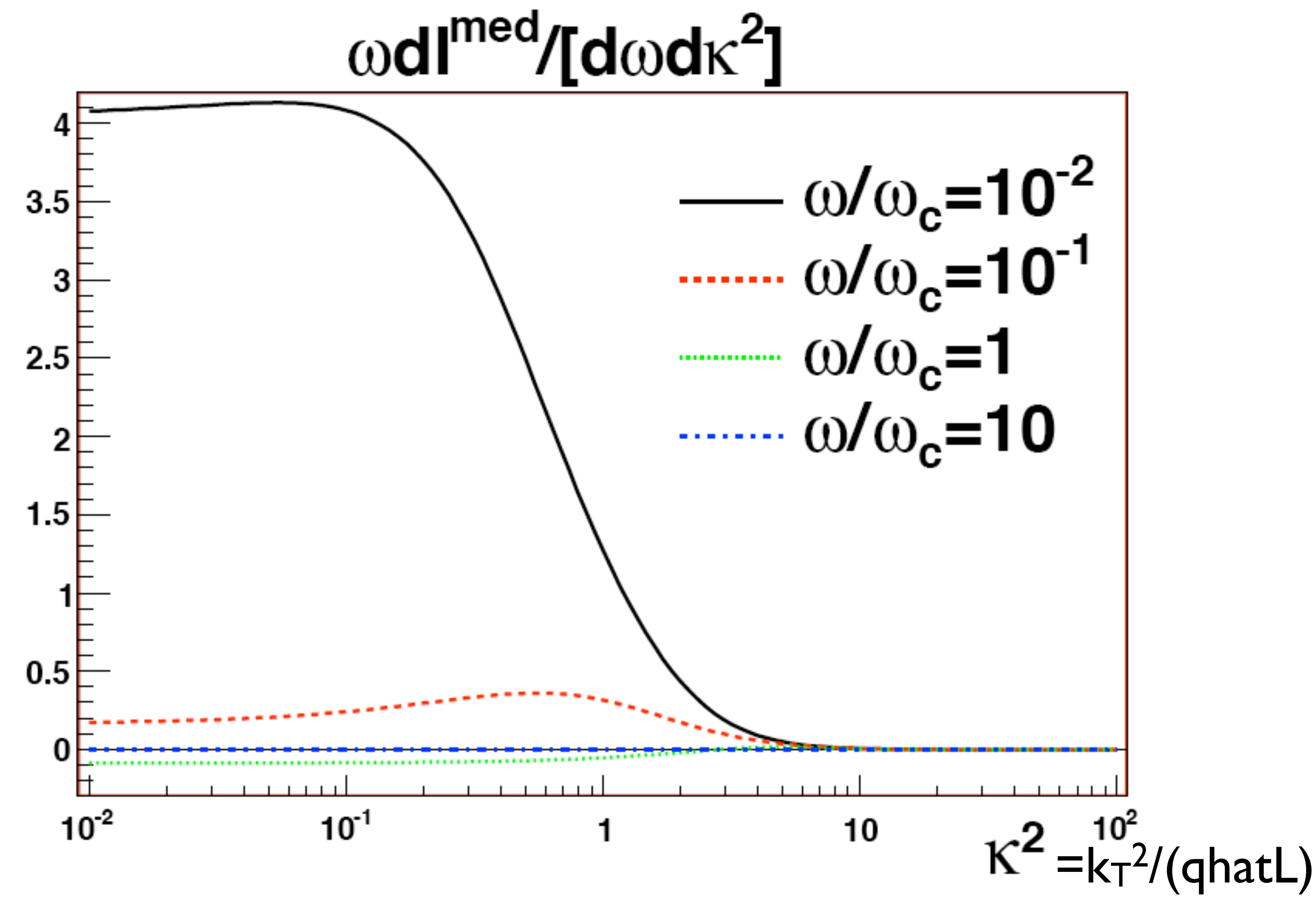

- Two parameters define
e medium: one
aracterizing the density
d strength of
eractions with the
edium, plus the length
eometry, dynamical
pansion).
- 'ou compute your
grams using modified
on-eikonal propagators:

$$G(x_{0+},\mathbf{x}_{0\perp};L_+,\mathbf{x}_\perp|p_+)=\int_{\mathbf{r}_\perp(x_{0+})=\mathbf{x}_{0\perp}}^{\mathbf{r}_\perp(L_+)=\mathbf{x}_\perp}\mathcal{D}\mathbf{r}_\perp(\xi)\exp\left\{\frac{ip_+}{2}\int_{x_{0+}}^{L_+}d\xi\,\left(\frac{d\mathbf{r}_\perp}{d\xi}\right)^2\right\}$$
$$\times W(x_{0+},L_+;\mathbf{r}_\perp(\xi)),$$

Initial/Final coordinates

Phenomenology:

- Using collinear factorisation with modified fragmentation functions, we can extract qhat from single-particle spectra and reproduce high p_T azimuthal asymmetries:

$$D_{i\to h}^{med}(x,Q^2)=\int_0^1 \frac{d\epsilon}{1-\epsilon}\,P(\epsilon)\,D_{i\to h}^{vac}\left(\frac{x}{1-\epsilon},Q^2\right)$$

Phenomenology:

- Using collinear factorisation with modified fragmentation functions, we can extract qhat from single-particle spectra and reproduce high p_T azimuthal asymmetries:

$$D_{i\to h}^{med}(x,Q^2)=\int_0^1 \frac{d\epsilon}{1-\epsilon} P(\epsilon) D_{i\to h}^{vac}\left(\frac{x}{1-\epsilon},Q^2\right)$$

quenching weights: Poisson resummation of multiple emissions, valid for dense media

Phenomenology:

- Using collinear factorisation with modified fragmentation functions, we can extract qhat from single-particle spectra and reproduce high p_T azimuthal asymmetries:

$$D_{i\to h}^{med}(x,Q^2)=\int_0^1 \frac{d\epsilon}{1-\epsilon} P(\epsilon) D_{i\to h}^{vac}\left(\frac{x}{1-\epsilon},Q^2\right)$$

quenching weights: Poisson resummation of multiple emissions, valid for dense media

- Extract qhat embedding an eloss calculation in a hydro model for bulk and fitting $R_{AA}^{charged}$. Medium more opaque at RHIC than at the LHC [1312.5003, 1506.02854], but centrality???

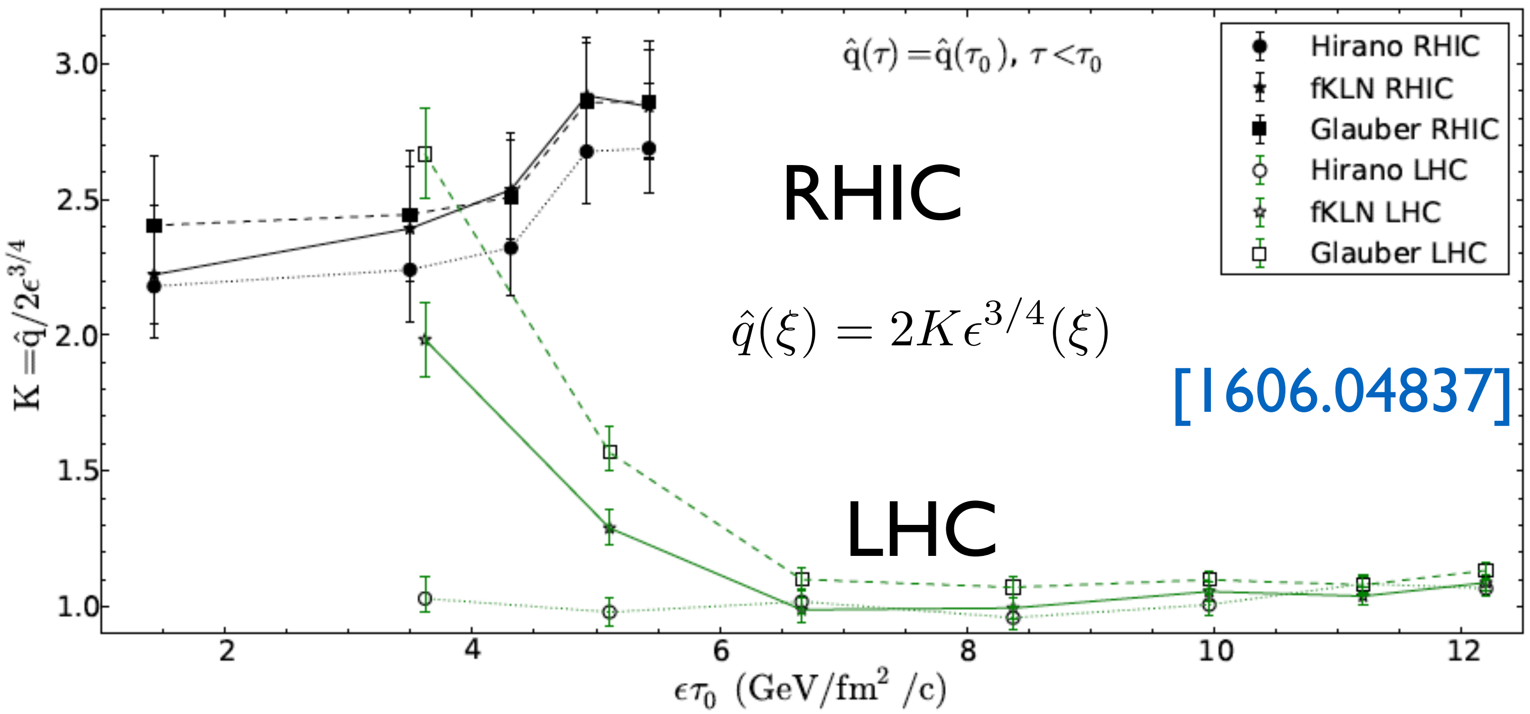

Problems:

- We do not consider properly energy-momentum (high-energy approximations), we need a full picture of parton propagation in a coloured medium (in-medium jet calculus), we need MCs.

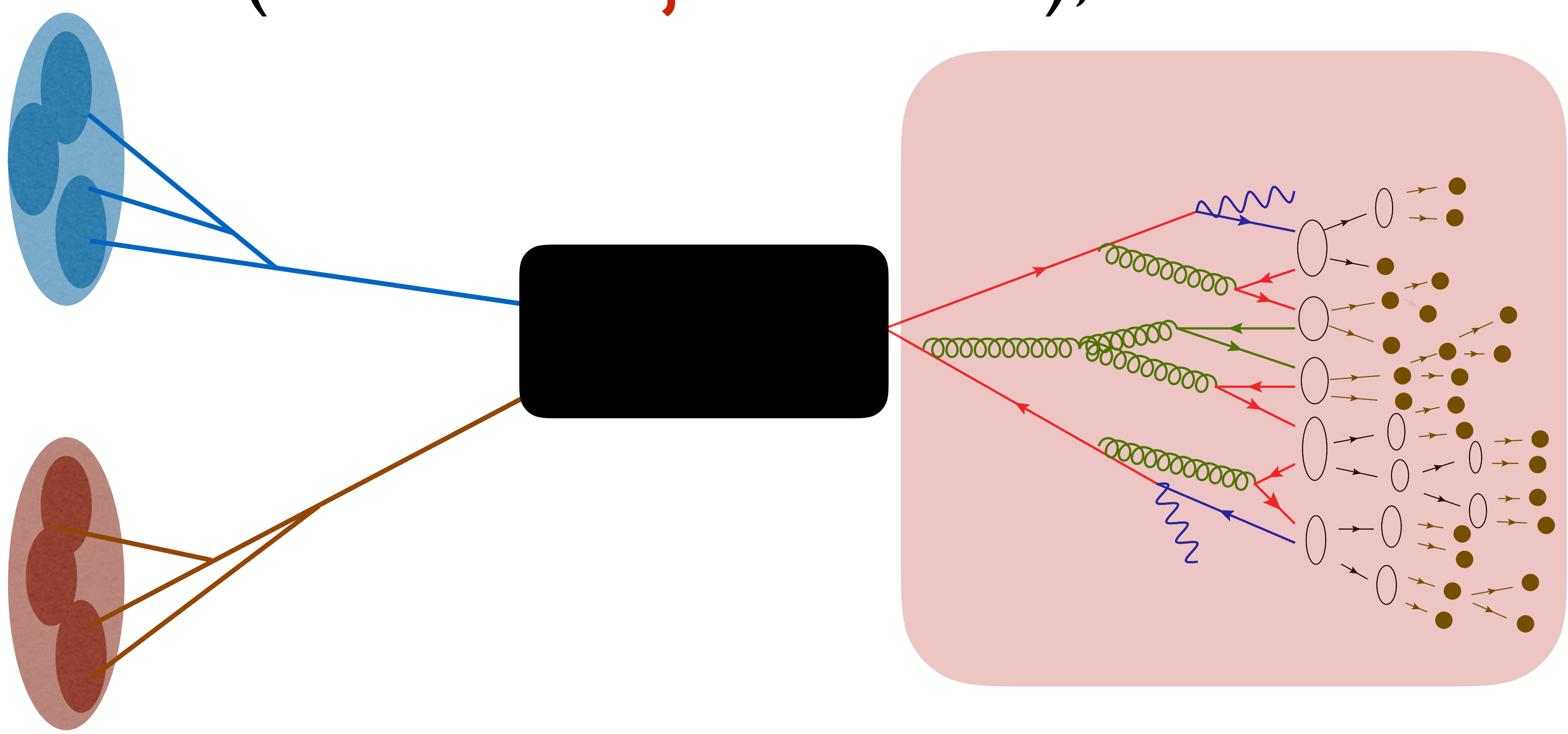

- Jet observables at the LHC (see Leticia's talk) show dijet momentum imbalance (👍), but little broadening (😕), large angle transport of momenta through soft particles (😐), and very little disruption of the core of the jet (👎): challenge to traditional BDMPS-Z-W/GLV like models.

Two emitters: vacuum

- Two-gluon tradition was essential to arrive at QCD jet calculus in the late '70s: the antenna setup offers a simplified frame to study this both in vacuum and in medium, angular ordering appears!

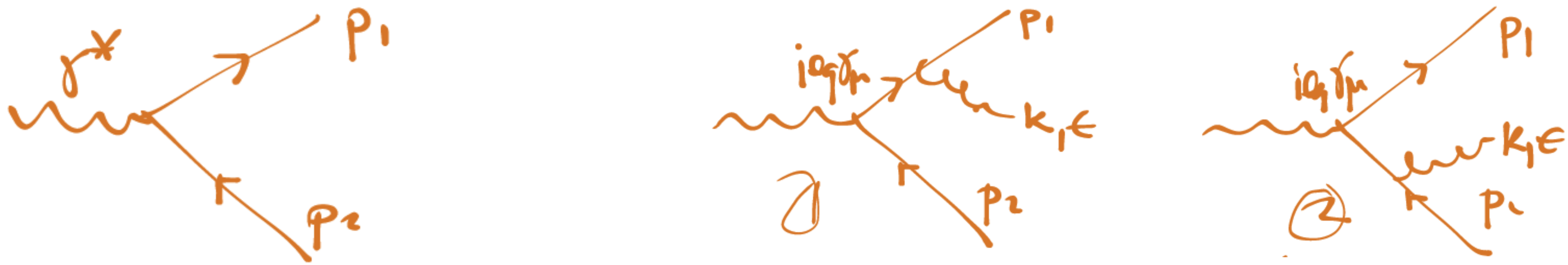

$$\mathcal{M}_{q\bar{q}g} = g_s t^a \mathcal{M}_{q\bar{q}} \left[\frac{p_1\cdot\epsilon}{p_1\cdot k} - \frac{p_2\cdot\epsilon}{p_2\cdot k} \right]$$

$$\overline{|\mathcal{M}_{q\bar{q}g}|^2} = \overline{|\mathcal{M}_{q\bar{q}}|^2}\, C_F\, g_s^2\, \frac{2\, p_1\cdot p_2}{(p_1\cdot k)(p_2\cdot k)}$$

Two emitters: vacuum

- Two-gluon tradition was essential to arrive at QCD jet calculus in the late '70s: the antenna setup offers a simplified frame to study this both in vacuum and in medium, angular ordering appears!

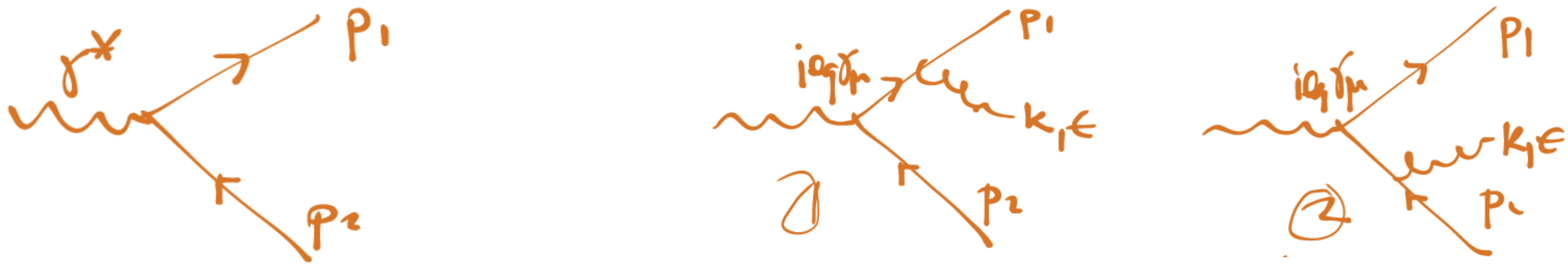

$$dN = \frac{d\omega}{\omega}\frac{d\Omega}{2\pi}\frac{\alpha_s C_F}{2\pi}\left[R_q + R_{\bar{q}} - 2J\right] =$$

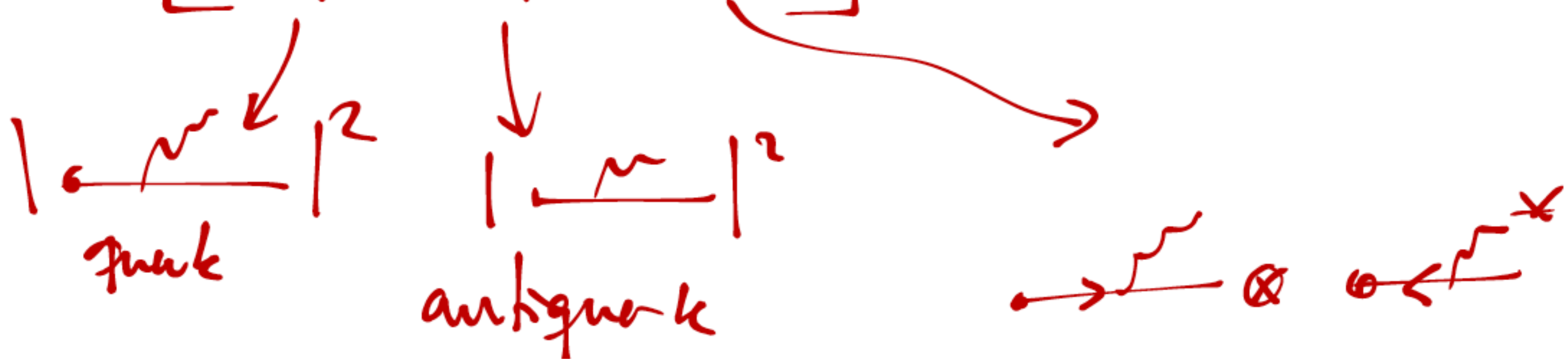

Two emitters: vacuum

- Two-gluon tradition was essential to arrive at QCD jet calculus in the late '70s: the antenna setup offers a simplified frame to study this both in vacuum and in medium, angular ordering appears!

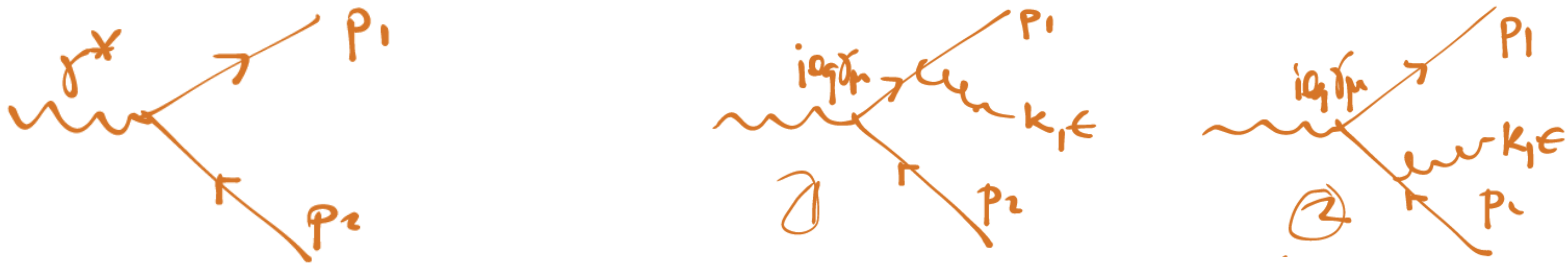

$$dN = \frac{d\omega}{\omega}\frac{d\Omega}{2\pi}\frac{\alpha_s C_F}{2\pi}\left[P_q + P_{\bar q}\right]; \quad P_q = R_q - J, \quad P_{\bar q} = R_{\bar q} - J$$

$$\int \frac{d\phi}{2\pi} P_q = \frac{1}{1-\cos\theta_q}\,\Theta\left[\theta_{q\bar q} - \theta_q\right]$$

Two emitters: vacuum

- Two-gluon tradition was essential to arrive at QCD jet calculus in the late '70s: the antenna setup offers a simplified frame to study this both in vacuum and in medium, angular ordering appears!

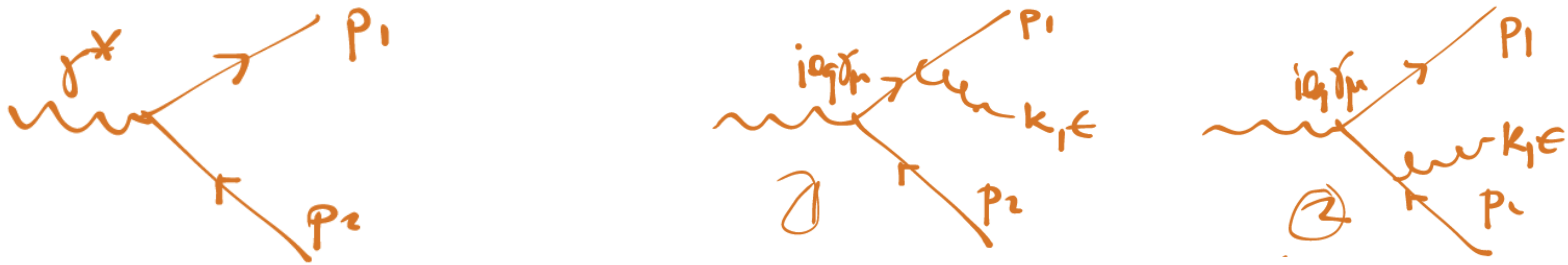

transverse size of gluon $\lambda_\perp \sim \frac{1}{k_\perp} = \frac{1}{\omega\theta}$

size of dipole at t_f $\quad r_\perp \sim \theta_{q\bar{q}}\, t_f = \frac{\theta_{q\bar{q}}}{\omega\theta^2}$

$\lambda_\perp > r_\perp \Leftrightarrow \theta > \theta_{q\bar{q}} \rightarrow$ gluon cannot resolve the dipole $\rightarrow$ suppression

Two emitters: vacuum

- Two-gluon tradition was essential to arrive at QCD jet calculus in the late '70s: the antenna setup offers a simplified frame to study this both in vacuum and in medium, angular ordering appears!

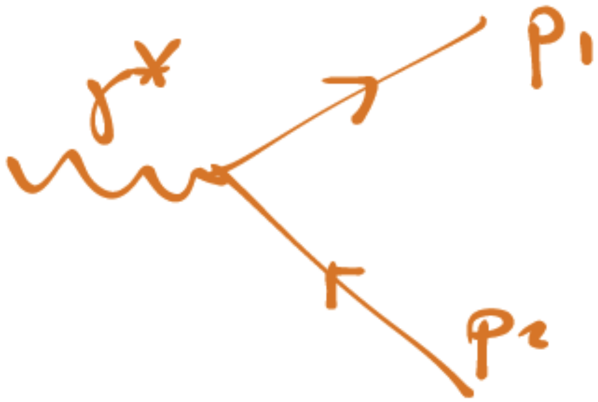

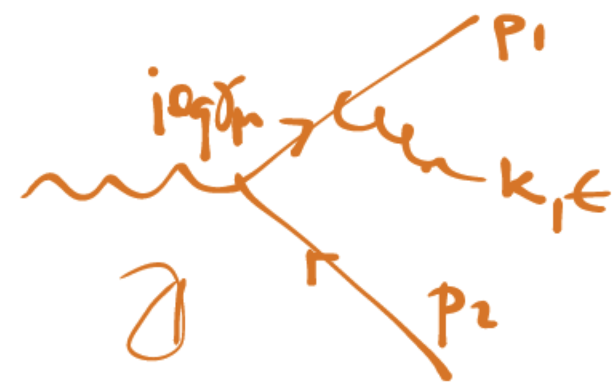

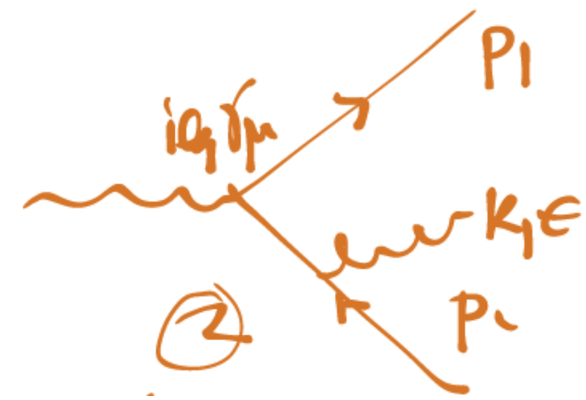

- In all colour representations, angularly ordered, soft-collinear divergent radiation: only gluons emitted within the antenna aperture.

$$\omega \frac{dN}{d^3k} = \frac{\alpha_s}{(2\pi)^2}\left[C_F\left(R_q + R_{\bar{q}} - 2J\right) + C_A J\right]$$

$$\omega \frac{dN}{d^3k} = \frac{\alpha_s}{(2\pi)^2}\left[C_F R_q + C_A R_g - C_A J\right]$$

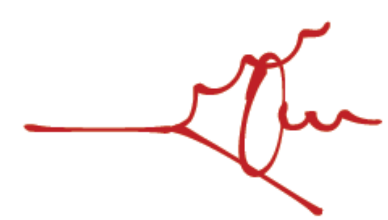

Two emitters: medium

- We consider the soft limit $\omega \to 0$.

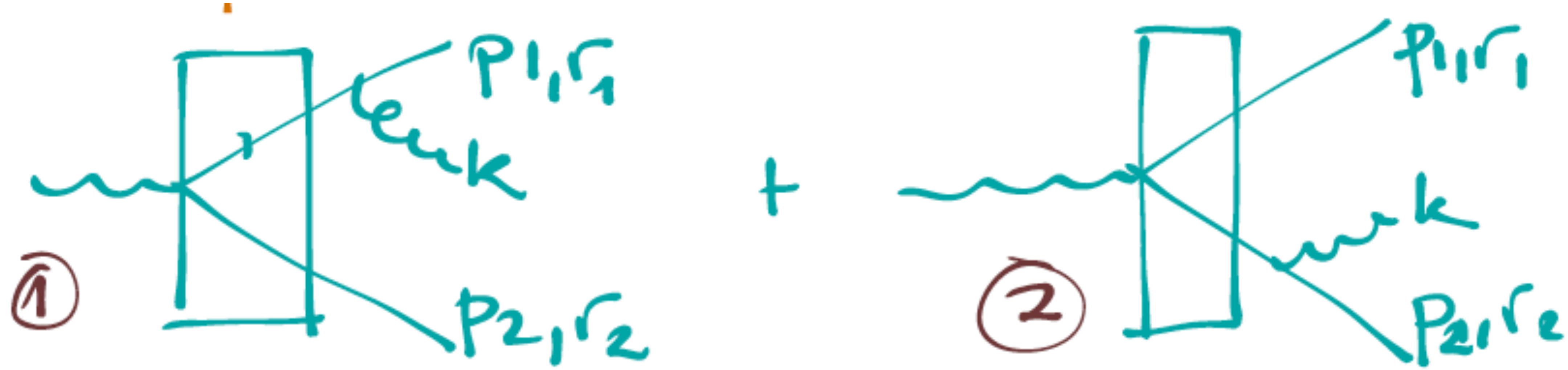

$$①^2 = |M_{q\bar{q}}|^2 C_F g_s^2 \left(\frac{p_1\cdot\epsilon}{p_1\cdot k}\right)^2 \qquad ②^2 = R_{\bar{q}}$$

$$1\otimes 2^* = |M_{q\bar{q}}|^2 \frac{1}{N} \sum \langle \mathrm{tr}\left(W^\dagger(r_2)\, W(r_1)\, t^a\, W^\dagger(r_1)\, W(r_2)\, t^a\right)\rangle \times g_s^2 \frac{p_1\cdot p_2}{p_1\cdot k\; p_2\cdot k}$$

$$= \langle \mathrm{tr}\left(\underbrace{W(r_2)\, t^a\, W^\dagger(r_2)}\; \underbrace{W(r_1)\, t^a\, W^\dagger(r_1)}\right)\rangle$$

$$= C_F \frac{1}{N_c^2-1}\, \mathrm{tr}\langle W_A(r_1)\, W_A(r_2)\rangle$$

Two emitters: medium

- We consider the soft limit ω→0.

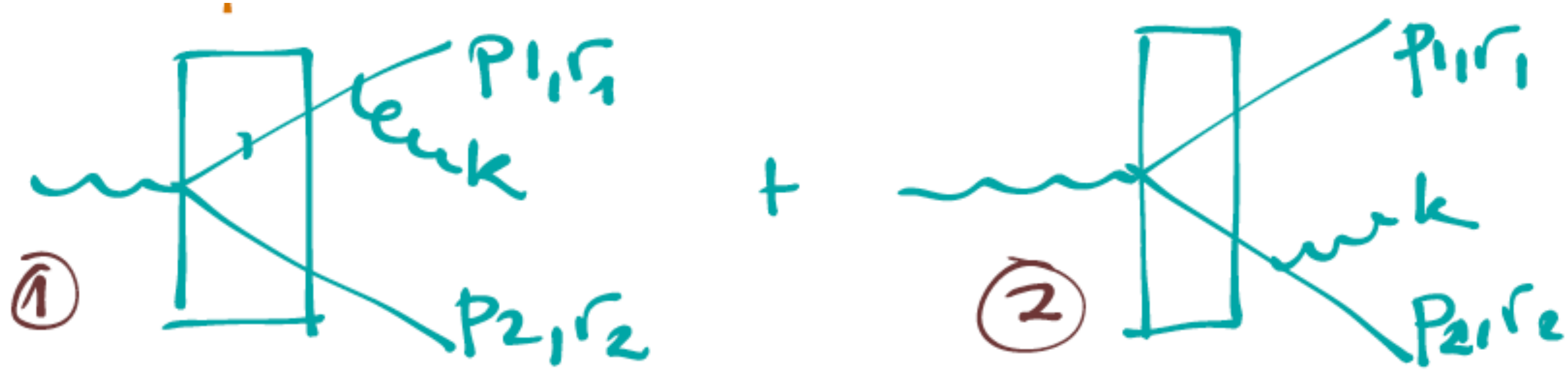

$$dN = \frac{d\omega}{\omega}\frac{d\Omega}{2\pi}\frac{\alpha_s C_F}{2\pi}\left[R_q + R_{\bar q} - (1-\Delta_{med})\, 2J\right]$$

$$* \quad 1-\Delta_{med} = \frac{1}{N^2-1}\, tr\langle W_A(r_1)\, W_A(r_2)\rangle \quad [\text{Survival prob}]$$

Two regimes

⊛ $\Delta_{med} \to 1 \Rightarrow dN \sim R_q + R_{\bar q}$ (independent)

OPAQUE MED — Decoherence

⊛ $\Delta_{med} \to 0 \Rightarrow dN \sim R_q + R_{\bar q} - 2J \Rightarrow$ vacuum

DILUTE MEDIUM — (Angular ordering)

Summarising:

- Traditional (BDMPS-Z-W/GLV) picture: semihard large angle gluon radiation (interference with several scattering centres).
- Present picture, developed in CGC-like schemes, SCET,…: interplay between the medium resolving power and the jet scale [Mehtar-Tani-Salgado-Tywoniuk, Casaderrey-Iancu, Vitev et al.].

Summarising:

• Traditional (BDMPS-Z-W/GLV) picture: semihard large angle gluon radiation (interference with several scattering centres).

• Present picture, developed in CGC-like schemes, SCET,...: interplay between the medium resolving power and the jet scale [Mehtar-Tani-Salgado-Tywoniuk, Casaderrey-Iancu, Vitev et al.].

$$\Delta_{med} \approx 1 - \mathrm{e}^{-\frac{1}{12}Q_s^2 r_\perp^2} \qquad Q_s^2 = \hat{q}L \qquad r_\perp = \theta_{\rm jet} L$$

Summarising:

- Traditional (BDMPS-Z-W/GLV) picture: semihard large angle gluon radiation (interference with several scattering centres).
- Present picture, developed in CGC-like schemes, SCET,...: interplay between the medium resolving power and the jet scale [Mehtar-Tani-Salgado-Tywoniuk, Casaderrey-Iancu, Vitev et al.].

$$\Delta_{med} \approx 1 - e^{-\frac{1}{12}Q_s^2 r_\perp^2} \qquad Q_s^2 = \hat{q}L \qquad r_\perp = \theta_{\rm jet} L$$

Soft limit

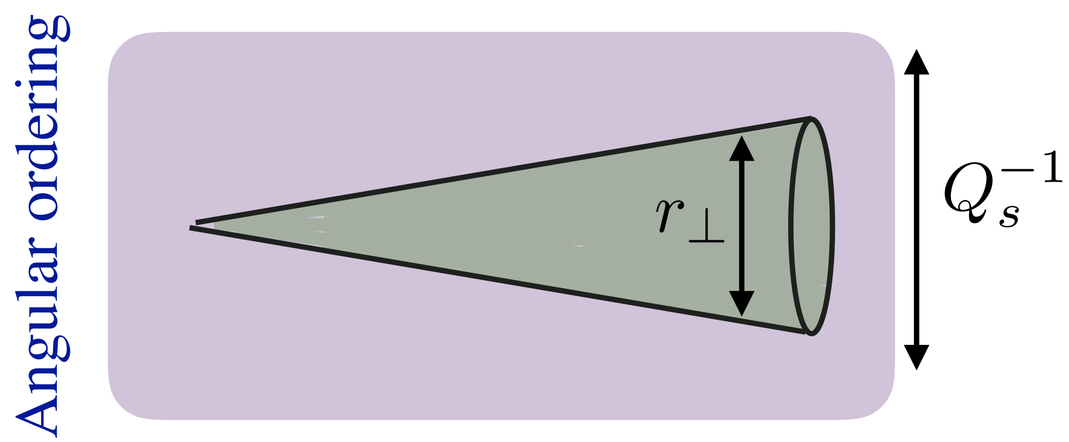

$$\Delta_{med} \to 0$$

Summarising:

- Traditional (BDMPS-Z-W/GLV) picture: semihard large angle gluon radiation (interference with several scattering centres).
- Present picture, developed in CGC-like schemes, SCET,...: interplay between the medium resolving power and the jet scale [Mehtar-Tani-Salgado-Tywoniuk, Casaderrey-Iancu, Vitev et al.].

$$\Delta_{med} \approx 1 - \mathrm{e}^{-\frac{1}{12}Q_s^2 r_\perp^2} \qquad Q_s^2 = \hat{q}L \qquad r_\perp = \theta_{\mathrm{jet}} L$$

Soft limit

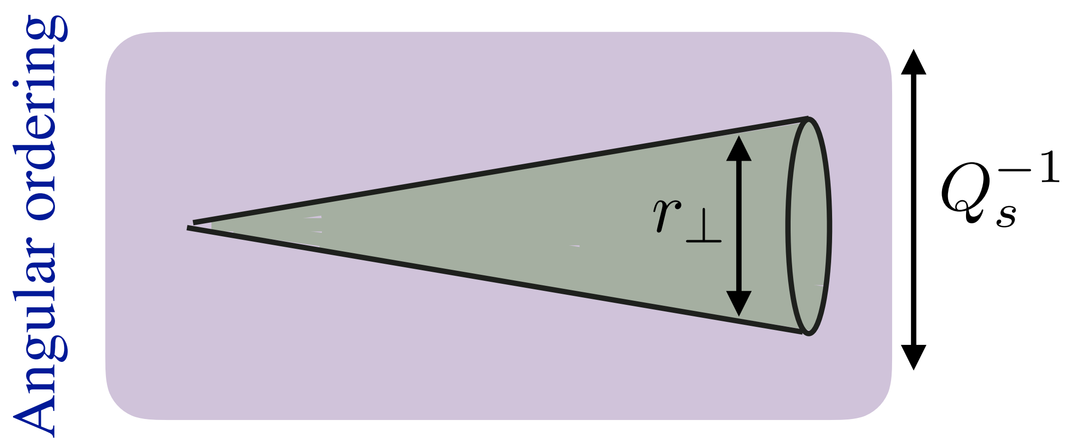

$$\Delta_{med} \to 0$$

➜ Vacuum-like radiation (angular ordering AO) + radiated gluons off the total colour charge: hard part of jet FF preserved, little jet broadening.

Summarising:

- Traditional (BDMPS-Z-W/GLV) picture: semihard large angle gluon radiation (interference with several scattering centres).
- Present picture, developed in CGC-like schemes, SCET,…: interplay between the medium resolving power and the jet scale [Mehtar-Tani-Salgado-Tywoniuk, Casaderrey-Iancu, Vitev et al.].

$\Delta_{med} \approx 1 - e^{-\frac{1}{12}Q_s^2 r_\perp^2}$ $Q_s^2 = \hat{q}L$ $r_\perp = \theta_{\rm jet} L$

Soft limit

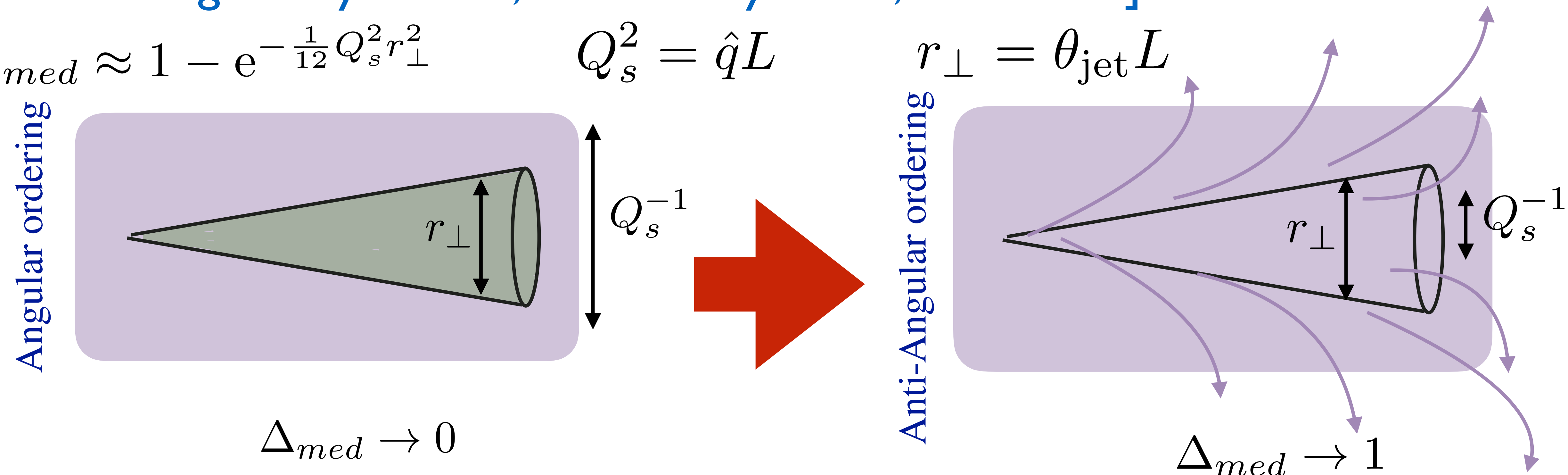

➜ Vacuum-like radiation (angular ordering AO) + radiated gluons off the total colour charge: hard part of jet FF preserved, little jet broadening.

Summarising:

- Traditional (BDMPS-Z-W/GLV) picture: semihard large angle gluon radiation (interference with several scattering centres).
- Present picture, developed in CGC-like schemes, SCET,...: interplay between the medium resolving power and the jet scale [Mehtar-Tani-Salgado-Tywoniuk, Casaderrey-Iancu, Vitev et al.].

$$\Delta_{med} \approx 1 - e^{-\frac{1}{12} Q_s^2 r_\perp^2} \qquad Q_s^2 = \hat{q} L \qquad r_\perp = \theta_{\rm jet} L$$

Soft limit

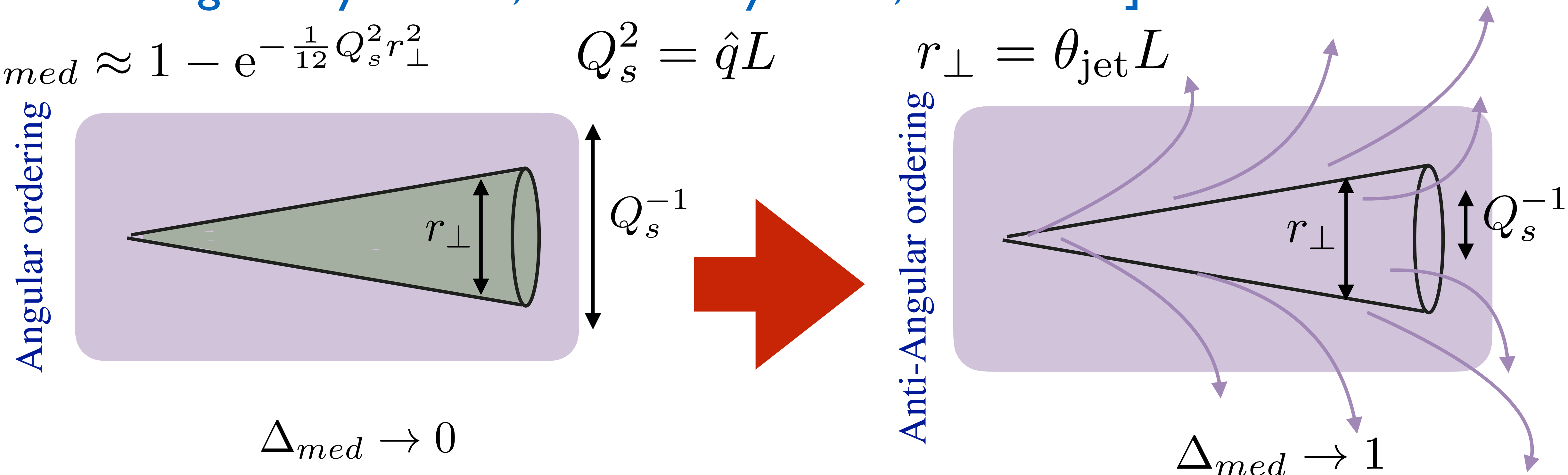

➜ Vacuum-like radiation (angular ordering AO) + radiated gluons off the total colour charge: hard part of jet FF preserved, little jet broadening.

➜ Vacuum-like radiation (~~AO~~) + radiated gluons off the individual colour charges: large angle jet shapes, large angle momentum imbalance (turbulence picture for large dense media).

Summarising:

• Traditional (BDMPS-Z-W/GLV) picture: semihard large angle gluon radiation (interference with several scattering centres).

• Our picture of radiative energy loss is based on coherence, both for the rescattering with the medium and for the emission from composite systems.

• We are close to see the limits in which an in-medium jet calculus is valid, to establish the basis for better MC implementations.

• Partial implementations of coherence exists in several MC: Jewell, QPYTHIA,…

• For single inclusive production, these ideas support the traditional picture.

Summary and outlook:

• I have tried to illustrate some of the uses of coherence for the initial and final stages of high-energy hadronic and nuclear collisions:

➜ Nuclear shadowing, single inclusive particle production and correlations (ridge).

➜ Medium-induced gluon radiation leading to radiative energy loss.

Summary and outlook:

- I have tried to illustrate some of the uses of coherence for the initial and final stages of high-energy hadronic and nuclear collisions:
  - ➜ Nuclear shadowing, single inclusive particle production and correlations (ridge).
  - ➜ Medium-induced gluon radiation leading to radiative energy loss.
- In the initial stage, these ideas are required to:
  - ➜ Help to understand the success of hydrodynamics for small systems and its eventual limits.
  - ➜ Establish the initial conditions for hydro evolution.

Summary and outlook:

- I have tried to illustrate some of the uses of coherence for the initial and final stages of high-energy hadronic and nuclear collisions:

  ➜ Nuclear shadowing, single inclusive particle production and correlations (ridge).

  ➜ Medium-induced gluon radiation leading to radiative energy loss.

- In the initial stage, these ideas are required to:

  ➜ Help to understand the success of hydrodynamics for small systems and its eventual limits.

  ➜ Establish the initial conditions for hydro evolution.

- In the final stage, these ideas are required to:

  ➜ Set the basis for an in-medium jet calculus and its eventual limitations.

  ➜ Understand the relative importance of radiative processes with respect to elastic and medium response, to reduce the theoretical uncertainties in the extraction of medium parameters.

Summary and outlook:

- I have tried to illustrate some of the uses of coherence for the initial and final stages of high-energy hadronic and nuclear collisions:
  - ➜ Nuclear shadowing, single inclusive particle production and correlations (ridge).
  - ➜ Medium-induced gluon radiation leading to radiative energy loss.
- In the initial stage, these ideas are required to:
  - ➜ Help to understand the success of hydrodynamics for small systems and its eventual limits.
  - ➜ Establish the initial conditions for hydro evolution.
- In the final stage, these ideas are required to:
  - ➜ Set the basis for an in-medium jet calculus and its eventual limitations.
  - ➜ Understand the relative importance of radiative processes with respect to elastic and medium response, to reduce the theoretical uncertainties in the extraction of medium parameters.
- Note that the techniques are very similar, with extensions from one to other: semiclassical approach for radiative energy loss, non-eikonal corrections for CGC,…

Summary and outlook:

- I have tried to illustrate some of the uses of coherence for the initial and final stages of high-energy hadronic and nuclear collisions:
  - ➜ Nuclear shadowing, single inclusive particle production and correlations (ridge).
  - ➜ Medium-induced gluon radiation leading to radiative energy loss.
- In the initial stage, these ideas are required to:

Many thanks to:

➜ *Those whose plots/slides I have used: Brian Cole, Liliana Apolinario, François Gelis, Carlos Salgado, Urs Wiedemann, …*

➜ *The **organisers** for their invitation to provide this talk.*

➜ *You all for your attention.*

- Note that the techniques are very similar, with extensions from one to other: semiclassical approach for radiative energy loss, non-eikonal corrections for CGC,…

Backup:

Hydrodynamics:

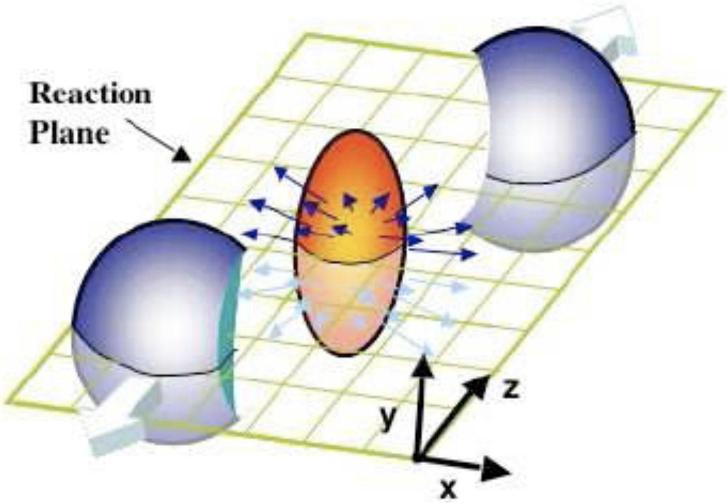

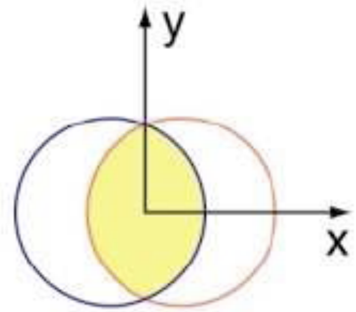

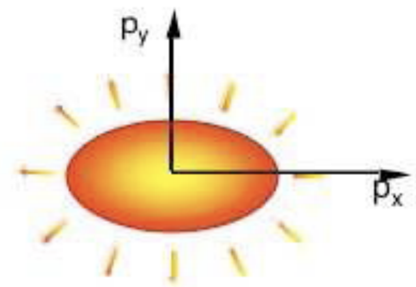

$$\frac{dN_k}{dy dp_T^2 d\phi} = \frac{dN_k}{dy dp_T^2} \frac{1}{2\pi} [1 + 2v_1 \cos(\phi - \phi_R) + 2v_2 \cos 2(\phi - \phi_R) + \ldots]$$

- Viscous relativistic hydrodynamics very successful in reproducing azimuthal asymmetries if started very early (< 1 fm/c).
- Initial space anisotropy ⇒ final momentum anisotropy: it

generates correlations between any number of particles.

- It requires EoS plus initial conditions (averaged or fluctuating) plus a hadronisation prescription, and several constants determined from data: relaxation time, bulk and shear viscosity,…
- Hydro requires $\lambda=(\rho\sigma)^{-1} << R$ (interactions) and equilibrium: large opacities for the particles, equilibrium/isotropization problem.